Doctoral Dissertation

(Shinshu University)

Fabrication of nanofibers composites for biomedical and textile applications

March 2019

KHAN Muhammad Qamar

17ST103H

Doctor of Engineering Thesis

Supervisor: Prof Ick Soo Kim (Dr. Eng)

Department of Bioscience and Textile Technology

Interdisciplinary Graduate School of science and Technology

Shinshu University

ABSTRACT

Fabrication of nanofibers composites for biomedical and textile applications

KHAN Muhammad Qamar

Directed by: Prof Ick Soo Kim

The nanofibers has become very interesting topic for the researchers due to its applications ground, and it is being used in various research fields such as biotechnology, biomedical, electrical & electronics, environmental and energy resources due to its advanced properties and high potentials applications. Therefore, this thesis covered the series of experiments related to biomedical applications and functional textiles. For this purpose, we started to the formation of blended nanofibers by incorporating natural biomaterials with the synthetic polymer which has a great interest in recent years. We reported the successful fabrication of novel nanofibers using naturally occurring antimicrobial honey incorporated in Poly (1, 4 cyclohexane dimethylene isosorbide trephthalate) (PICT) for the potential wound dressing applications. On the basis of characterizations results, it was concluded that PICT/honey nanofibers containing 15% of honey are more suitable for good elastic behavior and tensile strength as compared to other concentrations of honey used in the polymer solution and in the study of "Preparation and Characterizations of Multifunctional PVA/ZnO Nanofibers Composite membranes for Surgical Gown Application" authors developed the multifunctional; antibacterial, ultraviolet rays (UV) protected and self-cleaning surgical gown by blending of zinc oxide (ZnO) nanoparticles with poly vinyl alcohol (PVA). On the behalf of characterization results, PVA/ZnO nanofibers were exhibited the desired objectives for the surgical gown. This multifunctional surgical gown is beneficial for medical surgeon against the bacteria, stains, and UV blocking to save his/her life.

The fabrication of an artificial blood vessel remains an ongoing challenge for cardiovascular tissue engineering. Full biocompatibility, proper physiological and immediate availability have emerged as central issues. To address these issues, the dual network composite scaffolds were fabricated by coating the electrospun nanofibres based tubes with PVA hydrogel, which could increase the cell viability and show the potential for controlling the composition, structure and mechanical properties of scaffolds. The authors also tried to form a model for axon, where nanofibers based tubes as scaffolds for potential neuroscience application in the axon were fabricated by Polyvinylpyrrolidone incorporated with gold nanoparticle

(PVP/Au) in five different diameters via electrospinning. So the nanofibers based tubes having diameter 0.2 mm made from PVP/Au is the better substrate for farther in vivo or in vitro investigation which will make this material more useful for tissue engineering.

Metals and their nanoparticles, sodium alginate, honey and bacterial cellulose were widely used in the fabrication of scaffolds and wound dressings due to their biocompatibility, but silver sulfadiazine (SSD) is a leading topical antibacterial agent especially for the treatment of burn wound infections. In this novel research study, first time SSD was embedded with nanofibers. The objective of this study was to fabricate high profiled antibacterial properties with lowest toxicity and high cell adhesion. The resultant CA/SSD nanofibers exhibited the appreciable antimicrobial activity against Gram-negative Escherichia Coli and Gram-positive Bacillus Subtilis bacteria with considerable sustainability for repetitive use. In another study, for functional textiles related to biomedical field, were focused. Herein, a self-cleaning effect of electrospun poly (1,4-cyclohexanedimethylene isosorbide terephthalate) nanofibers embedded with ZnO nanoparticles and comparative study of self-cleaning properties of electrospun PVA/TiO2 and PVA/ZnO Nanofibers Composite were examined. On the base of the characterization results, it was concluded that these PVA/ZnO & PVA/TiO2 nanofibers have self cleaning properties, but PVA/ZnO nanofibers have higher self-cleaning properties than PVA/TiO2 nanofibers because PVA/ZnO nanofibers have 95% self-cleaning properties, which is higher than PVA/TiO2 nanofibers.

Acknowledgements

First of all the praise is to Allah, the Almighty, on whom eventually we are governed by for provisions and assistance. Each and every part of work is waged according to the degree of devotion and dedication to it. I sets my sincere and humble thanks for Him, Who shaped the universe and donated the mankind with knowledge, awareness, and intelligence to examine for its underground and invigorated us with the courage and capability to accomplish our research effort and enabled us to participate as a drop in the present oceans of systematic knowledge. Shuddering lips and drizzling eyes tribute and praise for **Holy Prophet (S.A.W)** who is endlessly a torch of direction for the whole humanity. During my Ph.D. I received support and assistance of many individuals and organization whom I acknowledged at this time I first want to thank faculty, staff, administrators of **Shinshu University Ueda campus** in particular. I want to thank my supervisor **Rising Star Professor Ick Soo Kim (Dr.Eng).** I am appreciative of advice, information and materials that I receive from him. I am also appreciative of guidance and help that I received from Kim lab members specially, **Tanveer Hussain, Davood kharaghani, Yusuke Saito, Sanaullah, Yamamoto, Inove, Nam, Husegawa, Otani, Uemra, Zeeshan Khatri, Murai and Ishikawa san**. I will never forget the efforts and sincerity that they give me in my research.

My final acknowledgement is to my **Mother and Wife**. Without their support and complete understanding I would never have been able to complete this project.

Table of Contents

Chapter # 01 Introduction

1.1. Background

The fiber has the primary role to fabricate the textiles or biomedical product due to length to volume ratio, sustainable flexibility with certain strength. Nanofiber has the great important over the conventional fiber because its diameter is very low around >100 nm with light weight and high length to volume ratio [1]. Nanofibers can be manufactured using various methods but most prominent is electrospinning. Electrospinning is the only way through which we can produce continuous nonwoven fabric in form of nanofibers [2]. This nonwoven fabric/web is used for various applications in biotechnology such as nanofibers for wound dressing, drugs for treatment of diseases, bone regeneration and other artificial vital organs of human beings and this web can also use for functional textiles like multifunctional surgical gown, self-cleaning fabrics and etc [3].

Electrospinning is the fiber production method in which electric force is applied to draw charged threads of polymer solutions to fiber diameters in the order of nanometer. In the electrospinning, when a sufficiently voltage is supplied to a liquid droplet, it becomes charged and electrostatic repulsion counteracts the surface tension and droplet is stretched at a critical point of stream where liquid droplet erupts from the surface and then it becomes the fiber as shown in the Figure 1.1. [4,5].

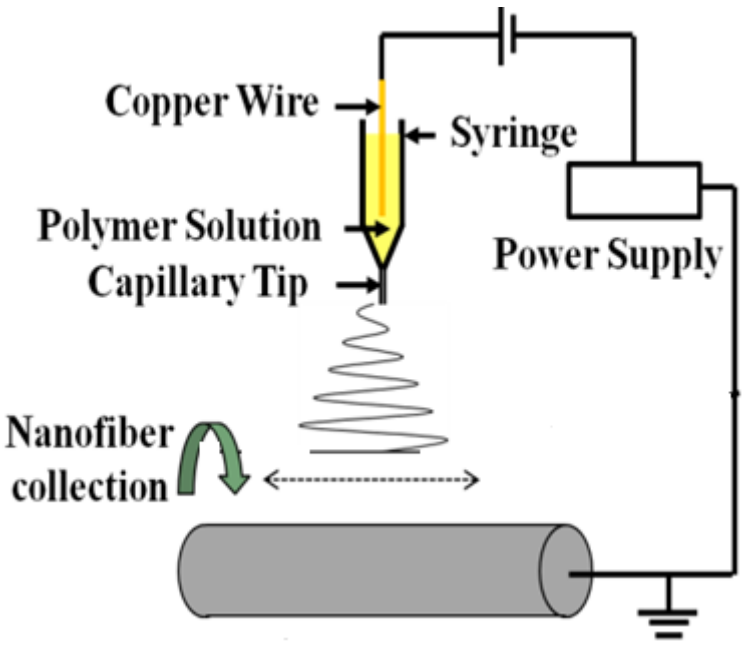

Figure 1.1: Illustration scheme of electrospinning

1.2. Nanofibers for biomedical applications

Biomedical engineering is defined as the application of engineering fields to maintain and restore existing cell/tissue/skin structure or to enable their growth. They are usually organized into three-dimensional structures as required for the body that believed to the development of specific biological function in them. When used to develop the artificial tissue substitutes, the engineering approaches emphasize the importance of the structural design of the biomaterial employed as scaffolding structure. These scaffolds or wound dressings are used to protect the skin from various microbials or maintain and restore the cells and tissues [6, 7].

The development of nanofibers has enhanced the scope for fabricating the scaffolds that can potentially mimic the architecture of human tissue at stated requirements. The high surface area to volume ratio of the nanofibers combined with their microporous structure favors the cell adhesion, proliferation, migration, and differentions are the highly desired properties for the tissue engineering applications. Therefore the current research in this area was driven towards the fabrication, characterization, and application of nanofibers as scaffolds for biomedical engineering in many fields like ophthalmology, bone regeneration, drug delivery, wound dressings, neuroscience and vascular transplantation [8-10].

Since past few years, the nanofibers based tissue engineering has been increasing and progress is obvious in various fields such as blood vessels, artificial cornea, retina, veins, blood filter for kidney and other implantable artificial vital organs of animals and also for human beings. A huge numbers of people used nanofibers for this field because nanofibers are fruitful for medical textiles due to its biodegradable and non biodegradable properties as required for the organs [11- 13].

1.2.1. Nanofibers for antibacterial properties

The skin is the largest organ of the human body and serves as an important barrier that protects the body from microbial infestation and maintains homeostasis. The damage skin can allow pathogens to invade the human body or its part/parts and cause the infections. However, it is necessary to cover the skin with proper wound dressings to protect the wound from further contaminations. To ensure the effectiveness of wound healing, wound dressings should be biocompatible, non-allergic and non-toxic and in addition, it should maintain a moist environment around the wound, rapid the wound

recovery, reduce the risk of infection and should possess antibacterial activity to prevent the microbial invasion. Multidisciplinary Alliance Against Device-Related Infections (MAADRI) reported that medical device related infections are the major cause of more than half of the hospital acquired infections. Together with the rise in antibiotic resistant Staphylococcus aureus & Escherichia Coli, there is a pressing demand for next generation anti-infective materials for protecting wounds and medical devices against microbes. In the United States, an estimated seven million people suffer from chronic skin ulcers while more than one million burns have been reported annually [14,15].

Staphylococcus aureus, bacillus subtilis & Escherichia Coli are the major etiological agents responsible for invasive infections in wounds around the globe. The advent of topical antimicrobial agent impregnated wound dressings such as silver, iodine, polyhexamethylenebiguanide and honey have provided a tangible alternative in the development of wound dressing for the control of wound infections [16,17].

1.2.2. Nanofibers based tubes

Since past few years, the nanofibers based tissue engineering has been increasing and progress is obvious in various fields such as blood vessels [11], artificial cornea, retina, veins, blood filter for kidney and other implantable artificial vital organs of animals and also for human beings. A huge numbers of people used nanofibers for this field because nanofibers are fruitful for medical textiles due to its biodegradable and non biodegradable properties as required for the organs [18, 19]. These organs are damaged due to the accidental situations and the medical treatment required the secondary surgery for planting the organs. The artificial organs are best option to for replace the damaged organs of human beings [20]. One of them is the axon for continues supply of neurosignals in the nerves of human's body. These signals need some amount of potential voltage for the information carrying from any point of body to brain. This potential voltage is not harmful for brain because around the axon there is insulated layer which protect the nerve [21-23]. The fabrication of artificial blood vessel remains an ongoing challenge for cardiovascular tissue engineering. Full biocompatibility, proper physiological and immediate availability have emerged as central issues. To address these issues, the dual network composite scaffolds were fabricated by coating the electrospun nanofibres based tubes with PVA hydrogel, which could increase the cell viability and show the potential for controlling the composition, structure and mechanical properties of scaffolds [24, 25].

The electrospinning setup for making nanofibers tubes is shown in Figure 1.2, in which a rotating and resiprotating element is used to collect the nanofibers in front of main collector of nanofibers.

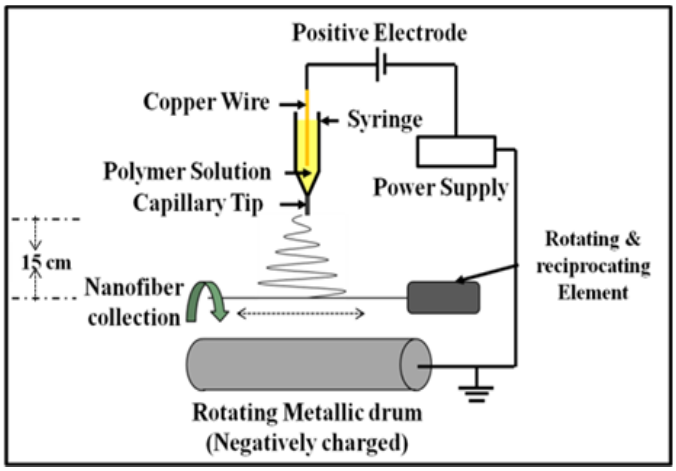

Figure 1.2: Illustration scheme of electrospinning for nanofibers based tubes.

1.3. Nanofibers for functional textiles

Nanofibers are ideally suited to form the functional or multifunctional textiles [26]. The protected products are needed to reduce occupational exposure for individual involved with the hospital, chemical industry, emergency response and also military. A number of methods for development of nonwoven and non-washable technical textiles like surgical gowns but the use of electrospun nanofibers for the non-washable protective garments has grown over the past few decades since they are relatively inexpensive, lightweight and effective protection [27]. The electrospun nanofibers can be used for various functional applications, such as protection from exposure to UV light, as an anti-microbial product, as a flame retardant, to enhance the shape-memory behavior of apparel, and self-cleaning. Especially, various approaches have been suggested to introduce the self-cleaning property to nanofibers [28, 29]. Since ZnO is a promising material for introducing the self-cleaning property to composite materials, it is of great interest to researchers who want to make self-cleaning materials [30]. It is non-toxic and could be used extensively in industry due to its low cost. In addition, it provides better efficiency in photo-catalytic applications than other chemicals (e.g., TiO_2 and WO_3) due to its large energy gap (3.37 eV) and its large excitation binding energy (60 meV) [31].

References

1) Bang, Hyunsik, Kei Watanabe, Ryu Nakashima, Wei Kai, Kyung-Hun Song, Jung Soon Lee, Mayakrishnan Gopiraman, and Ick-Soo Kim. "A highly hydrophilic water-insoluble nanofiber composite

as an efficient and easily-handleable adsorbent for the rapid adsorption of cesium from radioactive wastewater." *Rsc Advances* 4, no. 103 (2014): 59571-59578.

2) Ashraf, Roqia, Hasham S. Sofi, Aijaz Malik, Mushtaq A. Beigh, Rabia Hamid, and Faheem A. Sheikh. "Recent Trends in the Fabrication of Starch Nanofibers: Electrospinning and Non-electrospinning Routes and Their Applications in Biotechnology." *Applied biochemistry and biotechnology*(2018): 1-28.

3) Kurtz, Irene, and Jessica Schiffman. "Current and Emerging Approaches to Engineer Antibacterial and Antifouling Electrospun Nanofibers." *Materials* 11, no. 7 (2018): 1059.

4) Yurova, Nadezhda S., Alexandra Danchuk, Sarah N. Mobarez, Nongnoot Wongkaew, Tatiana Rusanova, Antje J. Baeumner, and Axel Duerkop. "Functional electrospun nanofibers for multimodal sensitive detection of biogenic amines in food via a simple dipstick assay." *Analytical and bioanalytical chemistry*410, no. 3 (2018): 1111-1121.

5) Li, Dan, Yuliang Wang, and Younan Xia. "Electrospinning nanofibers as uniaxially aligned arrays and layer‐by‐layer stacked films." *Advanced materials* 16, no. 4 (2004): 361-366.

6) Laschke, Matthias W., and Michael D. Menger. "Life is 3D: boosting spheroid function for tissue engineering." *Trends in biotechnology* 35, no. 2 (2017): 133-144.

7) Moreno-Jiménez, Inés, Janos M. Kanczler, Gry Hulsart-Billstrom, Stefanie Inglis, and Richard OC Oreffo. "The chorioallantoic membrane assay for biomaterial testing in tissue engineering: a short-term in vivo preclinical model." *Tissue Engineering Part C: Methods* 23, no. 12 (2017): 938-952.

8) Khan, Muhammad Qamar, Hoik Lee, Zeeshan Khatri, Davood Kharaghani, Muzamil Khatri, Takahiro Ishikawa, Seung-Soon Im, and Ick Soo Kim. "Fabrication and characterization of nanofibers of honey/poly (1, 4-cyclohexane dimethylene isosorbide trephthalate) by electrospinning." *Materials Science and Engineering: C* 81 (2017): 247-251.

9) Hu, Jue, Dan Kai, Hongye Ye, Lingling Tian, Xin Ding, Seeram Ramakrishna, and Xian Jun Loh. "Electrospinning of poly (glycerol sebacate)-based nanofibers for nerve tissue engineering." *Materials Science and Engineering: C* 70 (2017): 1089-1094.

10) Lee, Hoik, Gang Xu, Davood Kharaghani, Masayoshi Nishino, Kyung Hun Song, Jung Soon Lee, and Ick Soo Kim. "Electrospun tri-layered zein/PVP-GO/zein nanofiber mats for providing biphasic drug release profiles." *International journal of pharmaceutics* 531, no. 1 (2017): 101-107.

11) Ma, Zuwei, Masaya Kotaki, Thomas Yong, Wei He, and Seeram Ramakrishna. "Surface engineering of electrospun polyethylene terephthalate (PET) nanofibers towards development of a new material for blood vessel engineering." *Biomaterials* 26, no. 15 (2005): 2527-2536.

12) Bakhshandeh, Haleh, Masoud Soleimani, Saied Shah Hosseini, Hassan Hashemi, Iman Shabani, Abbas Shafiee, Amir Houshang Behesht Nejad, Mohammad Erfan, Rassoul Dinarvand, and Fatemeh Atyabi. "Poly (ε-caprolactone) nanofibrous ring surrounding a polyvinyl alcohol hydrogel for the development of a biocompatible two-part artificial cornea." *International journal of nanomedicine* 6 (2011): 1509.

13) Khan, Muhammad Qamar, Davood Kharaghani, Nazish Nishat, Takahiro Ishikawa, Sana Ullah, Hoik Lee, Zeeshan Khatri, and Ick Soo Kim. "The development of nanofiber tubes based on nanocomposites of polyvinylpyrrolidone incorporated gold nanoparticles as scaffolds for neuroscience application in axons." *Textile Research Journal* (2018): 0040517518801185.

14) Chen, Honglei, Guangqian Lan, Luoxiao Ran, Yang Xiao, Kun Yu, Bitao Lu, Fangying Dai, Dayang Wu, and Fei Lu. "A novel wound dressing based on a Konjac glucomannan/silver nanoparticle composite sponge effectively kills bacteria and accelerates wound healing." *Carbohydrate polymers* 183 (2018): 70-80.

15) Siafaka, Panoraia I., Asimina P. Zisi, Maria K. Exindari, Ioannis D. Karantas, and Dimitrios N. Bikiaris. "Porous dressings of modified chitosan with poly (2-hydroxyethyl acrylate) for topical wound delivery of levofloxacin." *Carbohydrate polymers* 143 (2016): 90-99.

16) Dhand, Chetna, Mayandi Venkatesh, Veluchami Amutha Barathi, Sriram Harini, Samiran Bairagi, Eunice Goh Tze Leng, Nandhakumar Muruganandham et al. "Bio-inspired crosslinking and matrix-drug interactions for advanced wound dressings with long-term antimicrobial activity." *Biomaterials*138 (2017): 153-168.

17) Mele, Elisa. "Electrospinning of natural polymers for advanced wound care: towards responsive and adaptive dressings." *Journal of Materials Chemistry B* 4, no. 28 (2016): 4801-4812.

18) Li, Yumei, Xiang Li, Rui Zhao, Chuying Wang, Fangping Qiu, Bolun Sun, He Ji, Ju Qiu, and Ce Wang. "Enhanced adhesion and proliferation of human umbilical vein endothelial cells on conductive PANI-PCL fiber scaffold by electrical stimulation." *Materials Science and Engineering: C* 72 (2017): 106-112.

19) Namekawa, Koki, Makoto Tokoro Schreiber, Takao Aoyagi, and Mitsuhiro Ebara. "Fabrication of zeolite–polymer composite nanofibers for removal of uremic toxins from kidney failure patients." *Biomaterials Science* 2, no. 5 (2014): 674-679.

20) Ma, Zuwei, Masaya Kotaki, Thomas Yong, Wei He, and Seeram Ramakrishna. "Surface engineering of electrospun polyethylene terephthalate (PET) nanofibers towards development of a new material for blood vessel engineering." *Biomaterials* 26, no. 15 (2005): 2527-2536.

21) Albreiki, Salhah, Alanoud AlAli, and Raed M. Shubair. "Coding brain neurons via electrical network models for neuro-signal synthesis in computational neuroscience." In *Electronic Devices, Systems and Applications (ICEDSA), 2016 5th International Conference on*, pp. 1-5. IEEE, 2016.

22) Liedler, Angela, and Gregor Remmert. "Neurostimulation using AC and/or DC stimulation pulses." U.S. Patent Application 15/647,905, filed January 18, 2018.

23) Yogev, Shaul, and Kang Shen. "Establishing neuronal polarity with environmental and intrinsic mechanisms." *Neuron* 96, no. 3 (2017): 638-650.

24) Muhammad Qamar Khan, Davood Kharaghani, Nazish Nishat, Sanaullah, Amir Shahzad,Takayuki Yamamoto, Yuma Inoue, Ick Soo Kim. J. Applied Polymer Sci. DOI: 10.1002/app.47222

25) Laschke, Matthias W., and Michael D. Menger. "Life is 3D: boosting spheroid function for tissue engineering." *Trends in biotechnology* 35, no. 2 (2017): 133-144.

26) Khan, Muhammad Qamar, Hoik Lee, Jun Mo Koo, Zeeshan Khatri, Jianhua Sui, Seung Soon Im, Chunhong Zhu, and Ick Soo Kim. "Self-cleaning effect of electrospun poly (1, 4-cyclohexanedimethylene isosorbide terephthalate) nanofibers embedded with zinc oxide nanoparticles." *Textile Research Journal* (2017): 0040517517723026.

27) Zhu, Chunhong, Jian Shi, Sijun Xu, Minori Ishimori, Jianhua Sui, and Hideaki Morikawa. "Design and characterization of self-cleaning cotton fabrics exploiting zinc oxide nanoparticle-triggered photocatalytic degradation." *Cellulose* 24, no. 6 (2017): 2657-2667.

28) Saad, Siti Rohani, Norsuria Mahmed, Mohd Mustafa Al Bakri Abdullah, and Andrei Victor Sandu. "Self-cleaning technology in fabric: A review." In *IOP Conference Series: Materials Science and Engineering*, vol. 133, no. 1, p. 012028. IOP Publishing, 2016.

29) Fu, Qiuxia, Cheng Duan, Zishuo Yan, Yan Li, Yang Si, Lifang Liu, Jianyong Yu, and Bin Ding. "Nanofiber‐Based Hydrogels: Controllable Synthesis and Multifunctional Applications." *Macromolecular rapid communications* 39, no. 10 (2018): 1800058.

30) Li, Jia, Boxiang Wang, Jie Lin, Dehong Cheng, and Yanhua Lu. "Multifunctional Surface Modification of Mulberry Silk Fabric via PNIPAAm/Chitosan/PEO Nanofibers Coating and Cross-Linking Technology." *Coatings* 8, no. 2 (2018): 68.

31) Khan, Muhammad, Davood Kharaghani, Sana Ullah, Muhammad Waqas, Abdul Abbasi, Yusuke Saito, Chunhong Zhu, and Ick Kim. "Self-Cleaning Properties of Electrospun PVA/TiO2 and PVA/ZnO Nanofibers Composites." *Nanomaterials* 8, no. 9 (2018): 644.

Chapter # 02

Fabrication and characterization of nanofibers of honey/poly (1, 4 cyclohexane dimethylene isosorbide trephthalate) by electrospinning

2.1. Introduction

The applications ground of nanofibers is becoming vast day by day and it is being used in various research fields such as biotechnology, biomedical [1-10], electrical & electronics [11], environmental [12] and energy resources [13] due to its advance properties and high potentials applications. Nanofibers can be manufactured using various methods but most prominent is electrospinning [14]. Electrospinning is the only way through which we can produce continuous nonwoven fabric in form of nanofibers [15]. This nonwoven fabric is used for various applications in biotechnology [16] such as nanofibers for wound dressing [17], drugs for treatment of diseases [18], bone regeneration [19] and other artificial vital organs of human beings [20]. The formation of blend nanofibers by incorporating natural biomaterials with the synthetic polymer has great interest in recent years [21]. Herein, we attempted to fabricate the nanofibers by incorporating natural Honey in Poly (1, 4 cyclohexane dimethylene isosorbide trephthalate) (PICT) by electrospinning for the very first time. PICT is an aromatic semicrytalline & biodegradable co-polyester [22] and honey is an aromatic hydrocarbon, which has many organic compounds and used as a medical treatment since ancient time [23]. Honey is the most efficient antimicrobial compound for safe and effective antimicrobial wound dressings, throughout the naturally occurring compounds such as tea tree oil, mastic gum and cranberry juice which demonstrated the antimicrobial efficiency [24]. Recently a few approaches were adopted to fabricate honey with different polymers, such as; A. Arslan et al. (2014) tried to fabricate honey based polyethylene terephthalate nanofibers by electrospinning and nanofibers had the beaded & ribbon-like morphology but the fiber deposition's area was increased [25] and H. Maleki et al. (2013) tried to fabricate the honey based nanofibers with PVA by electrospinning at different concentrations of honey. The nanofibers diameter was reduced as the concentration of honey increased and the release was completed in one hour [26].

The nanofibers of PICT/honey were fabricated successfully and no beads were observed. The release behavior was completed in 30 minutes and good tensile strength & elongation as compared to previous works and having potential for wound dressing and other antimicrobial properties. The morphology of nanofibers was examined under SEM and TEM. The chemical structural change was studied with FT-IR, the mechanical

properties were assessed using tensile strength tester and the release behavior was investigated by UV-visible Spectrophotometer.

2.2. Experimental

2.2.1. Materials

PICT polymer (99.8%) with 70 mol % isosorbide (99.8%) purchased from SK Chemical Korea, Triflouric acid (99.9%) was purchased from Sigma-Aldrich Corporation (USA), Honey was extracted by Bee insects from Pakistan forest and chloroform was purchased from Wako Pure Chemical Industries, Ltd.

2.2.2. Preparation of Nanofibers

Polymer solution was prepared by weight using 10% of PICT dissolved in the TFA and chloroform at ratios 1:3 respectively. After stirring polymer solution for 3 hours, honey was dissolved with 10% & 20% by weight separately. Both polymer solutions (10% honey contained and 20% honey contained) were kept on stirring for 2 hours. After two hours of stirring both polymer solutions were used for electrospinning and loaded separately in two different syringes to carry out electrospinning process. An electrode of copper wire was adjusted in the syringe and the distance from capillary tips to collector was kept 12 cm. A 10 kV was applied to produce the nanofibers.

2.2.3. Characterization

The surface morphology of these nanofibers was evaluated by SEM (JSM-5300, JEOL Ltd., Japan) accelerated with the voltage of 12 kV, TEM (JEM-2100 JEOL Japan) accelerated with 200 kV, FT-IR spectra (IR Prestige-21 by shinmadzu Japan) was done for the evaluation of chemical reaction or bonding with Honey & PICT, the Tensile strength test was performed to check the mechanical behavior of nanofibers by using the Universal Testing Machine (Tesilon RTC 250A, A&D Company Ltd., Japan), wetting behavior of PICT/honey nanofibers surface was characterized by measuring the static contact angle with a contact angle meter (Digidrop, GBX, France), X-ray photoelectron spectroscopy (XPS) was performed on a Kratos Axis-ultra DLD spectrometer (Kratos Analytical Ltd., Manchester, U.K.) and the UV-visible Spectrophotometer (Lambda 900, perkin-Elmer, USA) was used to evaluate the releasing behavior of honey in the wavelength range of 100-900 nm.

2.3. Results and discussions

2.3.1. Morphology of Nanofibers

In order to investigate the surface morphology of PICT nanofibers and PICT/honey nanofibers, SEM images were taken. It was investigated that nanofiber diameter is affected by blending of honey in PICT. When the percentage of honey was increased in PICT then diameter of nanofibers was also increased. In Fig. 2.1a it can be clearly observed that the nanofibers are fine with average diameter 190nm and in Fig. 2.1b PICT nanofiber embedded with 10% honey showed smooth morphology and bead free nanofibers with average diameter of 328 nm and greater in average diameter than pure PICT nanofibers and in Fig. 2.1c the nanofibers of PICT with 15% honey showed further increment in average diameter up to 412 nm and in Fig. 2.1d the nanofibers of PICT with 20% honey showed further increment in average diameter than PICT/honey nanofibers with 15% honey up to 482 nm and it is the largest diameter of the all concentrations of honey used in the nanofibers.

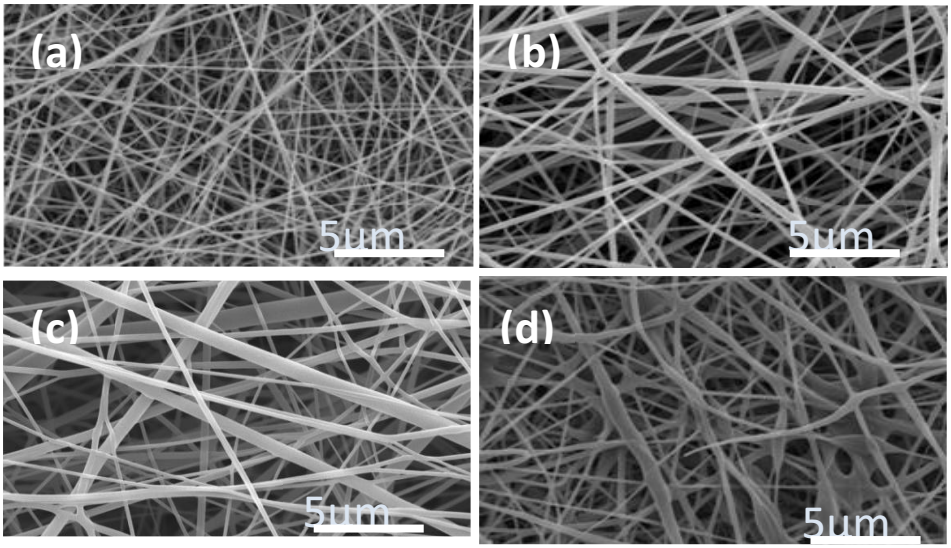

Figure. 2.1. Results of SEM (a) pure PICT nanofibers (b) 10% PICT/honey nanofibers (c) 15% PICT/honey nanofibers (d) 20% PICT/honey nanofibers

Table 2.1. Average diameter of PICT and PICT/honey Nanofibers

Sr. No.	Composition of Samples	Concentration of Honey	Average Diameter
1	Neat PICT	0	190 ±30 nm
2	PICT/honey	10%	328±20 nm
3	PICT/honey	15%	412±50 nm
4	PICT/honey	20%	482±35 nm

The average diameter of all samples was calculated by image analysis software (Image J, version 1.49) as shown in Table 2.1. The average diameter of neat PICT is

190 nm which is very fine as compared to PICT/honey nanofibers having concentration of honey 10%, 15% and 20%.

For the study of average diameter distributions, a graph against each concentration of honey was drawn between diameter in nm of nanofibers and the frequency of fibers in the same range of diameter. It was analyzed that in Fig. 2.2a there are very low diameter distributions in neat PICT nanofibers, most of the nanofibers were in the range of 100-200 nm. In Fig. 2.2b there are diameter distributions in 10% PICT/honey nanofibers. This distribution is greater than neat PICT; most of the nanofibers are in the range of 100-200, 300-400 nm. In Fig. 2.2c there are high diameter distributions in 15% than neat PICT & PICT/honey nanofibers with 10% honey, in this case most of the nanfibers lies in the range of 300-400 nm. In Fig. 2.2d there are highest diameter distributions in 20% PICT/honey nanofibers than neat PICT, PICT/honey nanofibers with 10% honey and PICT/honey nanofibers with 15% honey. In this case nanifibers have also diameter of 900-1000 nm. So when concentration of honey increased the diameter distributions are also increased.

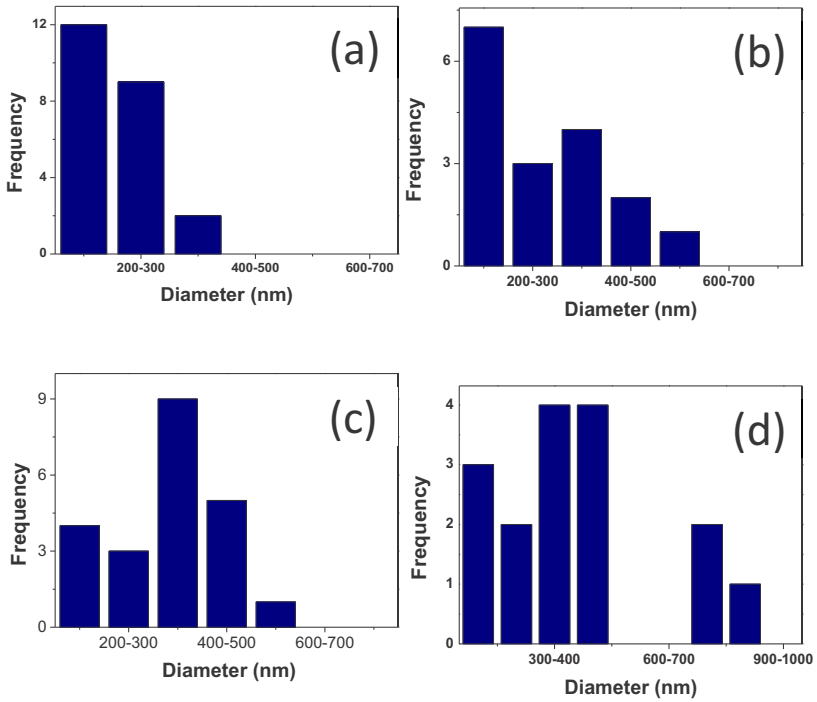

Figure 2..2. Results of diameter distributions (a) Neat PICT nanofibers (b) 10% PICT/honey nanofibers (c) 15% PICT/honey nanofibers (d) 20% PICT/honey nanofibers

To investigate further, the morphology of nanofibers was examined under TEM. It was investigated that diameter and morphology of nanofibers were changed by blending of honey with PICT. The neat PICT nanofibers having diameter size very small and smooth surface as compared to 10%, 15%& 20% by weight PICT/honey nanofibers. When concentration of honey was increased, the surface became lesser smooth than pure PICT nanofibers, and the nanofibers having 20% of honey showed rougher surface morphology compared to PICT nanofibers containing amount of honey 10% and 15% at magnification 200nm. The Fig. 2.3 revealed the obvious change in the diameter and exterior surface morphology of nanofibers. The Fig.2.3d showed the highest diameter size than other Fig. 2.3a, 2.3b and 2.3c.

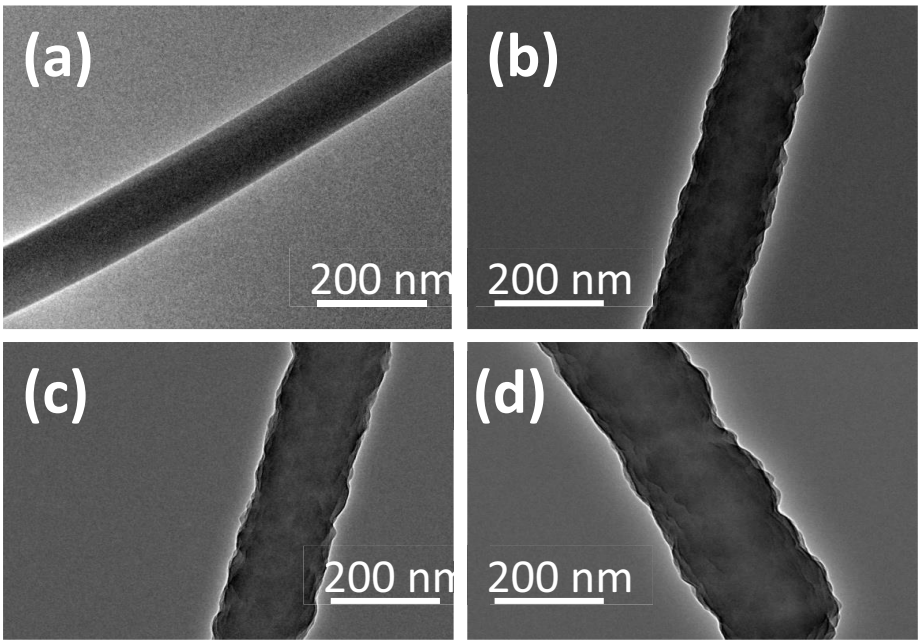

Fig. 2.3. Results of TEM (a) pure PICT nanofiber, (b) 10% PICT/honey& (c) 15% PICT/honey nanofiber (d) 20% PICT/honey nanofiber

2.3.2. Tensile Strength

The tensile strength of PICT/honey nanofibers was investigated for the mechanical behavior of the nanofibers, we prepared five specimens for each category of the samples where the initial length and width was kept at 26 mm and 2.8 mm respectively but the thickness for the samples was not the same. The stress and strain were calculated according to the following formula A and formula B respectively.

$$S(MPa) = \frac{\text{all average values of load(N)}}{\text{area (m2)}} \qquad A$$

$$\boldsymbol{S}(\%) = \frac{\text{change in length}(\Delta \text{l})}{\text{initial length(l)}} \times 100 \qquad B$$

The Fig. 2.4 showed the elastic and plastic behavior of the PICT/honey nanofibers. The nanofibers without honey showed has high young modulus up to 6 MPa along with 9% elongation, But the blended PICT/honey nanofibers with increased amount of honey were observed under tensile test, an increase in percentage of elongation was observed but the tensile strength was decreased with young modulus because of concentration of honey was increased. 90:10 PICT/honey nanofibers has the low strength than pure nanofibers, It has 3 MPa and showed more elongation up upto 39%. Similarly, 85:15 PICT/honey nanofibers has the good strength but less than neat PICT and 90:10 PICT/honey nanofibers, which has 2.7 MPa strength and showed highest elongations (45%) than neat PICT, 90:10 PICT/honey nanofibers and 80:20 PICT/honey nanofibers, but 80:20 PICT/honey nanofibers has lowest strength than 90:10, 85:15 and neat PICT nanofibers; it has 0.7 MPa strength and showed 37% elongation which is good elastic behavior. So PICT/honey nanofibers having 15% concentration of honey are suitable for good elastic behavior and for tensile strength as compared to other concentrations.

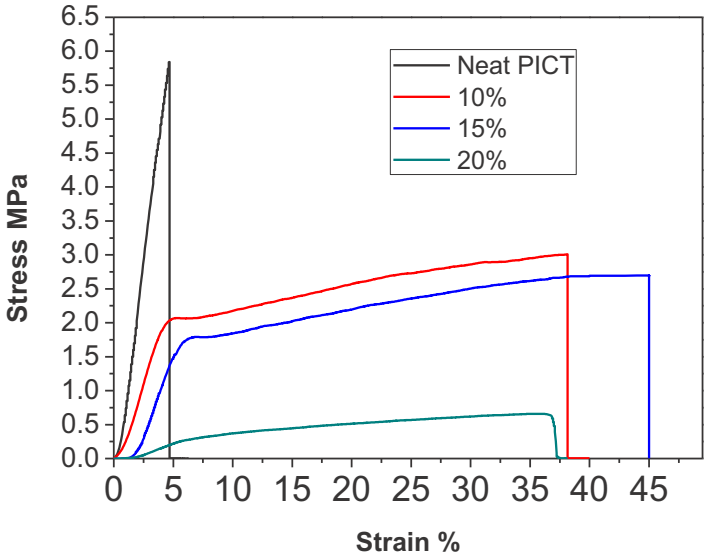

Fig. 2.4. Stress Strain curve of PICT/honey Nanofibers

2.3.3. FT-IR study

Pure PICT nanofibers, PICT/honey nanofibers embedded with 10% and 20% honey were investigated under FT-IR Spectroscopy. Fig. 2.5 showed the successful reaction of PICT with honey as it can be observed that in neat PICT there are aromatic strong stretching at 1600 cm^{-1}, C=C stretching at 1680 cm^{-1} and C-O stretching at 1050 cm^{-1}. After bending of honey with PICT there is significant interactions between PICT and

honey which showed the bonding of O, C and H at 1270 cm^{-1}& 1850 cm^{-1} C-O stretching and C-H bending respectively. So, FT-IR confirmed the presence of honey in PICT/honey nanofibers.

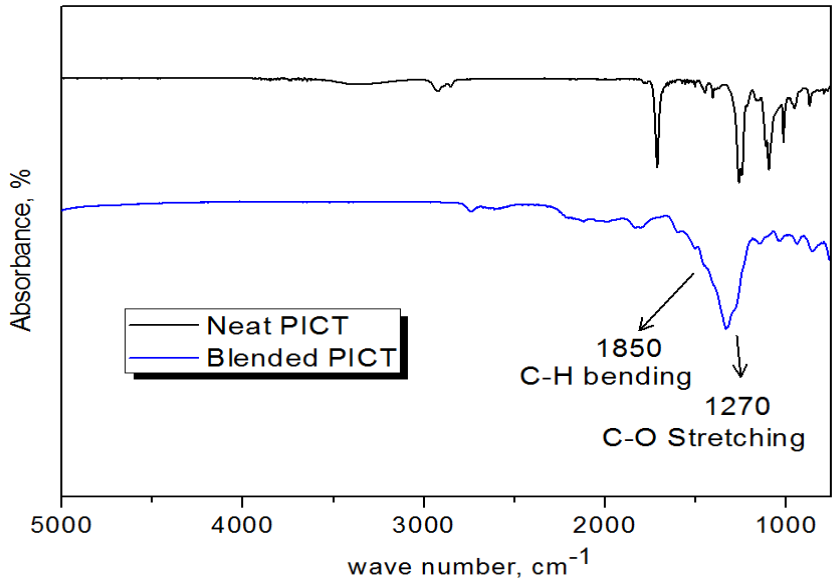

Fig. 2.5. FT-IR spectra of PICT/honey Nanofibers

2.3.4. Release behavior of honey

UV visible Spectrophotometer was used to investigate the releasing behavior of honey. It was observed that releasing efficiency was good. Honey was started to release within the 3 min. and showed maximum releasing behavior in 10 min. and gradually increased up to 10 minutes. The maximum release of honey was 56% (72 mg/L) and minimum was 4% (8 mg/L) in the range of weaves length 250-325 nm as shown in Fig. 2.6b.

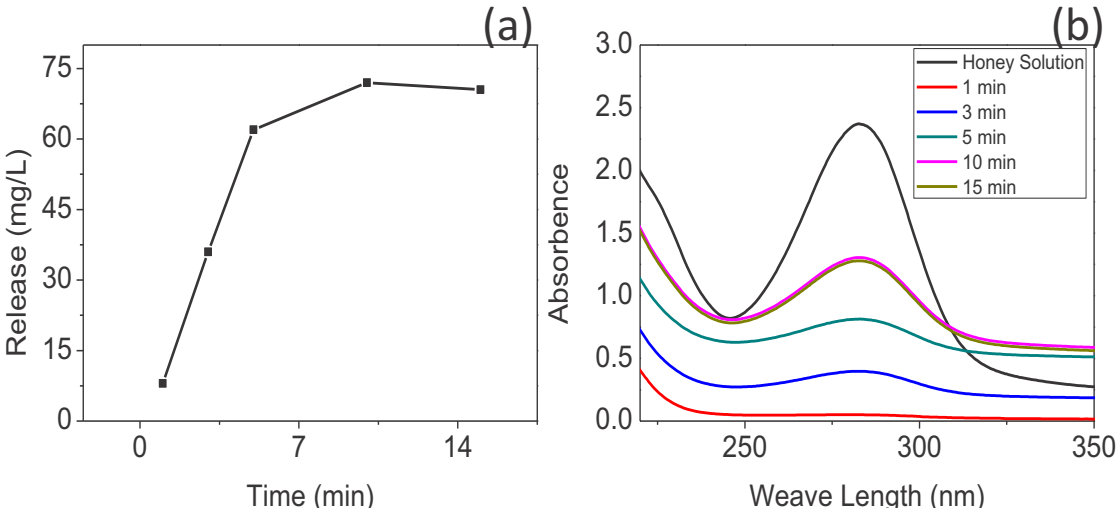

Fig. 2.6. Release behavior of honey

2.3.5. Water contact angle measurements

The wetting behavior of PICT/honey nanofibers was investigated by measuring the static angle with a contact angle meter by drop method. It was analyzed that neat PICT nanofibers is hydrophobic with contact angle 135° as mentioned all images of water droplet on the surface of electrospun PICT & PICT/honey nanofibers in Figure 2.7. When the concentration of honey was increased the hydrophobicity was decreased. At 20% of honey in PICT/honey nanofibers the hydrophilic property was increased.

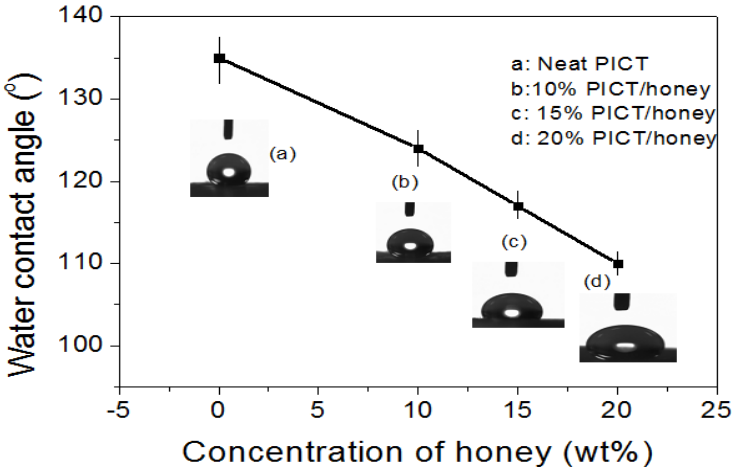

Fig. 2.7. Images of water droplet on PICT/honey nanofibers (a) neat PICT, (b) 10% PICT/honey (c) 15% PICT/honey (a) 20% PICT/honey

2.3.6. X-ray photoelectron spectroscopy (XPS)

XPS spectra were recorded to study the formation of carbon, oxygen and nitrogen functional groups in PICT/honey nanofibers. As expected, PICT/honey nanofibers strated an N1s peak, O1s peak and C1s peak at binding energy of 398, 533 and 285 eV respectively as shown in Figure 2.8 and there is no N1s peak in neat PICT nanofibers.

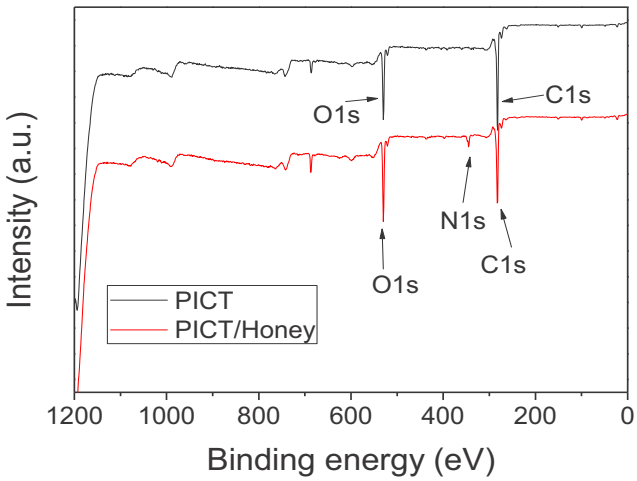

Fig. 2.8. XPS spectra of PICT & PICT/honey nanofibers

2.4. Conclusion

Here in, PICT/honey nanofibers were successfully fabricated by electrospinning. The elastic behavior of PICT/honey nanofibers was improved by increasing concentration of honey in the polymer solution but this increase in concentration was also the cause of decrease in young's modulus. The morphology of PICT/honey nanofibers observed was rough on the surface. Moreover, increasing concentration of honey in the polymer solution was the reason of more diameter distributions of PICT/honey nanofibers. Polymer solution containing 20% of the honey was maximum percentage to obtain bead free PICT/honey nanofibers. Water contact angle measurements were done with the static contact angle by a contact angle meter, which showed that hydrophobacity was decreased by adding the honey. The XPS spectra showed that honey was present in the PICT/honey nanofibers. The release of honey was complete in 15 minutes and the maximum release of honey was 72 mg/L in 10 minutes. Therefore, PICT/honey nanofibers containing 15% of honey are more suitable for good elastic behavior and tensile strength as compared to other concentrations of honey used in the polymer solution.

References

1. Cha, Kim, et al. Biopolymers 101, (2014) 307.
2. Jian, Yan, et al., ACS Sustainable Chemistry & Engineering, (2017).
3. Hu, Jue, et al., Materials Science and Engineering: C 70 (2017): 1089-1094.
4. Kai, Dan, et al., Colloids and Surfaces B: Biointerfaces 148 (2016): 557-565.
5. Kai, Dan, et al., ACS Sustainable Chemistry & Engineering 4.10 (2016): 5268-5276.
6. Sun, Yuqiao, et al., Biomedical Materials 12.1 (2016): 015007.
7. Kai, Dan, et al., Journal of Materials Chemistry B 3.30 (2015): 6194-6204.
8. Lakshminarayanan, Rajamani, et al., International journal of nanomedicine 9 (2014): 2439.
9. Kai, Dan, Sing Shy Liow, and Xian Jun Loh. Materials Science and Engineering: C 45 (2014): 659-670.
10. Loh, Xian Jun, et al., Journal of Controlled Release 143.2 (2010): 175-182.
11. M. Muneeswaram, I.S. Kim and N. V. Giridharan, Applied Phys. A 114, (2014) 853.
12. H. Bang, M. Gopiraman and I. S. Kim, RSC Adv. 103, (2014) 59571.

13. K. Wei and I. S. Kim, Handbook of Applications of Nanofibers in super capacitors, Springer, (2014) p.163.
14. N. Kimura, T. Sakumoto, Y. Mori and I. S. Kim, Composites Sci. and Technol. 92, (2014) 120.
15. Z. Khatri, F. Ahmed and I. S. Kim, Material Letters 71, (2016) 178.
16. Kwak, I. S. Kim et al., I.J. Biological Macromoleules 63, (2014) 198.
17. Abdelgawad, S. M. Hudson and O. J. Rojas, Carbohydrate Polymers 100, (2014) 166.
18. Gagandeep, T. Garg, and A. K. Goyal, Euro. J. Pharmaceutical Sci. 53, (2014) 10.
19. K. Kim, L. Jeong, H. Park and C. Chung, J. Biotechnol. 120, (2005) 327.
20. Prabhakaran, P. Molamma and Seeram, J. Nanosci. and Nanotechnol. 11, (2011) 3039.
21. Y. Dzenis, Science 304, (2004) 1917.
22. H. Lee, I. S. Kim and S.Soon Im, RSC Advance 6, (2016) 40383.
23. T. Wang, X. Xue and D. Wu, Carbohydrate Polymers 88, (2012) 75.
24. Y. Qin, Medical Textile Materials, Wood head publishing, 174(2016).
25. A. Arslan, N.M. Kazaroglu and G. Menemse, J. Biomaterial Sci. Polymer Edition 999, (2014) 25.
26. H. Maleki, A. A. Gharehaghaji and P.J. Dijkstra, J. Applied Polymer Sci. 4086, 127(2013).

Chapter # 03

Self-cleaning effect of electrospun poly (1, 4-cyclohexanedimethylene isosorbide terephthalate) nanofibers embedded with ZnO nanoparticles

3.1. Introduction

Over the past decade, the sustainable conversion of biomass to specific chemicals has been an active research area in academia and industry. Due to the high stability of isosorbide (a biomass material) at 256 ^{o}C and its compatibility with different polymers, it has become a significant chemical platform for further chemical modifications [1-4]. Recently, a terephthalate-based polymer, i.e., poly (1, 4-cyclohexanedimethylene isosorbide terephthalate) (PICT), was synthesized using isosorbide, and this new polymer has various significant properties, including its aromaticity, its semi-crystalline structure, thermal stability, and biodegradability [5-7]. To date, PICT has been used in various industrial applications, such as baby bottles, electrical outlets, and dishware suitable for cleaning in dishwashers [7, 8]. However, until now, there have been no studies of the nanofibers made from this new polymer. Based on their unique properties, this polymer has great potential for use in the textile industry, so we made the first attempt to fabricate PICT nanofibers using the electrospinning process. Electrospinning is a useful technique for fabricating nanofibers [9, 10] for various functional applications [11], such as protection from exposure to UV light [12], as an anti-microbial product [13], as a flame retardant [14], to enhance the shape-memory behavior of apparel [15], and self-cleaning [16]. Especially, various approaches have been suggested to introduce the self-cleaning property to nanofibers [17]. Since ZnO is a promising material for introducing the self-cleaning property to composite materials, it is of great interest to researchers who want to make self-cleaning materials [18]. It is non-toxic and could be used extensively in industry due to its low cost. In addition, it provides better efficiency in photo-catalytic applications than other chemicals (e.g., TiO_2 and WO_3) due to its large energy gap (3.37 eV) and its large excitation binding energy (60 meV) [19, 20]. Chutima S, et. al. demonstrated the silver decorated TiO_2 nanofibers with different concentration of silver. [17] They demonstrated the degradation efficiency of methylene blue with prepared nanofiber. The maximum value of degradation was 77% and the minimum value was 22% within 2hrs.

Herein, we report a novel ZnO/PICT nanofiber via electrospinning, and we investigated the effect of different ZnO concentrations on the nanofiber's self-cleaning properties. The resultant nanofibers were characterized by Fourier Transform Infrared Spectroscopy (FT-IR) to determine their chemical composition, and a

scanning electron microscope (SEM) was used to investigate their surface morphology. Also, transmission electron microscopy (TEM) was used to investigate the dispersion of the nanoparticles, and their photo-catalytic activity was determined to assess their self-cleaning properties. It was observed that the ZnO nanoparticles were well-located along the nanofibers, and they provided a high photodegradable property as their concentration was increased. Since this was the first attempt to fabricate ZnO/PICT nanofibers, it is our opinion that these nanofibers provide a significant opportunity for extending their applications in various areas, including their use in home textile products and eliminating stains in non-woven or non-washable products, such as surgical gowns, wound dressings, pillows, and curtains. Thus, we believe this new product has great potential for extensive use in the textile industry.

3.2. Experimental

3.2.1. Materials

Pellet-type PICT was supplied by SK chemicals, Republic of Korea. Trifluoroacetic acid (99.9%), chloroform (99%), ZnO nanoparticles (50.1 wt%), and methylene blue (powder form, solubility of 1 mg/ml) were purchased from Sigma-Aldrich (USA).

3.2.2. Preparation of nanofibers

PICT was dissolved in trifluoroacetic acid and chloroform (volumetric ratio of 1:3). ZnO was blended in the solution of PICT in different concentrations, i.e., 0, 3, 5, 7, and 9%, but the concentration of PICT was constant at 10% by weight. The nanofibers were formed at room temperature at 45% humidity using an electrospinning machine. The solution was loaded in a plastic syringe connected with capillary tips that had an inner diameter of 0.60 mm, in which an electrode of Cu wire was adjusted. The distance from tip of the capillary to the collector was 15 cm, the flow rate was 0.75 ml/hr, and the supply voltage was 10 kV.

3.2.3. Characterization

The morphology of the nanofibers was evaluated by SEM (JSM-5300, JEOL Ltd., Japan) and TEM (JEM-2100, JEOL Ltd., Japan). The average diameter and distribution of the nanofibers were measured from the SEM micrographs using image analysis software (Image J, version 1.49). To obtain an average value for the diameter, 50 points were selected randomly in a single SEM image. The photo-catalytic activity was investigated in two ways. The first way was to determine the photo-catalytic property of pure PICT nanofibers and 9 wt% ZnO/PICT nanofibers by changing the irradiation time. The second way was to investigate the

effect of different concentrations of the ZnO-embedded PICT nanofibers during irradiation with sunlight for 3 hr. For the first way, a solar simulator (XES-40S3, San-ei Electric, Japan) was used to simulate sunlight, and it had an intensity of 1000 W/m^2 with a wavelength range of 350 - 1100 nm. For the two ways mentioned above, FT-IR spectra were acquired using an IR Prestige-21 instrument (Shimadzu, Japan). The spectra were recorded from 400 to 4000 cm^{-1} with a resolution of 4 cm^{-1} and the addition of 128 scans. The degradation value was obtained by the following equation:

$$\text{Degradation } (\%) = (I_i - I_d)/(I_i) \times 100$$

where I_i and I_d are the peak intensity of the initial, dyed nanofiber and the degraded dyed nanofiber, respectively, extracted at 1275 cm^{-1} in the FT-IR spectrum.

3.3. Results and discussion

3.3.1. Morphology of the nanofibers

SEM images were acquired and average fiber diameters of PICT and ZnO/PICT were determined in order to study the average fiber diameters when different concentrations of ZnO were loaded into the PICT nanofibers. Figure 3.1(f) shows the average diameters of the ZnO/PICT nanofibers with different concentrations of ZnO. The average diameters were not changed significantly as the ZnO concentration was increased, and all of the nanofibers had an average diameter of ~500 nm. This result implied that the concentration of ZnO did not affect the diameters of the diameters of the PICT nanofibers.

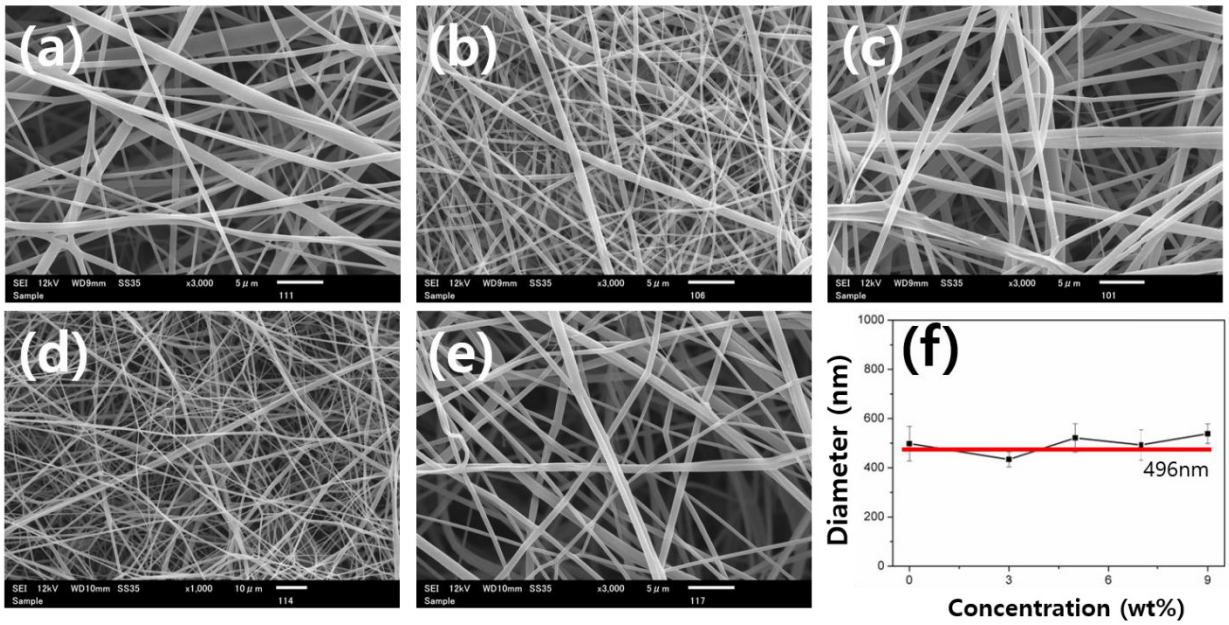

Figure 3.1. (a) Neat PICT nanofibers; (b) 3 wt% of ZnO in PICT nanofibers; (c) 5 wt% of ZnO in PICT nanofibers; (d) 7 wt% of ZnO in PICT nanofibers; (e) 9 wt % of ZnO in PICT nanofibers; (f) graph of average diameter versus concentrations.

To investigate the dispersion of ZnO into the PICT nanofibers, TEM images were taken for ZnO/PICT. Figure 3.2 shows that the ZnO particles were incorporated along the axes of the nanofibers, and the amount of ZnO particles increased as the ZnO concentration increased. Interestingly, for the low concentrations of ZnO (3 and 5 wt%), almost no ZnO particles were imbedded in the PICT nanofibers, resulting in fewer ZnO particles being observed on the surfaces of the nanofibers. It was clearly observed that most of the ZnO particles were attached to the surfaces of the nanofibers in the samples of ZnO that had relatively high concentrations (7 and 9 wt%). Considering that the degradation reaction occurred on the surfaces of the ZnO particles, it is reasonable that 9 wt% of ZnO/PICT nanofibers would have a higher degradation efficiency than the other samples.

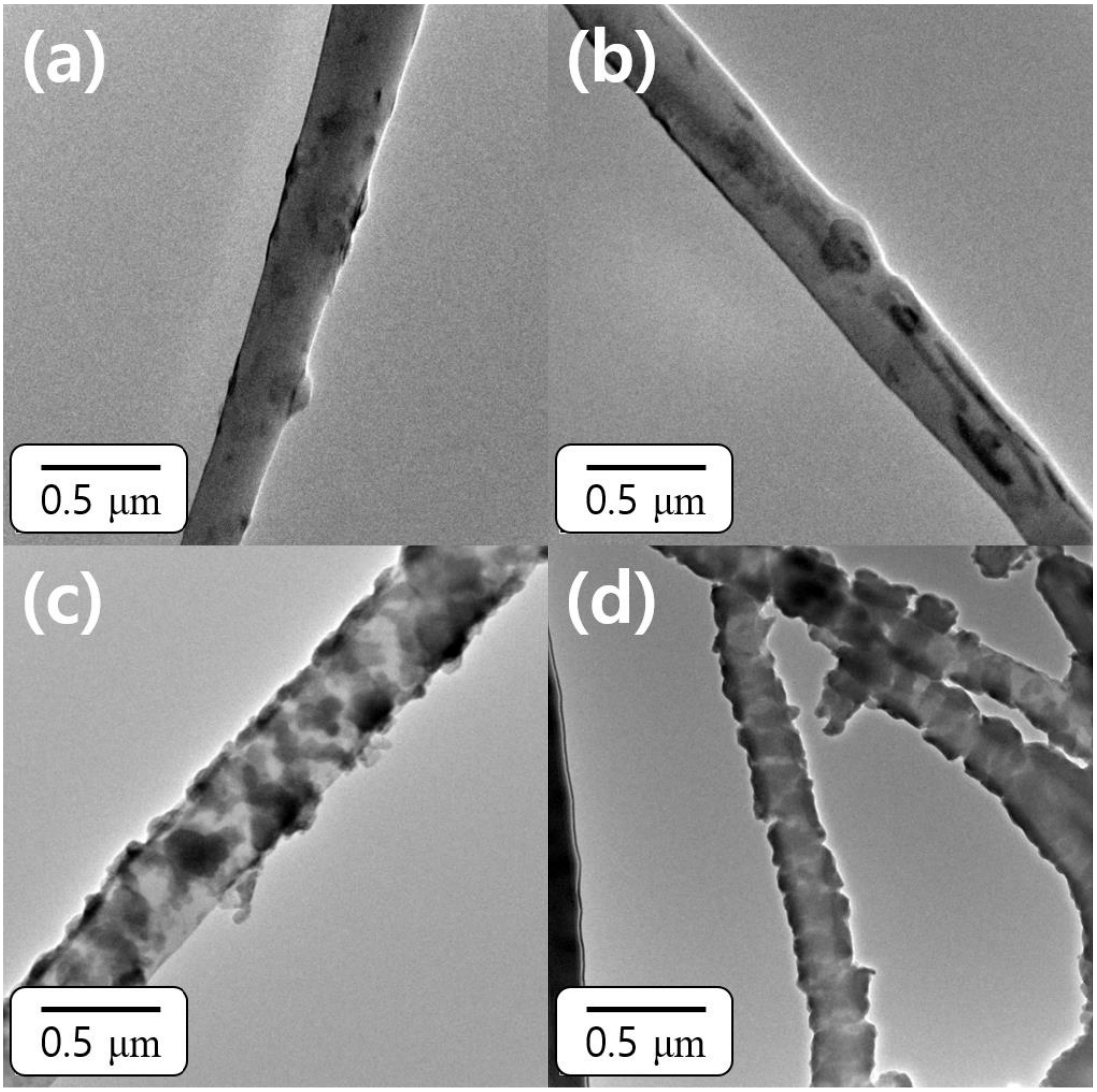

Figure 3.2. TEM results: (a) 3 wt% of ZnO particle in PICT nanofibers; (b) 5 wt% of ZnO particle in PICT nanofibers; (c) 7 wt% of ZnO particle in PICT nanofibers; (d) 9 wt% of ZnO particle in PICT nanofibers.

3.3.2. Photo-catalytic activity

A photo-catalyst absorbs UV light and then converts H_2O into hydroxyl radicals (OH^-), which have the ability to degrade the contaminant to small molecules and finally into CO_2 and H_2O [21, 22]. Two microliters of methylene blue were dropped onto each sample to evaluate the self-cleaning performance. The photo-catalytic activity was designed in two ways. First, the methylene blue was applied to pure and 9 wt% ZnO/PICT nanofibers for different times and the results are shown in Figure 3.3(a). The self-cleaning properties of those nanofibers were observed by the naked eye. The degradation result of photo-catalytic activity of the 9 wt% ZnO/PICT, as shown in Figure 3.3(c), was changed from 50% to 80% to 90% after 1, 2, and 3 hrs, respectively. In the second approach, the photo-catalytic activity was investigated using different concentrations of ZnO-embedded PICT nanofibers for a constant time (3 hours), and the results shown in

Fig. 3.4(b) indicate 40, 70, 90, and 99% of self-cleaning occurred when 3, 5, 7, and 9 wt% of ZnO were used, respectively. The photo-catalytic activity of the ZnO/PICT nanofibers depended on the concentration and time. In order to investigate the interactions of methylene blue with ZnO, FT-IR spectra were obtained for pure PICT and ZnO/PICT nanofibers (Figure. 3.3(b) and Figure 3.4(a)). The FT-IR spectrum of the pure nanofiber had no characteristic peak, but the FT-IR spectrum of the dyed nanofiber showed characteristic peaks at 1250 and 1275 cm^{-1} from methylene blue due to the stretching of N-H and C-N, respectively. The dyed nanofiber showed a high intensity of methylene blue, which decreased when the photo-catalytic activity increased as exposure time increased (Figure 3.3(b)). The photo-catalytic activity of the PICT nanofibers embedded with different concentrations of ZnO indicated that the intensity was inversely proportional to the concentration of ZnO (Figure 3.4(a)), and, at 9 wt% ZnO, there was a very low intensity of methylene blue in the nanofibers.

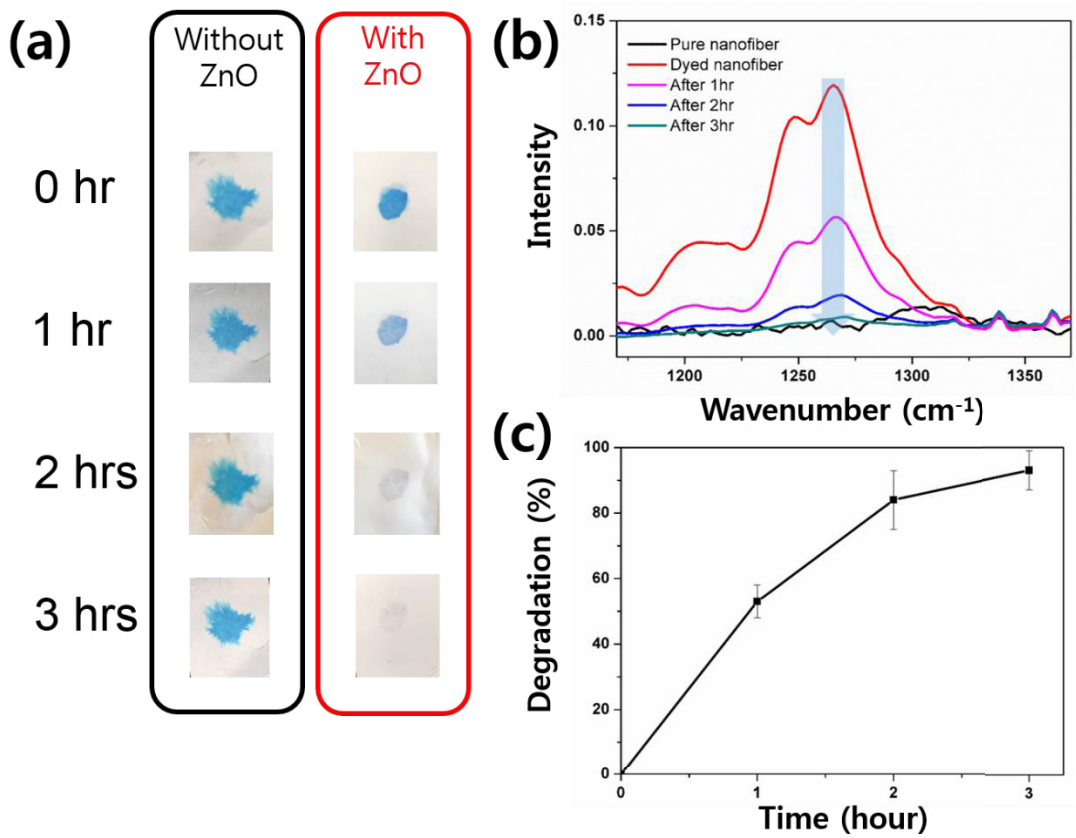

Figure 3.3. For different time intervals: (a) photo-catalytic activity; (b) FT-IR spectrum of dyed nanofiber; (c) degradation rate extracted from FT-IR spectrum.

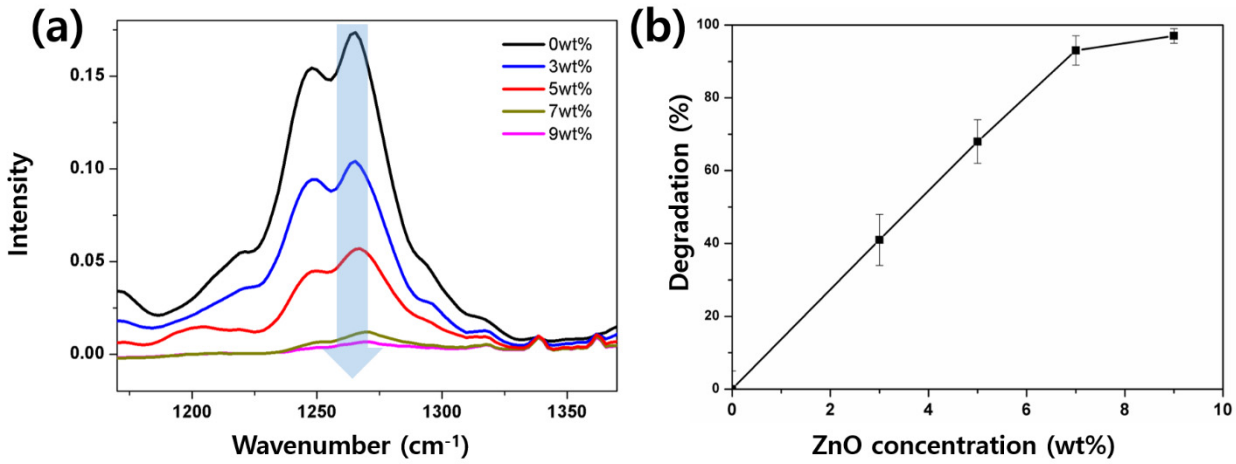

Figure 3.4. Photocatalytic activity of ZnO/PICT nanofibers at different concentrations of ZnO within 3 hrs: (a) FT of nanofibers; (b) degradation graph

3.4. Conclusions

We successfully fabricated ZnO/PICT nanofibers by the electrospinning technique. The electrospun nanofibers demonstrated efficient self-cleaning activity. The TEM results clearly showed that the uniformity in the dispersion of the ZnO nanoparticles on the PICT nanofibers was increased as the concentration increased. The photo-catalytic activity of 9 wt% ZnO/PICT nanofibers had about 50% efficiency within 1 hr, and it increased gradually to around 99% within 3 hrs, while, at 3 wt%, the ZnO/PICT had 40% self-cleaning efficiency in the same time. Based on these results, it was apparent that the higher concentration of ZnO provided a more effective self-cleaning performance, and the contamination was fully degraded and removed within3 hrs. The results of this innovative research should be very useful in developing intelligent textile products that self-eliminate stains. These results should be helpful in academic and industrial applications in that they can help textile researchers and manufacturers to meet the stated and implied needs of customers.

References

1. Lee H, Sohn D, Kim IS, et al. High thermal stability and high tensile strength terpolyester nanofibers containing biobased monomer: fabrication and characterization, *RSC Advances.* 2016; 6: 40383-40388.
2. Thombal RS and Jadhav VH, Application of glucose derived magnetic solid acid for etherification of 5-HMF, dehydration of sorbitol to isosorbide and fatty acid. *Tetrahedron Letters.* 2016; 57: 4398-4400.
3. Yamaguchi A, Muramatsu N, Mimura N, et al. Intermolecular dehydration of biomass-derived sugar alcohols in high temperature water, *Physical Chemistry Chemical Physics.* 2016; 11: 2421-2432.
4. Chatti S, Weindner SM, Fildier A, et al. Copolyester of isosorbide, succinic acid and isophthalic acid, *Polymer Sciences Part A: Polymer Chemistry* 2013; 511: 2464-2471.

5. Naves AF, Fernandes HT, Immich AP, et al. Enzymatic synthesis of unsaturated polyesters based on isosorbide, *Polymer Science, Part A: Polymer Chemistry* 2013; 51: 3881-3891.
6. Krcheldorf HR, Mix R and Weinder SM. Poly (ester urethane) derived from lactide, isosorbide, terephthalic acid, *Polymer Science, part A: Polymer Chemistry* 2014; 52: 867-875.
7. Koo JM, Hwang SY, Yoon WJ, et al. Structural and thermal properties of PCT containing isosorbide, *Polymer Chemistry* 2015; 6: 6973-6986.
8. Visakh PM and Liang M, Poly (Ethylene Terephthalate) Based Blends, Composites and Nanocomposites, Oxford: Elsevier, 2015, p.127.
9. Ali S, Khatri Z, Kim IS, et al. Preparation & characterization of hybrid polycaprolactone /cellulose ultrafine fiber via electrospinning, *Macromolecular Research* 2014; 22: 562-568.
10. Khatri Z, Jatoi AW, Kim IS, et al. Cell adhesion behavior of poly(caprolactone) /poly(L-lactic acid) nanofiber scaffold, *Material Letters* 2016; 71: 178-181.
11. Brown PJ and Stevens K, Nanofibers and Nano-technology in Textiles, 1st ed. Cambridge: Woodhead Publishing Ltd., 2007, p.11.
12. Khatri Z, Ali S, Khatri I, Kim IS, et al. UV responsive PVA- nanofibers, *Applied Surface Science* 2015; 342: 64-68.
13. Son WK, Youk JH and Park WH. Antimicrobial cellulose acetate nanofibers containing Ag-nanoparticles, *Carbohydrates Polymers* 2006; 65: 430-434.
14. Wu Z, Li C, Liang HW, et al. Ultralight, flexible and fire-resistant carbon nanaofiber, Angewandte Chemie International Edtion 2013; 125: 2997-3001.
15. Lee Y, Devarayan K, Kim IS, et al. Annealing effects on mechanical properties and shape memory behavior of silicone-coated elastomeric polycaprolatone nanofiber filaments, *Material Letters* 2014;131: 128-131.
16. Yuranova T, Mosteo R, Bandara J, et al. Self-cleaning cotton textiles surfaces modified by photoactive SiO2/TiO2 coating, J.Mol.Catal. A. Chem., 2006; 244, 160-167.
17. Chutima S, Voraluck P and Narupol I. The potential use of nanosilver-decorated titanium dioxide nanofibers for toxin decomposition with antimicrobial and self-cleaning properties, Applied Surf. Sci., 2011; 257, 8850-8856.

18. Hadi F, Shojaie AF and Zanjanchi MA. Photocatalytic self-cleaning properties of cellulosic fibers modified by nano-sized ZnO, *Thin Solid Films* 2011; 519: 3641-3646.
19. Siti RS, Norsuria M, Mohd M, et al. Self- cleaning technology in fabric: a review, *Material Science and Engineering* 2016; 133:1-9.
20. Zhu C, Shi J, Ishimori M, et al. Design and characterization of self-cleaning cotton fabrics exploiting zinc oxide nanoparticle-triggered photo-catalytic degradation, *Cellulose* 2017;24: 2657-2667.
21. Guan K. Relationship between photocatalytic activity, hydrophilicity and self-cleaning effect of TiO_2/SiO_2 films, *Surface and Coating Technology* 2005; 191: 155-160.

Chapter # 04

Self-Cleaning properties of electrospun PVA/TiO_2 and PVA/ZnO nanofibers composites

4.1. Introduction

In recent times nanofibres have been researched and studied widely because of their unique properties and applications [1]. Particularly, their high surface areas to volume ratio, large length to diameter ratio, and light weightiness have made them suitable for a number of applications [2]. They are widely used for filtration, drug delivery [3], tissue engineering, and sensors application in protective clothing for protection against biological and chemical hazards, food processing, and in microelectronics [4,5]. A number of methods for the production of nanofibers are being used, such as self-assembly, drawing, phase separation, and electrospinning [2]. Among these techniques electorspinning is more versatile due to its simple assembly and ease of production of continuous fibers [1,6].

There are a number of ways through which a self-cleaning property can be imparted to nanofibers [7]. Generally, in macro materials two basic methods that are used to develop self-cleaning surfaces are complete hydophobization or hydrophilization of a surface. In the case of hydrophobic surfaces, water takes away the dust particles and containments that are on the material surface, which has no adhesion because of a reduced wet ability also known as the lotus leaf effect [8–9]. While in case of hydrophilic surfaces developed by coating with semiconducting metal oxides dust, grease and organic containments decompose on exposure to light and are easily taken away by water or rain [10–12]. Use of photo-catalytic metallic oxides to develop hydrophilic self-cleaning surfaces is well known. When a photo-catalytic surface is exposed to light of suitable energy it causes the transition of the electrons from the valence band to the conduction band, leaving behind a hole that can react with water to produce hydroxyl radical. Both the hole and hydroxyl radical have very high oxidative power and can destroy organic matters and air pollutants [11].

To develop a nanofiber based photo-catalytic self-cleaning surface nanocomposite is the best option. Polymeric nanocomposites are unique structures that combine the properties of polymers and filler materials and provide improved properties compared to virgin materials [13]. TiO_2 and ZnO photo-catalysts are being widely used in a number of applications to remove environmental pollutants because of their excellent photo catalytic efficiency and non-toxicity [14,15]. TiO_2 coated on carbon nanotubes can be used to remove environmental pollutants and to kill microorganisms [16]. ZnO nano particles embedded poly (1,4-

cyclohexanedimethylene isosorbide terephthalate) fibers show excellent self-cleaning property [17]. If two exciting photo-catalysts, TiO_2 and ZnO, are embedded in a suitable polymer solution, then the resultant composite can effectively be used in a number of applications to destroy organic pollutants. In the literature no work is reported regarding the self-cleaning behavior of ZnO and TiO_2 embedded electrospun PVA nanofibers.

Therefore, in this work we have intended to explore the self-cleaning properties of ZnO and TiO_2 embedded PVA nanofibers. The use of the economical polymer, PVA, as a base material to develop TiO_2-PVA and ZnO-PVA nano-composites makes them particularly useful for commercial applications. The resultant nanofibers were characterized by Fourier-Transform Infrared Spectroscope (FT-IR). For the sake of chemical investigation, scanning electron microscope (SEM) was done to investigate the surface morphology, transmission electron microscope (TEM) was done to investigate the dispersion of nanoparticles, and photo-catalytic activity was done to check the self-cleaning properties of the nanofibers.

4. 2. Materials and Methods

4. 2.1. Materials

ZnO and TiO_2 nanoparticles (NPs) were purchased from the Sigma-Aldrich Corporation (Louis, Missouri, USA), with a dispersion concentration of 50.1 wt% and the size of particles was 50 nm. Methylene blue (powder form, soluble 4 mg/4 mL, was purchased from the Sigma-Aldrich Corporation (Louis, Missouri USA). Poly vinyl alcohol (MW: 85,000–124,000, 87–89% hydrolyzed) was purchased from the Sigma-Aldrich Corporation (Louis, Missouri, USA). Glutaraldehyde (GA, 50% in aqueous solution) was purchased from MP Biomedical (Tokyo, Japan).

4.2.2. Method

PVA 10% by weight was dissolved in de-ionized H_2O at 60 °C and stirred for 12 h. Glutaraldehyde was added in the solution at 2.5 wt% for cross-linking of the solution. Nanoaprticle suspensions of ZnO & TiO_2 were separately embedded in that PVA solution to fabricate the PVA/ZnO and PVA/TiO_2 nanofibers. For the fabrication of PVA/ZnO nanofibers three different concentrations; 5 wt%, 7 wt% and 9 wt% of ZnO nanoparticles were blended with PVA solution by stirring for 5 h and similarly to fabricate the PVA/TiO_2 nanofibers, TiO_2 nanoparticles in three different concentrations, 5 wt%, 7 wt%, and 9 wt%, were blended

with PVA solution by stirring for 5 h. The electrospinning of PVA/ZnO and PVA/TiO_2 solutions was done as the solution was loaded in the plastic syringe with an inner diameter of 0.60 mm, in which a Cu electrode was adjusted. The distance from capillary tip to collector was 15 cm and the supply of voltage was 12 kV. The PVA, PVA/ZnO, and PVA/TiO_2 nanofibers were formed without beads at room temperature and at 45% humidity. The resultant nanofibers were cross linked to form nanofibers that are water resistant yet can absorb water but are not soluble in water. The illustration scheme of cross-linking is shown in Figure 4.1. The hydrochloric acid (HCL) foaming of PVA/ZnO/GA & PVA/TiO_2/GA was done at 30 °C for 60 s. In this reaction, GA and HCl acted as a chemical cross-linking agent and a catalyst, respectively. To enhance the crystalline structure and for stable cross-linking, the PVA/ZnO nanofibers were kept at −20 °C for 3 h, which was followed by thawing at 15 °C for 3 h. This process was repeated three times and the resultant nanofibers were dried at room temperature for 24 h, and then estimated.

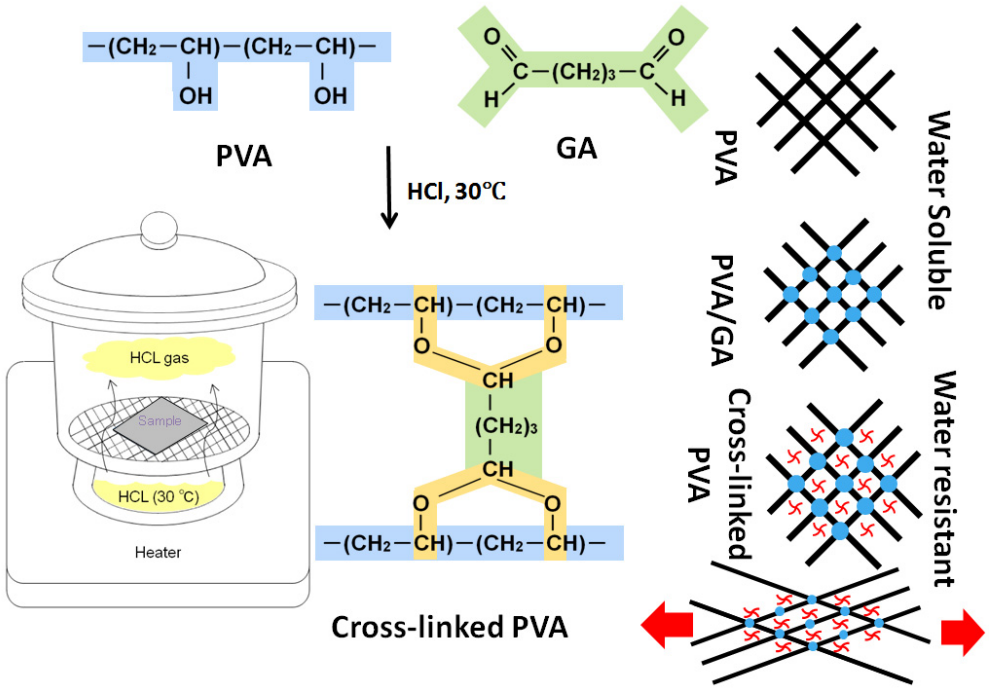

Figure 4.1. Illustration scheme of cross-linking nanofibers.

Figure 4.1. Illustration scheme of cross-linking nanofibers.

4.2.3. Characterizations

The morphology of the PVA, PVA/ZnO, and PVA/TiO_2 nanofibers was investigated by scan electron microscopy (SEM) (JSM-5300, JEOL Ltd., Tokyo, Japan) accelerated with voltage of 12 kV and

transmission electron microscopy (TEM) (JSM-5300, JEOL Ltd., Tokyo, Japan) accelerated with 200 kV. The chemical interactions were studied by FT-IR (IR Prestige-21 by shinmadzu, Nagano, Japan), Wide angle X-ray diffractions (WAXD) spectra were performed for the evaluation of the crystal structure at 25 °C with nanofiber samples using a Rotaflex RT300 mA (Rigaku manufacturer, Osaka, Japan) and Nickel-filtered Cu. Ka radiation was used for measurements, along with an angular angle of $5 \leq 2\,\theta \leq 50°$. Photo-catalytic activity was done by a solar simulator (XES-40S3, San-ei Electric, Nagano, Japan), stress-strain behavior was studied by a tensile strength tester (Universal Testing Machine, Tenilon RTC 250 A, A &D company Ltd., Tokyo, Japan), water contact angle measurements were done by a contact angle meter (Digidrop, GBX, Whitestone way, France) and photo-catalytic activity was done by a solar simulator (XES-40S3, San-ei Electric, Nagano, Japan). The light intensity was 1000 W/m^2, the wavelength range was 350–1100 nm, and the self-cleaning efficiency was calculated as the following Equation (1).

$$\text{Degradation } (\%) = \frac{\text{Ii} - \text{Id}}{\text{Ii}} \times 100 \quad (1)$$

Thermal degradation of PVA, PVA/ZnO & PVA/TiO_2 was performed by thermogravimetric analysis. This thermogravimetric analysis was performed on the thermo-plus TG 8120 (Rigaku Corporation, Osaka, Japan). It was operating in a static mode under air atmosphere at a heating rate of 10 °C/min and a temperature range of 0–700 °C.

4. 3. Results and Discussion

4.3.1. Morphology of nanofibers

In order to investigate the surface morphology of nanofibers, SEM images were analyzed as mentioned in Figure 4.2. All PVA, PVA/ZnO, and PVA/TiO_2 nanofibers were bead free and PVA/ZnO and PVA/TiO_2 nanofibers showed that the blending of the nanoparticles did not affect the surface morphology of the PVA nanofibers as mentioned in Figure 4.2b–g. It was also analyzed that both ZnO and TiO_2 nanoparticles did not change the surface morphology of the PVA nanofibers. Both nanoparticles affected the size of the nanofibers. When the concentration of nanoparticles was increased, the size of the nanofibers was also increased, as shown in Figure 4.2b–g.

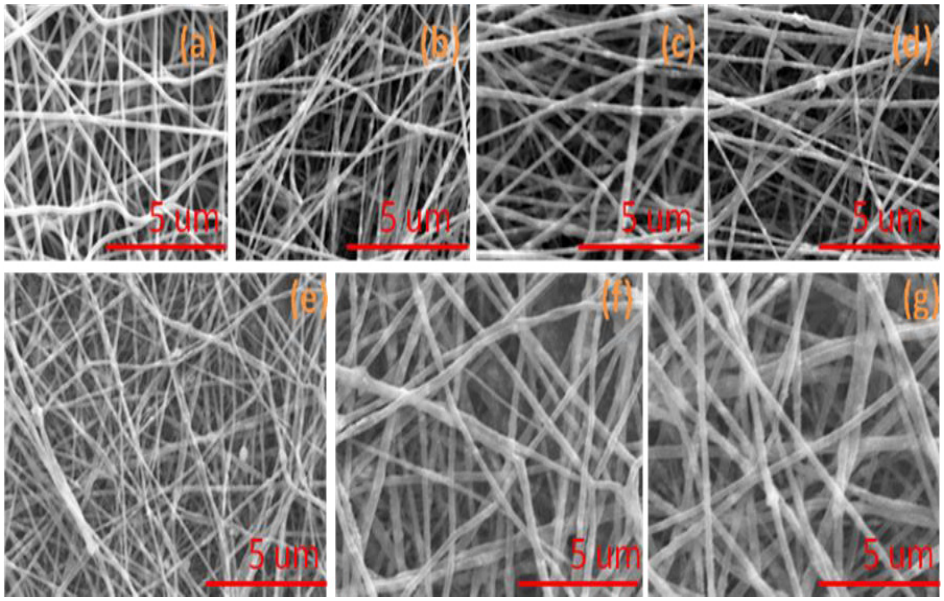

Figure 4.2. Scanning electron microscope (SEM) images of (**a**) Neat PVA nanofibers; (**b**) 5% PVA/ZnO nanofibers; (**c**) 7% PVA/ZnO nanofibers; (**d**) 9% PVA/ZnO nanofibers; (**e**) 5% PVA/TiO_2 nanofibers; (**f**) 7% PVA/TiO_2 nanofibers; (**g**) 9% PVA/TiO_2 nanofibers.

In order to investigate the effect of ZnO & TiO_2 nanoparticles on the average diameter of the PVA nanofibers, distribution graphs were studied, as shown in Figure 4.3. It was analyzed that the average diameter of PVA/ZnO and PVA/TiO_2 was affected by the blending of ZnO & TiO_2 nanoparticles. The average diameter of neat PVA nanofibers was 350 ± 10 nm but the average diameter of PVA/ZnO nanofibers was increased as the concentration of ZnO NPs was increased as mentioned in Figure 4.3b–d; 5%, 7% & 9% PVA/ZnO nanofibers have an average diameter of 380 ± 15, 385 ± 20, and 410 ± 10 nm, respectively. The average diameter of PVA/TiO_2 nanofibers was also increased when the concentration of TiO_2 was increased, as

mentioned in Figure 4.3e–g; 5%, 7% & 9% PVA/TiO_2 nanofibers have an average diameter of 383 ± 05, 390 ± 10 and 418 ± 15 nm, respectively. It showed that PVA/TiO_2 nanofibers have a greater average diameter than the PVA & PVA/ZnO nanofibers. It also means that the TiO_2 NPs have a greater effect on the PVA nanofibers than ZnO NPs.

In order to investigate the dispersion of the ZnO and TiO_2 nanoparticles on the PVA nanofibers, TEM images were analyzed, as shown in Figure 4.4. It was analyzed that there was uniform and well dispersion of both the ZnO and TiO_2 nanoparticles on the PVA nanofibers. TEM images also showed that when the concentrations of nanoparticles were increased, then the diameters of PVA/ZnO and PVA/TiO_2 were also increased. When the concentration of NPs was increased the dispersion of NPs on PVA nanofibers also was increased, as mentioned in Figure 4.4.

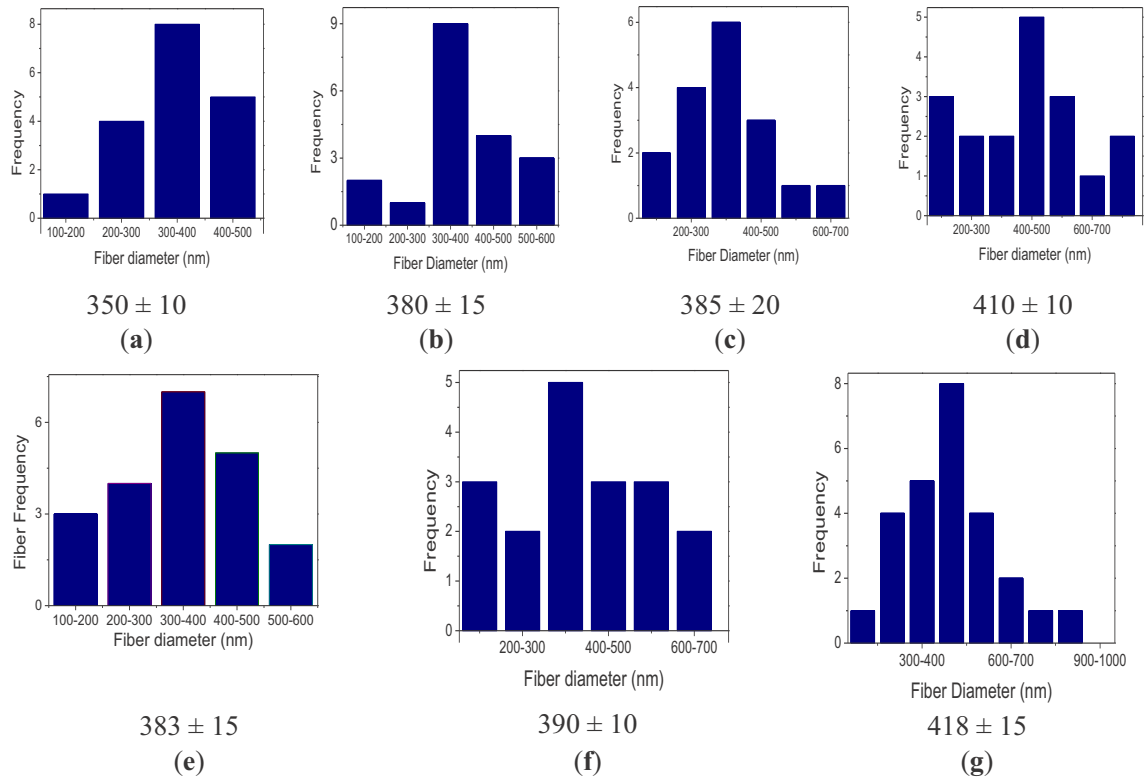

350 ± 10 (**a**) | 380 ± 15 (**b**) | 385 ± 20 (**c**) | 410 ± 10 (**d**)

383 ± 15 (**e**) | 390 ± 10 (**f**) | 418 ± 15 (**g**)

Figure 4.3. Average diameter distributions analysis of (**a**) Neat PVA nanofibers; (**b**) 5% PVA/ZnO nanofibers; (**c**) 7% PVA/ZnO nanofibers; (**d**) 9% PVA/ZnO nanofibers; (**e**) 5% PVA/TiO_2 nanofibers; (**f**) 7% PVA/TiO_2 nanofibers; (**g**) 9% PVA/TiO_2 nanofibers.

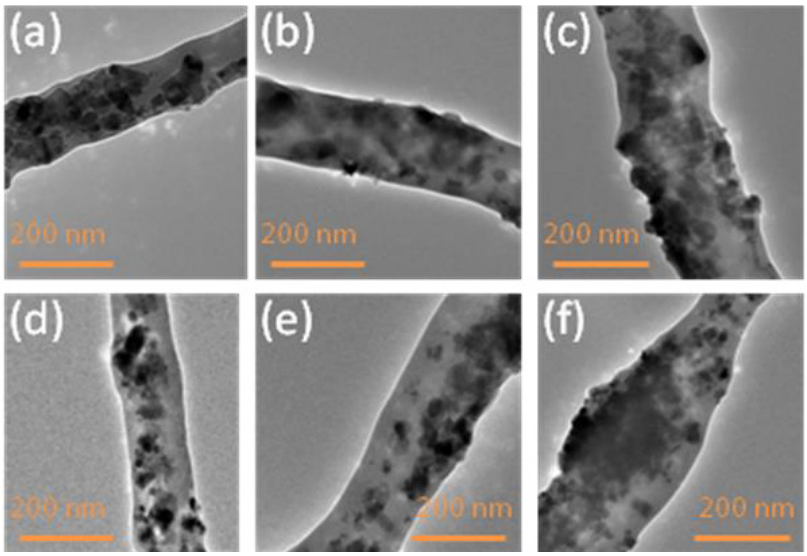

Figure 4. 4. Transmission electron microscope (TEM) analysis of (**a**) 5% PVA/ZnO nanofibers; (**b**) 7% PVA/ZnO nanofibers; (**c**) 9% PVA/ZnO nanofibers; (**d**) 5% PVA/TiO_2 nanofibers; (**e**) 7% PVA/TiO_2 nanofibers; (**f**) 9% PVA/TiO_2 nanofibers.

4.3.2. Chemical structure analysis

In order to investigate the chemical structure analysis of PVA, PVA/ZnO, and PVA/TiO_2 nanofibers, ATR-FTIR spectra were studied, as shown in Figure 4.5. It was analyzed that there were successful chemical interactions of functional groups between PVA and ZnO & TiO_2 NPs, as shown in Figure 4.5b–g. The spectra showed that in the neat PVA nanofibers, the bands at about 3320, 2940, 1437, 1093, and 850 cm^{-1} showed the vibrations of –OH, –CH_2CH, C–C & C–O functional groups of PVA, respectively [18]. The new intense broad bands at 1100 cm^{-1} to 1000 cm^{-1} and 750 cm^{-1} are assigned to metal oxide of the of Zn & Ti, because these oxides have a moderate dipole moment. The oxides of Zn & Ti with more than one oxygen atom bound to a single metal atom usually absorb in the region 1100 to 750 cm^{-1}. In this spectra of PVA/ZnO and PVA/TiO_2, it was shown that O–H bending at 1579 cm^{-1} and O–H stretching at 3320 cm^{-1} occurred, which was due to the –O bonding of TiO_2 & ZnO with the –H of PVA. There was stretching vibration of –O of TiO_2 & ZnO with –C and –O of PVA at 1050 and 850 cm^{-1}, respectively, as shown in Figure 4.5 [19–21]. Therefore, these spectra confirmed that this self cleaning composite was composed with PVA/ZnO and PVA/TiO_2.

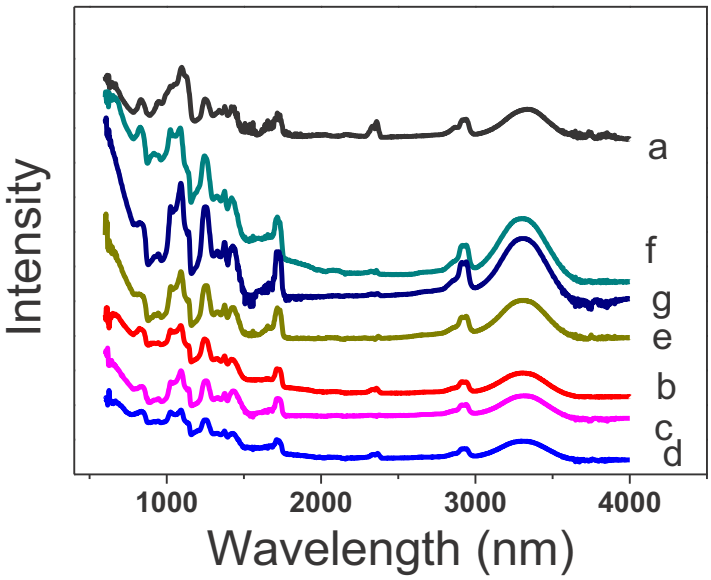

Figure 4.5. Fourier-transform infrared (FTIR) spectra of (a) Neat PVA nanofibers; (b) 5% PVA/ZnO nanofibers; (c) 7% PVA/ZnO nanofibers; (d) 9% PVA/ZnO nanofibers; (e) 5% PVA/TiO2 nanofibers;

(f) 7% PVA/TiO2 nanofibers; (g) 9% PVA/TiO2 nanofibers.

4.3.3. XRD Study

In order to investigate the crystalline structure of PVA, PVA/ZnO and PVA/TiO_2 nanofibers XRD spectra were studied, as shown in Figure 4.6. It was analyzed that the crystallinity of the PVA nanofibers was affected by blending the nanoparticles of ZnO and TiO_2, but ZnO NPs had a greater effect than TiO_2 NPs, as shown in Figure 4.6. PVA/ZnO nanofibers have a greater crystalline structure than PVA & PVA/TiO_2 nanofibers. 9% by weight ZnO/PVA nanofibers have a higher crystalline structure than other 7% & 5% by weight ZnO/PVA nanofibers, which exhibit the peak at 18°, 29°, 31° & 34° with high intensity, 7% & 5% by weight ZnO/PVA nanofibers exhibit the peak at at 18°, 29°, 31° & 34° with low intensity than 9% by weight ZnO/PVA nanofibers. 9% by weight TiO_2/PVA nanofibers exhibit the peak at 18°, 20° and 36° with high intensity than 5% & 7% by weight of TiO_2/PVA nanofibers but 5% by weight of TiO_2/PVA nanofibers did not show the crystalline structure at 36° [15,19]. Therefore, due to cross-linking, the crystalline structure of PVA/ZnO & PVA/TiO_2 was increased. This crystalline structure made them water resistant nanofibers.

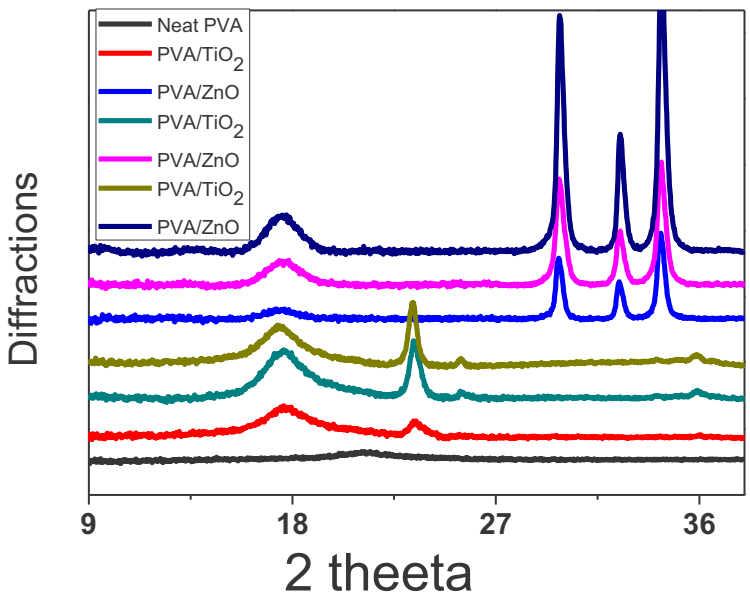

Figure 4.6. X-ray diffraction (XRD) spectra of Neat PVA nanofibers and PVA/ZnOnanofibers.

4.3.4. Water contact angle measurements

In order to investigate the wetting behavior of PVA, PVA/ZnO and PVA/TiO_2 nanofibers, water contact angle measurements were studied, as shown in Figure 4.7. It was analyzed that when crystallinity of PVA/ZnO & PVA/TiO_2 nanofibers was increased, the capacity of water absorbency was reduced. Therefore, these nanofibers showed more water contact angle values than neat PVA nanofibers, as mentioned in Figure 4.7. It was also analyzed that when the concentration of both ZnO and TiO_2 NPs was increased the water contact angle's value was increased, but TiO_2 NPs has a greater effect than ZnO NPs, as mentioned in Figure 4.7.

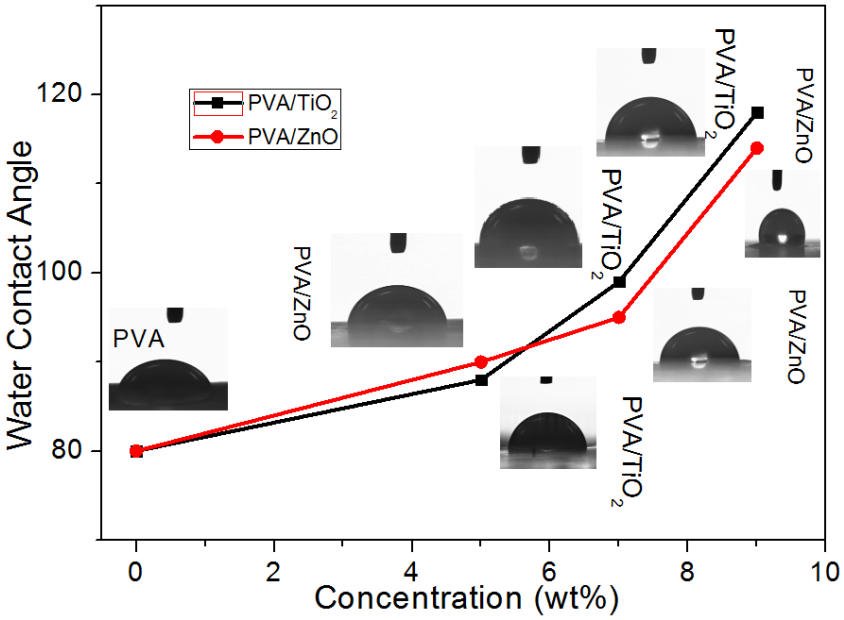

Figure 4.7. Wetting behavior of Neat PVA nanofibers; 5% PVA/ZnO nanofibers; 7% PVA/ZnO nanofibers; 9% PVA/ZnO nanofibers; 5% PVA/TiO_2 nanofibers; 7% PVA/TiO_2 nanofibers; (g) 9% PVA/TiO_2 nanofibers.

4.3.5. Photo-catalysis study

In order to investigate the self-cleaning efficiency of PVA, PVA/ZnO and PVA/TiO_2 nanofibers, a photo-catalysis study was conducted by solar simulator with a light intensity of 1000 W/m^2 and a wavelength range of 350–1100 nm. In this activity, the photo-catalyst absorbs the UV light, which convert the H_2O into hydroxyl radical (OH-1), which degrades the contaminants into small molecules and finally into CO_2 and H_2O [17]. The objective of this research was to develop the self-cleaning nanocomposites in two different ways: PVA/ZnO and PVA/TiO_2 nanofibers. Three different concentrations, 5%, 7% & 9% by weight, of ZnO and TiO_2 NPs were separately blended in PVA nanofibers, but the self-cleaning comparison of both was analyzed at 9% by weight PVA/ZnO and PVA/TiO_2 nanofibers, as shown in Figure 4.8. Methylene blue (MB) dye was used for analyzing the self-cleaning properties of these composites. 2 µL MB was dropped on each sample of PVA, PVA/ZnO & PVA/TiO_2 nanofibers. It was observed that there was no self-cleaning property in PVA but PVA/ZnO and PVA/TiO_2 nanofibers have self-cleaning properties, as mentioned in Figure 4.8. The comparative study between PVA/ZnO and PVA/TiO_2 nanofibers was done in two ways; first by the naked eye, as shown in Figure 4.8A, and second by ATR spectra, in which the intensity of the methylene blue was measured by using Equation (2).

$$\text{Degradation } (\%) = \frac{\text{Ii} - \text{Id}}{\text{Ii}} \times 100$$

Where Ii is the initial intensity of dyed nanofibers and Id is the degraded intensity of dyed nanofibers. Therefore, degradation efficiency/percentage was calculated from ATR spectra, which showed that PVA/ZnO nanofibers have a higher self-cleaning efficiency than PVA/TiO_2 nanofibers because PVA/ZnO nanofibers showed a 95% self-cleaning efficiency within three hours but the PVA/TiO_2 nanofibers showed less efficiency than the PVA/ZnO nanofibers, as shown in Figure 4.8b,c.

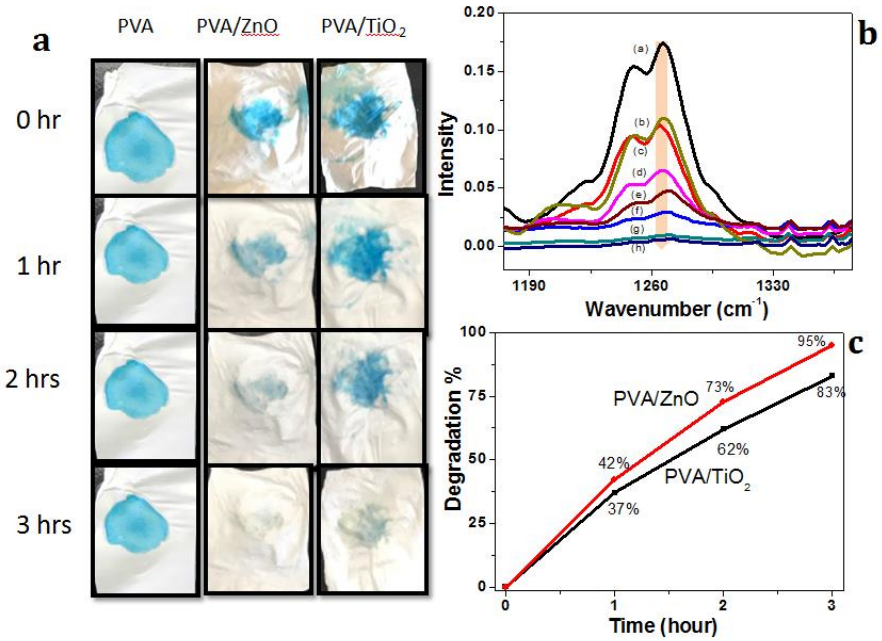

Figure 4.8. Photo-catalysis efficiency in 3 h of neat PVA nanofibers, 9% PVA/ZnO nanofibers and 9% PVA/TiO_2 nanofibers, (a) photocatalytic activity by solar simulator, (b) Self-cleaning efficiency calculated by FT-IR(c) profile of self cleaning efficiency of PVA/ZnO & PVA/TiO_2.

4.3.6. Thermogravimetric analysis (TGA)

Thermal degradation of PVA, PVA/ZnO & PVA/TiO_2 was performed by thermogravimetric analysis as shown in Figure 4.9. This thermogravimetric analysis was performed on the thermo-plus TG 8120 Rigaku Corporation Japan. It was operating in a static mode under air atmosphere at a heating rate of 10 °C/min and a temperature range from 30–500 °C. The samples weighing 6 mg were placed in the pans. The TGA curves of neat PVA, PVA/TiO_2 and PVA/ZnO nanofibers as shown in Figure 4.9 showed that PVA/TiO_2 & PVA/ZnO showed the same thermal stability as neat PVA nanofibers. In this test PVA nanofibers did show

smaller residual mass than PVA/TiO_2 & PVA/ZnO nanofibers. The PVA/TiO_2 & PVA/ZnO nanofibers showed the residual mass that confirmed the presence of nanoparticles of ZnO and TiO_2 as shown in the Figure 4.9. The neat PVA showed 93% degradation at 470 °C, but 5 wt% PVA/ZnO showed 73%, 7 wt% PVA/ZnO 64%, and 9 wt% PVA/ZnO 61% showed degradation, which confirmed that there was a good amount of ZnO nanoparticles. Similarly, PVA/TiO_2 also showed less degradation than PVA, which confirmed the presence of TiO_2 nanoparticles in the PVA/TiO_2 as shown in Figure 4.9B [22, 23].

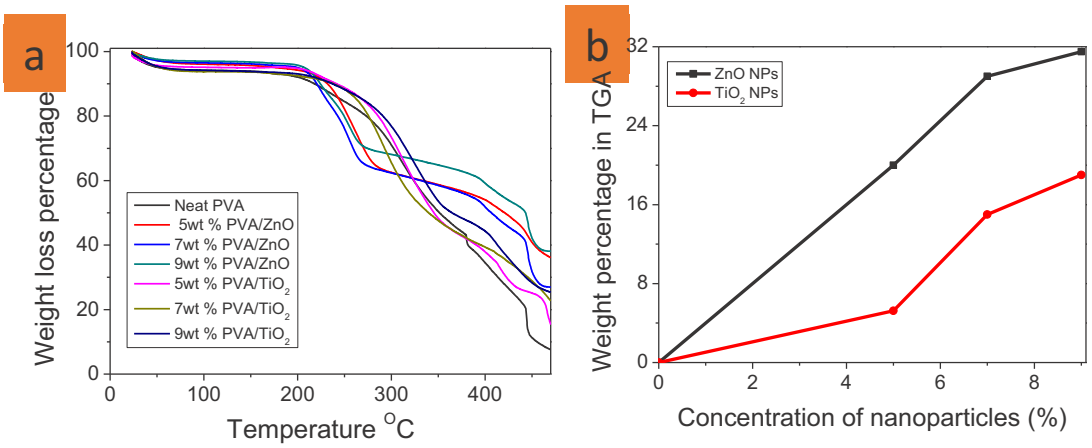

Figure 4.9. Results of TGA (**a**) showed the degradation behavior; (**b**) content percentage of ZnO and TiO_2 NPs in 6 mg of sample.

4.4. Conclusions

Herein, we successfully developed self-cleaning PVA/ZnO & PVA/TiO_2 nanofibers by electrospinning in three different concentrations of ZnO and TiO_2 NPs. On the basis of the characterization results, it was concluded that these PVA/ZnO & PVA/TiO_2 nanofibers have self-cleaning properties, but PVA/ZnO nanofibers have higher self-cleaning properties than PVA/TiO_2 nanofibers because 9% by weight PVA/ZnO nanofibers has 95% self-cleaning properties, which is higher than 9% by weight PVA/TiO_2 nanofibers. This innovative research is essential to form intelligent textiles for stain eliminating from non-washable & non-woven products, such as surgical gown, wound dressings, and home textiles. This research will be fruitful to fulfill the stated and implied needs of customers.

References

1. Czado, W.; Frese, T.; Schaper, A.; Hellwig, M.; Steinhart, M.; Greiner, A.; Wendorff, J.H.; Bognitzki, M. Nanostructured Fibers via Electrospinning. *Adv. Mater*. **2001**, *13*, 70–72.
2. Fujihara, K.; Teo, W.-E.; Lim, T.-C.; Ma, Z.; Ramakrishna, S. *An Introduction to Nanofibers and Electrospinning*; World Scientific Publishing Co. Pte. Ltd., Majulah, Singapore, 2005.
3. Sell, S.A.; Boland, E.D.; Simpson, D.G.; Bowlin, G.L.; Barnes, C.P. Nanofiber technology: Designing the next generation of tissue engineering scaffolds. *Sci. Dir*. **2007**, *59*, 1413–1433.
4. Bhat, G.S.; Tock, R.W.; Parameswaran, S.; Ramkumar, S.S.; Subbiah, T. Electrospinning of Nanofibers. *Wiley Intersci*. **2004**, *96*, 557–569.
5. Wei, Q. *Functional Nanofibers and Their Applications*; Woodhead Publishing: Cambridge, UK, 2012.
6. Kundu, S.C.; Bhardwaj, N. Electrospinning: A fascinating fiber fabrication technique. *Biotechnol. Adv*. **2010**, *28*, 325–347.
7. Bedford, N.M.; Steckl, A.J. Photocatalytic Self Cleaning Textile Fibers by coaxial electrospinning. *Appl. Mater. Interfaces* **2010**, *2*, 2448–2455.
8. Lyua, S.; Leea, S.; Kimb, Y.S.; Hwang, W.; Leea, K. Characteristics and self-cleaning effect of the transparent super-hydrophobic film having nanofibers array structures. *Appl. Surf. Sci*. **2010**, *256*, 6729–6735.
9. Tang, J.; Wang, R.; Lu, H.; Li, L.; Kong, Y.; Qi, K.; Xin, J.H.; Liu, Y. Artificial lotus leaf structures from assembling carbon nanotubes and their application in hydrophobic textile. *J. Mater. Chem.* **2007**, *17*, 1071–1078.
10. Guan, K. Relationship between photocatalytic activity, hydrophilicity and self-cleaning effect of TiO_2/SiO_2 films. *Surf. Coat. Technol.* **2005**, *191*, 155–160.
11. Dehn, F.; Quaas, J.; Orgass, M.; Benedix, R. Application of Titanium Dioxide Photocatalysis to Create Self-Cleaning Building Materials. In *Leipzig Annual Civil Engineering Report Lacer No. 5*; Publisher, Leipzing, Germany, 2005; pp. 157–167.
12. Zhang, Y.-Z.; Khotki, M.; Ramakrishna, S.; Huang, Z.-M. A review on polymer nanofibers by electrospinning and their applications in nanocomposites. *Compos. Sci. Technol.* **2003**, *63*, 2223–2253.
13. Luo, Z.; Rabenberg, L.; Heller, A.; Paz, Y. Photooxidative self-cleaning transparent titanium dioxide films on glass. *J. Mater. Res.* **1995**, *10*, 2842–2848.

14. Pyrgiotakis, G.; Sigmund, W.; Woan, K. Photocatalytic Carbon-Nanotube–TiO_2 Composites. *Adv. Mater.* **2009**, *21*, 2223–2239.
15. Jiang, X.; Wang, T. Influence of Preparation Method on Morphology and Photocatalysis Activity of Nanostructured TiO_2. *Environ. Sci. Technol.* **2007**, *41*, 4441–4446.
16. Jimmy, C.Y.; Yu, J.-G.; Kwok, Y.-C.; Che, Y.-K.; Zhao, J.-C.; Ding, L.; Ge, W.-K.; Wong, P.-K.; Yu, Y. Enhancement of photocatalytic activity of mesoporous TiO_2 by using carbon nanotubes. *Appl. Catal. A* **2005**, *289*, 186–196.
17. Lee, H.; Koo, J.M.; Khatri, Z.; Sui, J.; Im, S.S.; Zhu, C.; Kim, I.S.; Khan, M.Q. Self-cleaning effect of electrospun poly (1,4-cyclohexanedimethylene isosorbide terephthalate) nanofibers embedded with zinc oxide nanoparticles. *Text. Res. J.* **2017**, doi:10.1177/0040517517723026.
18. Kharaghani, D.; Lee, H.; Ishikawa, T.; Nagaishi, T.; Kim, S.H.; Kim, I.S. Comparison of fabrication methods for the effective loading of Ag onto PVA nanofibers. *Text. Res. J.* **2018**, doi:10.1177/0040517517753635.
19. Boyadjiev, S.I.; Kéri, O.; Bárdos, P.; Firkala, T.; Gáber, F.; Nagy, Z.K.; Baji, Z.; Takács, M.; Szilágyi, I.M. TiO_2/ZnO and ZnO/TiO_2 core/shell nanofibers prepared by electrospinning and atomic layer deposition for photocatalysis and gas sensing. *Appl. Surf. Sci.* **2017**, *424*, 190–197.
20. Kaviyarasu, K.; Geetha, N.; Kanimozhi, K.; Magdalane, C.M.; Sivaranjani, S.; Ayeshamariam, A.; Kennedy, J.; Maaza, M. In vitro cytotoxicity effect and antibacterial performance of human lung epithelial cells A549 activity of zinc oxide doped TiO_2 nanocrystals: Investigation of bio-medical application by chemical method. *Mater. Sci. Eng. C* **2017**, *74*, 325–333.
21. Boccuzzi, F.; Chiorino, A.; Tsubota, S.; Haruta, M. FTIR study of carbon monoxide oxidation and scrambling at room temperature over gold supported on ZnO and TiO_2. 2. *J. Phys. Chem.* **1996**, *100*, 3625–3631.
22. Ognibene, G.; Cristaldi, D.A.; Fiorenza, R.; Blanco, I.; Cicala, G.; Scire, S.; Fragala, M.E. Photoactivity of hierarchically nanostructured ZnO–PES fibre mats for water treatments. *RSC Adv.* **2016**, *6*, 42778–42785.
23. Juby, K.A.; Dwivedi, C.; Kumar, M.; Kota, S.; Misra, H.S.; Bajaj, P.N. Silver nanoparticle-loaded PVA/gum acacia hydrogel: Synthesis, characterization and antibacterial study. *Carbohydr. Polym.* **2012**, *89*,

Chapter # 05

Preparation and characterizations of multifunctional PVA/ZnO nanofibers composite membranes for surgical gown application

5.1. Introduction

Healthcare associated infection is one of the world's largest devastating problems, causing millions of deaths and billions of dollars in health care each year. Medical textile materials are very susceptible to microbial growth. Therefore, the antimicrobial treatment of medical textiles such as surgical gowns, bed-sheets, uniforms, aprons and masks, is essential to reduce the spreading of pathogenic microorganism [1].

Nanofibers are ideally suited to form the multifunctional medical products [2]. The protected products are needed to reduce occupational exposure for individual involved with the hospital, chemical industry, emergency response and also military. A number of methods for development of nonwoven and non-washable medical products like surgical gowns but the use of electrospun nanofibers for the non-washable protective garments has grown over the past few decades since they are relatively inexpensive, lightweight and effective protection [3,4]. Electrospinning is a potential technology for use as a platform for multifunctional and hierarchically organized composites because it allows extensive tenability in the materials properties and functions through the selection of the polymeric nanofibers and composite nanofibers [5-7,2,].

Recently, some researchers worked on the antibacterial surgical gown by different methods such as K Rajpreek and et al in 2004 used antibacterial finishing on nonwoven fabric [8], W Huang and et al in 2000 used antibacterial and fluorochemical repellent finishing on nonwoven fabric [9], AK Sarkar and et al in 2011 used different antibacterial agents on different types of fabric for medical textiles [10], M Radetic and et al in 2008 used Ag nanoparticles on the surface of fabric to form the antibacterial medical textiles [11] and RM Shistaway and et al in 2011 used Ag nanoparticles on the cotton fabric for medical textiles [12]. But none of them used antibacterial properties on nanofibers based surgical gown. Therefore we attempted to form the multifunctional surgical gown based on nanofibers by making the composite nanofibers by blending of ZnO nanoparticles in Poly vinyl alcohol (PVA/ZnO). ZnO nanoparticles can be used for antibacterial, UV protections and self-cleaning properties [13]. We are first to develop the nanofibers based multifunctional; antibacterial, UV protection and self-cleaning surgical gown.

In this report, we developed the multifunctional nanocomposite by blending of ZnO nanoparticles with PVA for the surgical gown. The morphology of nanofibers was investigated by SEM and TEM. The chemical interaction was studied by FT-IR, investigation of crystalline structure was done by XRD, photo-catalytic activity was done by solar simulator, stress-strain behavior was studied by tensile strength tester, water contact angles measurements were done by contact angle meter, and UV protection data was obtained by Ultraviolet transmission analyzer and for antibacterial agar diffusion test was done.

5.2. Experimental:

5.2.1. Materials

Poly vinyl alcohol (PVA) (MW: 85,000-124,000, 87-89% hydrolyzed) was purchased from Sigma-Aldrich Corporation USA. Glutaraldehyde (GA, 50% in aqueous solution) was purchased from MP Biomedical. ZnO nanoparticles were purchased from Sigma-Aldrich Corporation USA with a dispersion of concentration of 50.1 wt. %. Methylene blue (powder form soluble 4mg/4ml) was purchased from Sigma-Aldrich Corporation USA and Water.

5.2.2. Electrospinning

Poly vinyl alcohol (PVA) 10 % by weight was dissolved in water at 70 ^{o}C with stirring for five hours and GA was adding in that solution 2.5% by wt. for cross-linking of the solution. ZnO nanoparticles were embedding by stirring for 5 hours in three different concentrations 5%, 7% and 9% by weight. The solution was loaded in the plastic syringe having the diameter of 0.60 mm, in which a Cu electrode was adjusted. The distance from the capillary tip to the collector was 12 cm and the supply of voltage was 14 kV. The nanofibers were formed without beads at room temperature and at 45% humidity.

5.2.3. Characterization

The morphology of nanofibers was investigated by SEM (JSM-5300, JEOL Ltd., Japan) accelerated with the voltage of 12 kV and TEM (JSM-5300, JEOL Ltd., Japan) accelerated with 200 kV. The chemical interactions were study by FT-IR (IR Prestige-21 by shinmadzu Japan), Wide angle X ray diffractions (WAXD) were performed for evaluation of crystal structure at room temperature with nanofibers samples using a Rotaflex RT300 mA and Nickel-filtered Cu K_a radiation was used for measurements, along with an angular angle of $5 \leq 2\theta \leq 50^{o}$, photo-catalytic activity was done by solar simulator (XES-40S3, San-ei Electric,

Japan) in which light intensity was 1000 W/m^2 and wavelength range of 350-1100 nm and the self-cleaning efficiency was calculated as following equation 1.

$$\text{Degradation } (\%) = \frac{\text{Ii} - \text{Id}}{\text{Ii}} \times 100 \qquad 1$$

, stress-strain behavior was studied by tensile strength tester (Universal Testing Machine, Tenilon RTC 250A, A&D company Ltd., Japan), water contact angles measurements were done by contact angle meter (Digidrop, GBX France), UV protection data was obtained by UV-1000F, Ultraviolet transmission analyzer (Labsphere, USA) using EN 13758-1-2001and for antibacterial AATCC test was done.

5.3. Results and discussions

5.3.1. Morphology of nanofibers

The exterior morphology of PVA/ZnO nanofibers was evaluated by SEM in which it was investigated that nanofibers had the good cohesiveness to each other and beat free nanofibers as shown in Figure 5.1. With the blending of ZnO nanoparticles in the PVA solution there was no effect of morphology but diameter of nanofibers was increased as the concentration of ZnO was increased and in order to determine the presence of ZnO nanoparticles in the PVA/ZnO nanofibers scanning electron microscope images with corresponding energy dispersive spectrum was recorded as shown in Figure 5.1e. The weight percentage of ZnO in PVA/ZnO was 9 and uniform distribution over the surface area of the nanofibers as shown in Figure 5.1f, 5.1g.

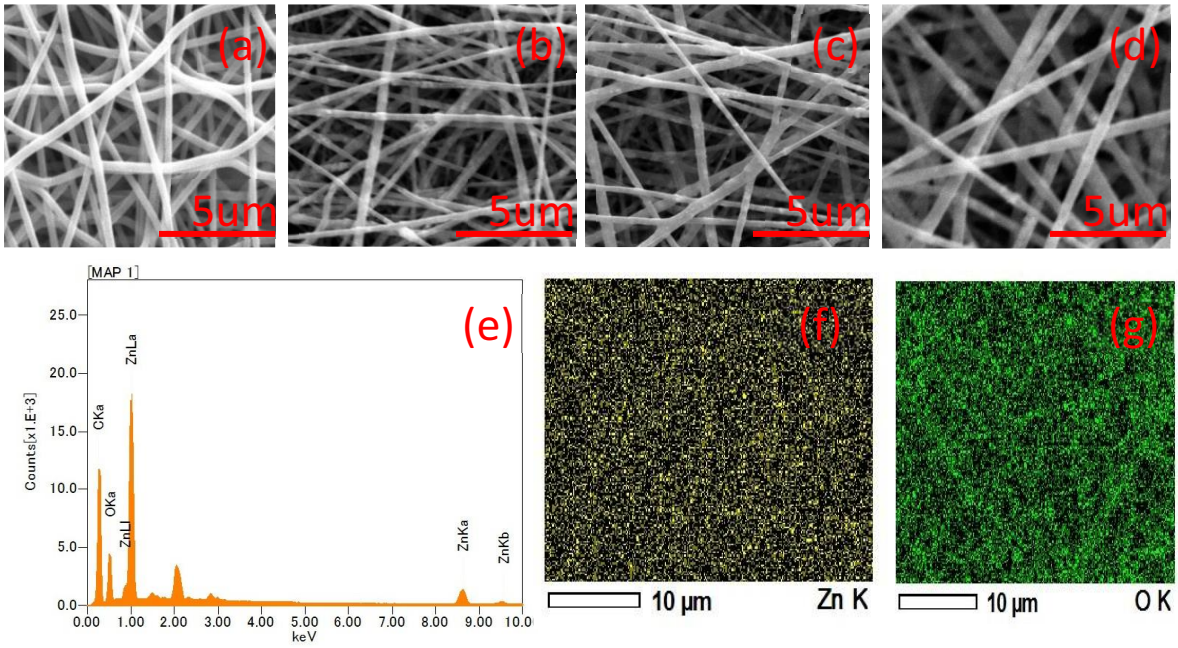

Figure 5.1. SEM images of (a) Neat PVA Nanofibers, (b) 5% PVA/ZnO Nanofibers, (c) 7% PVA/ZnO Nanofibers, (d) 9% PVA/ZnO Nanofibers & (e-g) EDS analysis of ZnO from PVA/ZnO Nanofibers.

In order to investigate the dispersion of ZnO nanoparticles in the PVA/ZnO nanofibers Transmission electron microscope study was done. As shown in Figure 5.2 ZnO nanoparticles were well embedded in the nanofibers during electrospinning process but ZnO nanoparticles affected the diameter size of nanofibers, as the concentration of ZnO was increased the diameter size of the nanofibers was also increased.

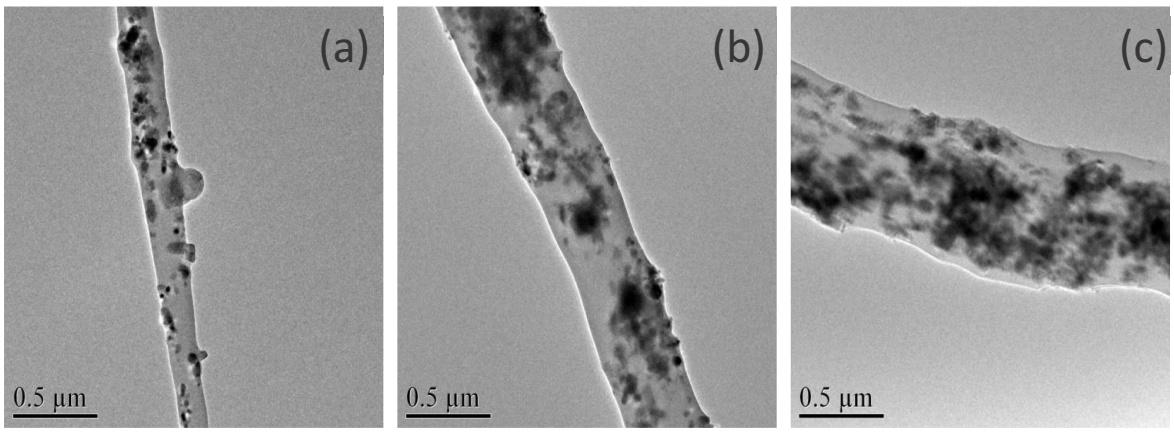

Figure 5.2. TEM images of (a) 5% PVA/ZnO Nanofibers, (b) 7% PVA/ZnO Nanofibers, (c) 9% PVA/ZnO Nanofibers

5.3.2. FT-IR study of nanofibers

In order to investigate the chemical interaction between PVA and ZnO nanoparticles, Fourier Transform Infrared spectroscope study was done as shown in Figure 5.3. Spectra showed that in the neat PVA nanofibers the bands at about 3320 cm^{-1}, 2940 cm^{-1}, 1437 cm^{-1}, 1093 cm^{-1} and 850 cm^{-1} are assigned to the vibrations of –OH, $–CH_2CH_2$, C-C and C-O group of PVA, respectively. The new intense broadbands 1100 cm^{-1} to 1000 cm^{-1} and at 750 cm^{-1} are assigned to Zn-O vibrations of ZnO nanoparticles that indicating the nanofibers composed of PVA and ZnO.

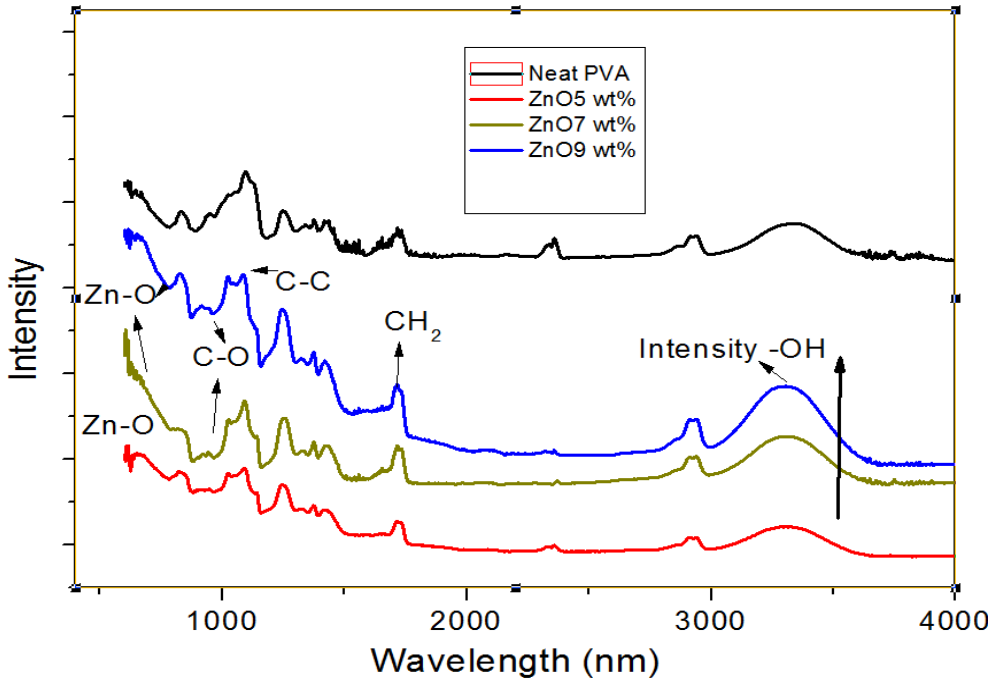

Figure 5.3. FT-IR spectra analysis of PVA Nanofibers and PVA/ZnO nanofibers

5.3.3. XRD analysis of nanofibers

In order to investigate the crystalline structure of PVA/ZnO nanofibers wide -angle X-ray diffraction (WAXD) was studied as shown in Figure 5.4. The neat PVA exhibits the peak at 20º but there were more peaks in PVA/ZnO nanofibers which were exhibited at 18, 28 º, 32 º, and 34 º. It means by addition of ZnO nanoparticles the crystallinity was increased and 9% ZnO by weight in PVA/ZnO nanofibers exhibited the peaks same at 18, 28, 32 and 34º but with high intensity [15] as shown in Figure 5.4.

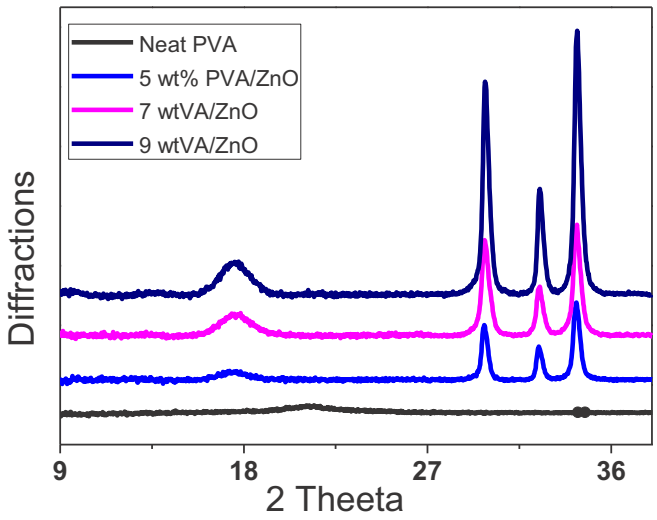

Figure 5.4. XRD Analysis of PVA Nanofibers and PVA/ZnO nanofibers

5.3.4. Tensile strength analysis of nanofibers

The stress-strain behavior of PVA/ZnO nanofibers was investigated by Universal Testing Machine as shown in Figure 5.5. It was observed that neat PVA nanofibers have the largest elongation at 93% but having a low capability of bearing load which is 0.25 MPa. The elongation of blended PVA/ZnO nanofibers was decreased as the concentration of ZnO nanoparticles was increased but capability of bearing load was increased as the concentration of ZnO nanoparticles was increased. The increasing the strength of PVA/ZnO nanofibers by blending of ZnO nanoparticles it is due to the effect of metallic nanoparticles because metallic nanoparticles; always increase the strength of their partner component in the composite [16]. Therefore, 9 wt% PVA/ZnO nanofibers have highest strength than others 7 wt% & 5 wt% PVA/ZnO nanofibers as shown in Figure 5.5.

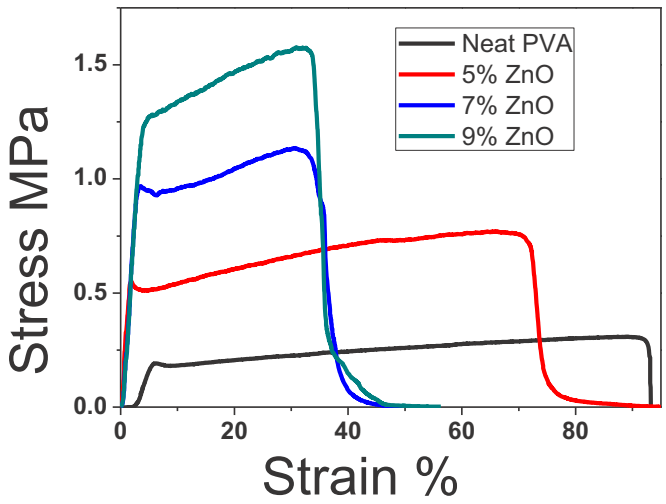

Figure 5.5. Stress-Strain Analysis of PVA Nanofibers and PVA/ZnO nanofibers

5.3.5. Water contact angle measurements of nanofibers

The wetting behavior of PVA/ZnO nanofibers was investigated by the static angle with a contact angle meter by drop method. It was analyzed that neat PVA nanofibers are hydrophilic with contact angle 88° as mentioned in Figure 5.6 but the water contact angle of blended nanofibers was reduced as the concentration of ZnO nanoparticles was increased. The 9% ZnO/PVA nanofibers has highest hydrophobicity with contact angle 118°.

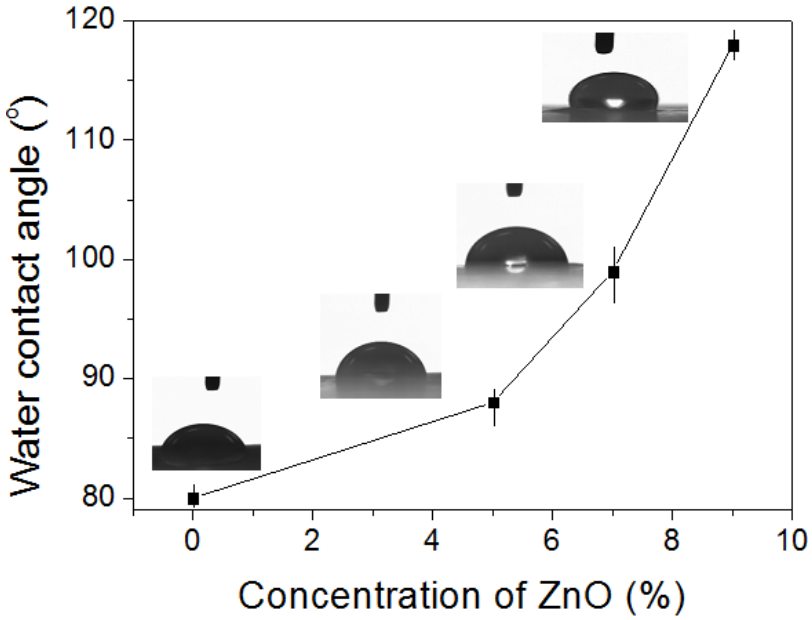

Figure 5.6. Water contact angle measurements of PVA Nanofibers and PVA/ZnO nanofibers

5.3.6. Photo-catalysis activity

The photo-catalysis activity was done by solar simulator in which light intensity was 1000 W/m^2 and wavelength range of 350-1100 nm. In this phenomenon, a photo-catalyst absorbs UV light and then converts H_2O into hydroxyl radicals (OH^-), which have the ability to degrade the contaminant to small molecules and finally into CO_2 and H_2O [14,4]. As we done in our previous work [4,15] for the evaluation of self-cleaning properties 2 micro liters of methylene blue was dropped onto each sample. The photo-catalysis activity was done between neat PVA and 9 wt% ZnO/PVA nanofibers for three hours as shown in Figure 5.7. It was observed that there was no self-cleaning property in PVA but PVA/ZnO has self-cleaning properties, as mentioned in Figure 5.7. The self-cleaning properties were done in two ways; first by the naked eye, as shown

in Figure 5.7A, and second by ATR spectra, in which the intensity of the methylene blue was measured by using Equation (1).

$$\text{Degradation } (\%) = \frac{\text{Ii} - \text{Id}}{\text{Ii}} \times 100$$

Where Ii is the initial intensity of dyed nanofibers and Id is the degraded intensity of dyed nanofibers. Therefore, degradation efficiency/percentage was calculated from ATR spectra, which showed that PVA/ZnO nanofibers have the appreciable self-cleaning efficiency because PVA/ZnO nanofibers showed a 98% self-cleaning efficiency within three hours in Figure 5.7b,c.

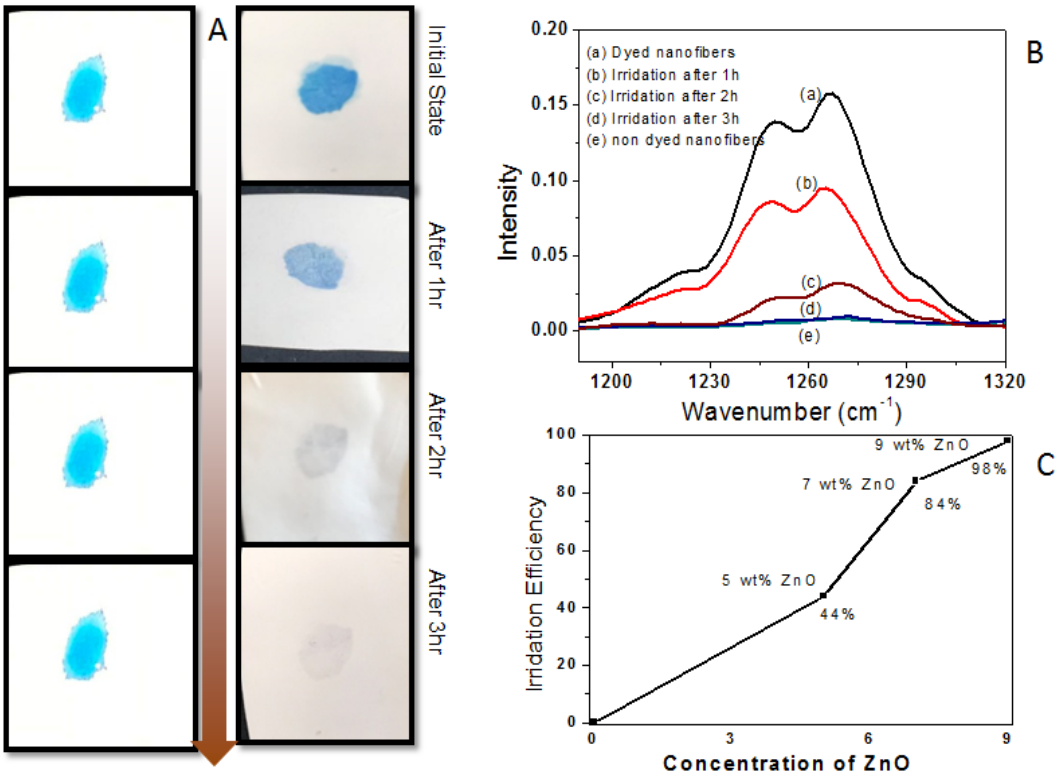

Figure 5.7. The photo-catalysis activity of PVA Nanofibers and 9wt% ZnO, PVA/ZnO nanofibers

Figure 5.7. The photo-catalysis activity of PVA Nanofibers and 9wt% ZnO, PVA/ZnO nanofibers

5.3.7. UV transmission

The ZnO nanoparticles strongly absorb in the UV region, so the PVA/ZnO nanofibers were expected to exhibit UV shielding properties. The black spectrum in Figure 5.8 shows that neat PVA had a high UV

transmission but all other PVA/ZnO nanofibers exhibited nearly 0% UV transmission, while transmission in the visible region showed no significant decline. Absorption by the ZnO nanoparticles was clearly responsible for the different transmissions in the UV and visible regions.

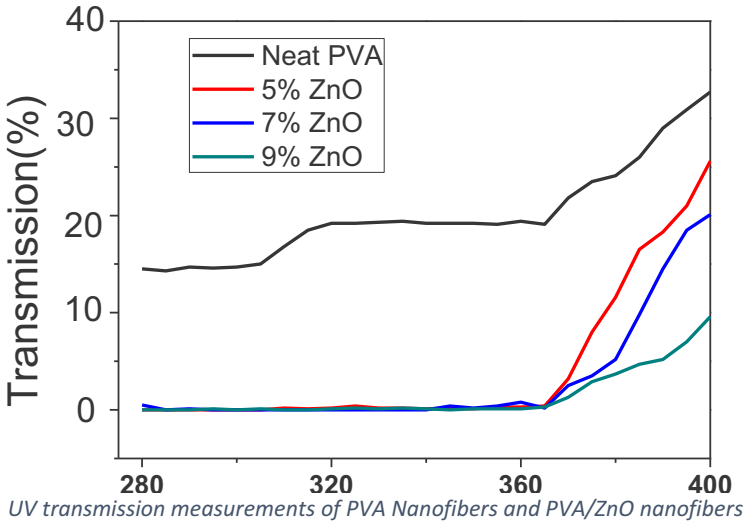

Figure 5.8. UV transmission measurements of PVA Nanofibers and PVA/ZnO nanofibers

5.3.8. Antibacterial activity

In order to investigate the antibacterial properties of the PVA/ZnO nanofibers, agar diffusion plate method was used. In this method, the staphylococcus aurous and Escherichia coli were used as model bacteria. The bacteria were used on the neat PVA nanofibers and PVA/ZnO nanofibers. The antibacterial results are shown in Figure 9. The results indicated that the treated nanofibers with ZnO nanoparticles have an effective antibacterial activity against staphylococcus aurous and Escherichia coli bacteria. When the concentration of ZnO nanoparticles was increased the killing process of bacteria was increased as shown in Figure 5.9 & Table 5.1. It was observed that neat PVA have no antibacterial properties but 9% by weight PVA/ZnO nanofibers membranes has the highest antibacterial properties against staphylococcus aureus as shown in Figure 5.9 and Table 5.1.

Table 5.1. Antibacterial activity by zone inhibition in mm

Sr. No	Sample specifications	E. Coli bacterium	S. Aureus bacterium
1	Neat PVA membranes	Not active	Not active
2	5% PVA/ZnO	1	1.3
3	7% PVA/ ZnO	2	4

4	9% PVA/ ZnO	5	10
	Rifampicin (+ve standard)	26	24

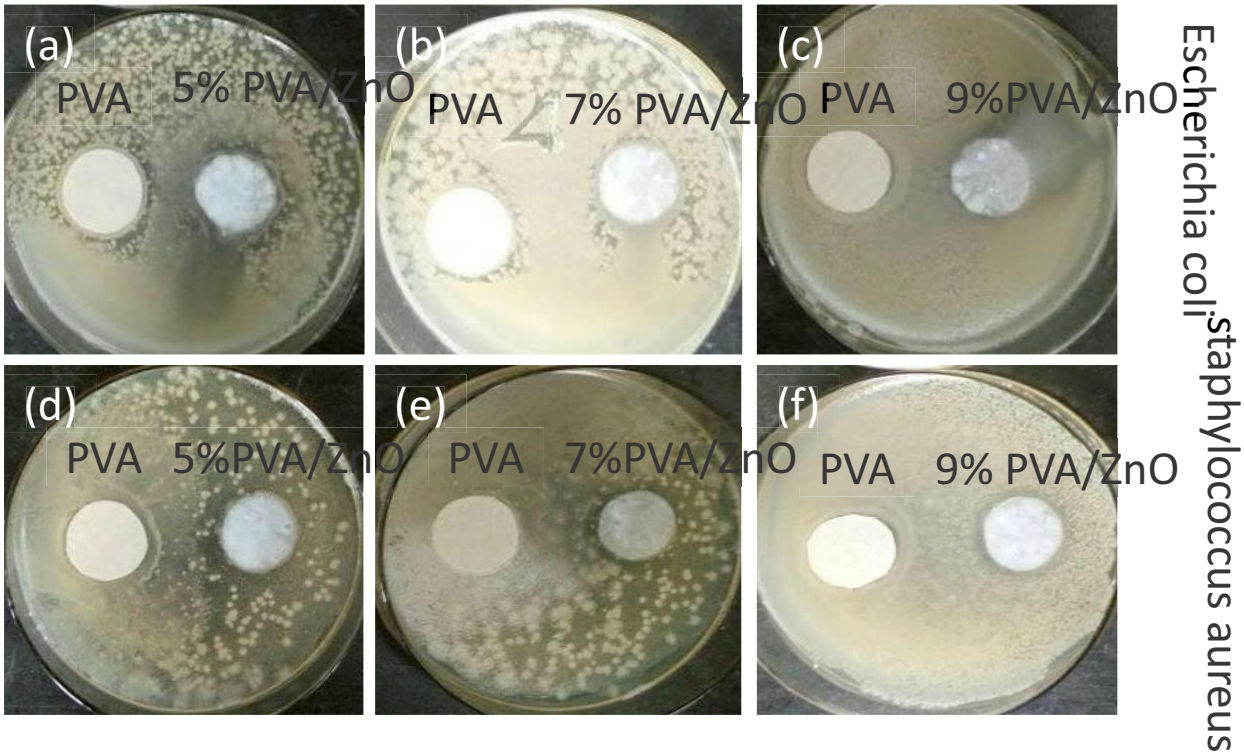

Figure 5.9. Antibacterial results of PVA Nanofibers and PVA/ZnO nanofibers

5.4. Conclusions

Herein, we successfully developed the multifunctional nanocomposite for the surgical gown by blending of PVA/ZnO through electrospinning. The blending of ZnO nanoparticles with PVA was in three different concentrations; 5wt%, 7wt% & 9wt% and uniformly dispersion on nanofibers was achieved. The resultant nanofibers have good chemical interactions between PVA & ZnO nanoparticles, crystallinity and strength of the blended nanofibers were increased as concentration of ZnO nanoparticles was increased. The photo-catalysis efficiency of the PVA/ZnO nanofibers was increased as the concentration of the ZnO nanoparticles was increased. The UV transmission of the PVA/ZnO nanofibers was decreased as the concentration of ZnO nanoparticles was increased. The antibacterial efficiency of PVA/ZnO nanofibers was increased as the concentration of the ZnO nanoparticles was increased. So this nanocomposite is very beneficial for the medical surgeon to fulfill the stated and implied needs of the customer.

References

1. Cerkez, Idris, Hasan B. Kocer, S. D. Worley, R. M. Broughton, and T. S. Huang. "Multifunctional cotton fabric: antimicrobial and durable press." *Journal of Applied Polymer Science* 124, no. 5 (2012): 4230-4238.
2. Teo, Wee-Eong, and Seeram Ramakrishna. "Electrospun nanofibers as a platform for multifunctional, hierarchically organized nanocomposite." *Composites Science and Technology*69, no. 11 (2009): 1804-1817.
3. Obendorf, S. Kay. "Improving personal protection through novel materials." *Aatcc Rev* 10, no. 4 (2010): 44-50.
4. Khan, Muhammad Qamar, Hoik Lee, Zeeshan Khatri, Davood Kharaghani, Muzamil Khatri, Takahiro Ishikawa, Seung-Soon Im, and Ick Soo Kim. "Fabrication and characterization of nanofibers of honey/poly (1, 4-cyclohexane dimethylene isosorbide trephthalate) by electrospinning." *Materials Science and Engineering: C* 81 (2017): 247-251.
5. Khan, Muhammad Qamar, Hoik Lee, Jun Mo Koo, Zeeshan Khatri, Jianhua Sui, Seung Soon Im, Chunhong Zhu, and Ick Soo Kim. "Self-cleaning effect of electrospun poly (1, 4-cyclohexanedimethylene isosorbide terephthalate) nanofibers embedded with zinc oxide nanoparticles." *Textile Research* Journal (2017): 0040517517723026.
6. Zhang, Yinhang, Deng Fei, Ge Xin, and Ur-Ryong Cho. "Surface modification of novel rice bran carbon functionalized with (3-Mercaptopropyl) trimethoxysilane and its influence on the properties of styrene-butadiene rubber composites." Journal of Composite Materials 50, no. 21 (2016): 2987-2999.
7. Zhang, Yinhang, and Soo‐Jin Park. "Enhanced interfacial interaction by grafting carboxylated‐macromolecular chains on nanodiamond surfaces for epoxy‐based thermosets." Journal of Polymer Science Part B: Polymer Physics 55, no. 24 (2017): 1890-1898.
8. Virk, Rajpreet K., Gita N. Ramaswamy, Mohamed Bourham, and Brian Lee Bures. "Plasma and antimicrobial treatment of nonwoven fabrics for surgical gowns." Textile research journal 74, no. 12 (2004): 1073-1079.
9. Huang, Wei, and Karen K. Leonas. "Evaluating a one-bath process for imparting antimicrobial activity and repellency to nonwoven surgical gown fabrics." Textile Research Journal 70, no. 9 (2000): 774-782.

10. Sarkar, Ajoy K., Subhash Appidi, and Anupama S. Ranganath. "Evaluation of berberine chloride as a new antibacterial agent against gram-positive bacteria for medical textiles." Fibres & Textiles in Eastern Europe 19, no. 4 (2011): 131-134.
11. Radetić, Maja, Vesna Ilić, Vesna Vodnik, Suzana Dimitrijević, Petar Jovančić, Zoran Šaponjić, and Jovan M. Nedeljković. "Antibacterial effect of silver nanoparticles deposited on corona‐treated polyester and polyamide fabrics." Polymers for advanced technologies 19, no. 12 (2008): 1816-1821.
12. El-Shishtawy, Reda M., Abdullah M. Asiri, Nayera AM Abdelwahed, and Maha M. Al-Otaibi. "In situ production of silver nanoparticle on cotton fabric and its antimicrobial evaluation." Cellulose 18, no. 1 (2011): 75-82.
13. Shafei, A. El, and A. Abou-Okeil. "ZnO/carboxymethyl chitosan bionano-composite to impart antibacterial and UV protection for cotton fabric." Carbohydrate polymers 83, no. 2 (2011): 920-925.
14. Zhu, Chunhong, Jian Shi, Sijun Xu, Minori Ishimori, Jianhua Sui, and Hideaki Morikawa. "Design and characterization of self-cleaning cotton fabrics exploiting zinc oxide nanoparticle-triggered photocatalytic degradation." Cellulose 24, no. 6 (2017): 2657-2667.
15. Khan et al. “Self-Cleaning Properties of Electrospun PVA/TiO2 and PVA/ZnO Nanofibers Composites”. Nanomaterials 2018, 8(9), 644; doi: 10.3390/nano8090644
16. Sami, Syed Kamran, Saqib Siddiqui, Sajal Shrivastava, Nae‐Eung Lee, and Chan‐Hwa Chung. "The Pine‐Needle‐Inspired Structure of Zinc Oxide Nanorods Grown on Electrospun Nanofibers for High‐Performance Flexible Supercapacitors." *Small* 13, no. 46 (2017): 1702142.

Chapter # 06

The development of nanofiber tubes based on nanocomposites of polyvinylpyrrolidone incorporated gold nanoparticles as scaffolds for neuroscience application in axons

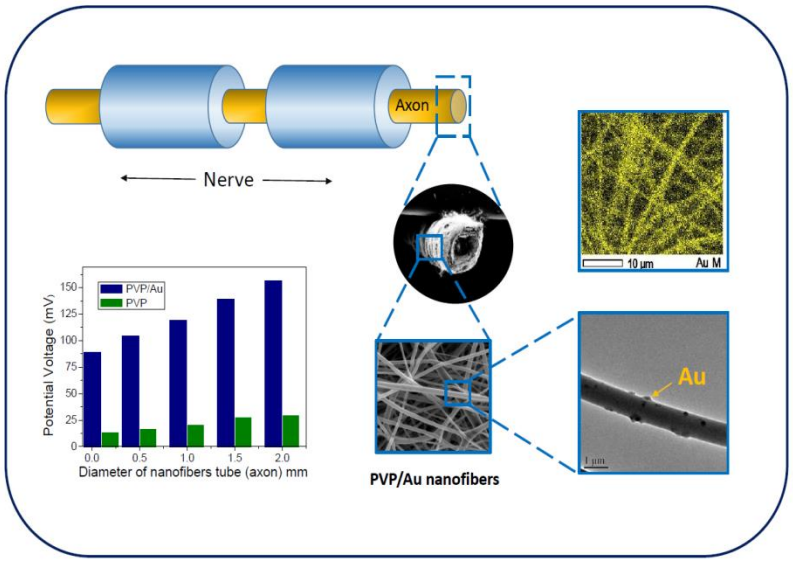

Figure 6.1: Graphical abstract

6.1. Introduction

Nanofibers have potential for research in various fields of life due to its high surface area, light weight [1] and having ability of growth for cell culturing in tissue engineering [2]. Tissue engineering is an emerging research area in the contemporary human health care administration, in which the basic understanding of cellular biology and the application of bioengineering are harnessed together for developing feasible substitutes to aid in the clinical treatment associated with human nervous system. More precisely, treatment of nerve tissue repair arising from the spinal cord injury requires an additional care or new medical therapy, because axons do not regenerate appreciably in their native environment [3-10].

Since past few years, the nanofibers based tissue engineering has been increasing and progress is obvious in various fields such as blood vessels [11], artificial cornea [12], retina [13], veins [14], blood filter for kidney [15] and other implantable artificial vital organs of animals and also for human beings [16]. A huge numbers of people used nanofibers for this field because nanofibers are fruitful for medical textiles due to its biodegradable and non biodegradable properties as required for the organs [17-19]. These organs are damaged due to the accidental situations and the medical treatment required the secondary surgery for planting the organs. The artificial organs are best option to for replace the damaged organs of human beings

[20]. One of them is the axon for continues supply of neurosignals in the nerves of human's body. These signals need some amount of potential voltage for the information carrying from any point of body to brain. This potential voltage is not harmful for brain because around the axon there is insulated layer which protect the nerve [21-24]. We attempted to develop the nanofibers based tubes for implantable axon for continuing the supply of the neurosignals from damaged place to any other place in axon throughout the nerve from nanocomposites of PVP/Au by electrospinning. Electrospun nanofibers have a unique 3D scaffold characteristics and potential for mimic native tissues and organs that favor the tissue engineering [25]. Polyvinylpyrolidone (PVP) is a biodegradable and nontoxic polymer for human health [26] and Au nanoparticles have the properties of conductivity and antimicrobial [27]. Therefore, PVP was blended with Au nanoparticles to enhance the capacity of potential voltage in axon. Recently, many attempts were done for neuro tissues growth, CNS regeneration, nerve guide by Eva Schnell et al in 2007, Vicki M. et al in 2008 and Zeeshan Khatri et al. in 2013 respectively, none of them work on neurosignal transmission in axon [28-30]. This report describes the development of axon for nerve by PVP/Au via electrospinning. All electrospun nanofibers were characterized for tensile strength by tensile testing, SEM & TEM for fiber morphology examinations, FT-IR & Raman for chemical structure changing, XRD was done to investigate the crystalline structure of the nano-composite, conductivity was measured by Ohm meter and the mechanical properties were assessed using tensile strength tester.

6.2. Experimental

6.2.1. Material

PVP was purchased from ALDRICH (product of USA) in form of solution (45% in H_2O) having molecular weight 160000. Gold (Au) nanoparticles of 5 nm in size were purchased from ALDRICH (product of USA) in form of suspension in 0.1 mM PBS having molecular weight 196.97 and ethanol (99.5%) was purchased from Wako Pure Chemical Industries, Ltd.

6.2.2. Electrospinning

The 20% by weight concentration of PVP was dissolved in ethanol, after 4 hrs stirring, the 2.5% by weight concentration of Au nanoparticles was blended in the solution of PVP and stirred for 3 hrs, after that ultrasonically dispersed for 2 hrs at intensity of 38 KHz. The solution PVP/Au nanoparticles was loaded in a plastic syringe connected with capillary tips having inner diameter of 0.60 mm, in which an electrode of Cu wire was adjusted. The distance from capillary tip to collector was 15 cm, flow rate was 0.75 ml/hr and the supply of voltage was 7 kV. The nanotubes for axon were prepared in 5 different sizes having internal

diameter of 2 mm, 1.5 mm, 1 mm, 0.5 mm and 0.2 mm. The 5 different types of collectors were used for the development of tubular structure having external diameter of 2 mm, 1.5 mm, 1 mm, 0.5 mm and 0.2 mm.

6.2.3. Characterization

The surface morphology of these nanofibers based tubes was evaluated by SEM (JSM-5300, JEOL Ltd., Japan) accelerated with the voltage of 12 kV and TEM (JEM-2100 JEOL Japan) accelerated with 200 kV. The average diameter of nanofibers was determined from 50 measurements of the random nanofibers using image analysis software (Image J, version 1.49) and thickness of tube wall was measured by digital micrometer MCD 130-25 with measuring sensitivity of ± 1μm. The chemical interactions between Au & PVP were studied by Fourier transform infrared (FT-IR) spectra achieved by IR Prestige -21 (Shimadzu, Japan). The spectra were recorded from 400-4000 cm^{-1} with a resolution of 4 cm^{-1} and the addition of 128 scanning, the tensile strength test was performed to check the mechanical behavior of nanofibers by using the Universal Testing Machine (Tesilon RTC 250 A, A&D Company Ltd., Japan) based on ISO 13634 methods. The 5 specimen for each tube of different diameter were prepared and the values of stress and strain were calculated by the following formulas 1 & 2 respectively.

$$\text{Stress (MPa)} = \frac{\text{All values of load(N)}}{\text{Area } (\pi r^2)} \qquad (1)$$

$$\text{Strain (\%)} = \frac{\text{change in length}(\Delta l)}{\text{initial length(l)}} \times 100 \qquad (2)$$

The potential voltage was measured by PCE-DC2 Voltmeter; PCE Instruments UK Ltd, which can detect AC& DC voltage, AC/DC current and frequency. Its sector and accuracy for AC voltage is 600 VAC ± (1.5% + 8 digits). This voltmeter can detect without contact and it takes power by 2 AAA batteries and Wide angle X ray diffraction (WAXD) were performed for evaluation of crystal structure of nanofibers samples at room temperature by using a Rotaflex RT 300 mA and Nickel-filtered Cu K_a radiation was used for measurements, along with an angular angle (θ) of $5 \leq 2\theta \leq 50^o$.

6.3. Results and Discussion

6.3.1. Morphology of the nanofibers based tubes

Figure 6.2 shows the SEM images for all nanofibers based tubes having different inner diameter of 0.2, 0.5, 1.0, 1.5 and 2 mm. The PVP/Au nanofibers had relatively good cohesiveness in nanofibers that led the scaffolds compact with cross section close to a circular shape. The morphology of nanofibers of each scaffolds surface is shown in Figure 6.2 (a-e) and 6.2f shows the wall thickness of PVP/Au nanofibers based

tubes. These nanofibers demonstrated smooth morphologies with no beads that were produced via continuous electrospinning. The Table 6.1 shows the specifications of the each nanofibers based tube in which inner diameter of tubes, average diameter of nanofibers in tubes, length of nanofibers based tubes and thickness of nanofibers tubes are mentioned. The average diameter of nanofibers was determined from 50 measurements of the random nanofibers using image analysis software (Image J, version 1.49). Diameter of nanofibers was increased when inner diameter of tubes was increased due to the use of rod like collector for the development of tubular structure when rod's external diameter was increased then diameter of nanofibers was increased because larger diameter has higher surface area than smaller diameter. Therefore high surface area has larger amount of lied nanofibers which also increased the thickness of tubes. The tube which has 0.2 mm diameter has thickness of 0.039 mm which smaller than the tube having diameter of 2.0 mm as shown in Table 6.1. Therefore, when thickness of tubes was increased, the size of nanofibers was also increased. The nanofibers based tube of 2 mm diameter having the highest average diameter 285±30 nm of the nanofibers than other tubes as mentioned in Table 6.1.

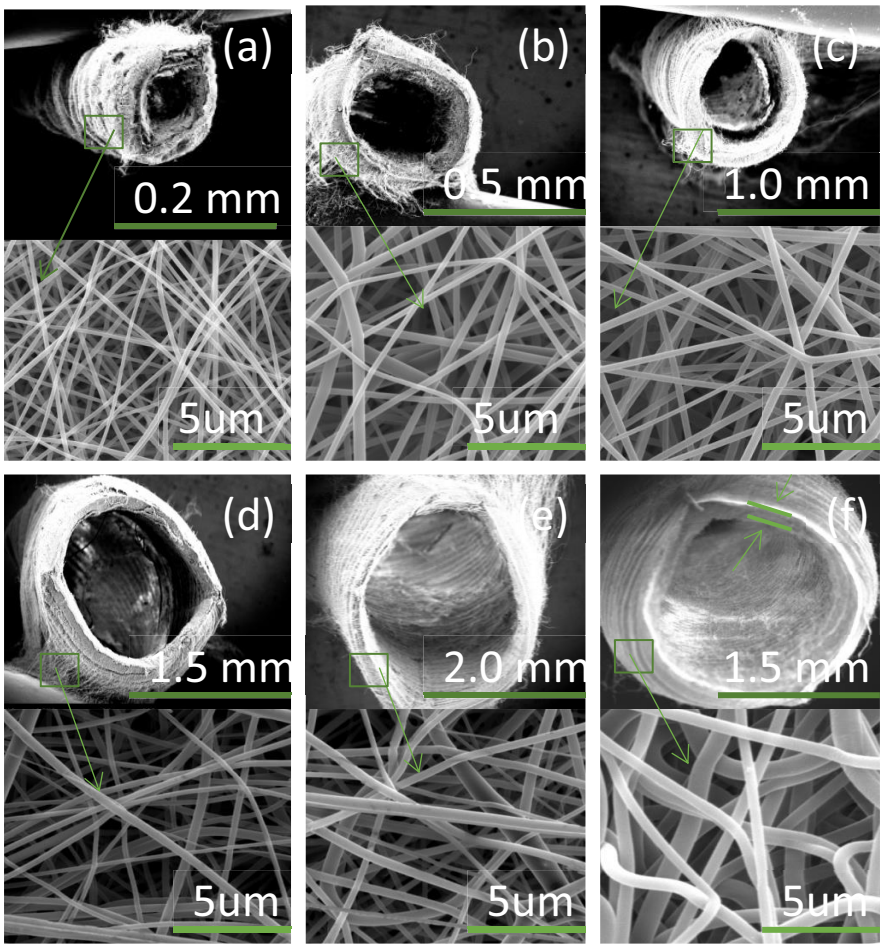

Figure 6.2. SEM images of (a) PVP/Au nanofibers based tube having diameter 0.2 mm, (b) PVP/Au nanofibers based tube having diameter 0.5 mm, (c) PVP/Au nanofibers based tube having diameter 1.0 mm,

(d) PVP/Au nanofibers based tube having diameter 1.5 mm, (e) PVP/Au nanofibers based tube having diameter 2.0 mm, (f) Neat PVP nanofibers based tube having diameter 2 mm & wall thickness of nanofibers based tube.

Table 6.1. Specifications of each nanofibers tube (Axon)

Diameter of Nanofiber based tubes (mm)	Average Diameter of nanofibers (nm)	Thickness of tube wall (mm)
0.2	210 ± 25	0.039
0.5	240 ± 10	0.040
1	255 ± 15	0.044
1.5	262 ± 20	0.046
2	285 ± 30	0.050

In order to investigate the dispersion of gold nanoparticles in PVP/Au nanofibers based tubes, Transmission Electron Microscope study was done. As seen in Figure 6.3, the morphology showed that Au nanoparticles were well embedded in the nanofibers during electrospinning process.

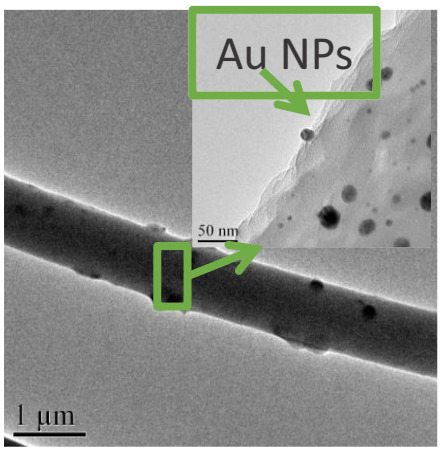

Figure 6.3. TEM image of PVP/Au nanofibers

6.3.2. EDS Analysis

Scanning electron microscope images with corresponding energy dispersive spectrum was recorded as shown in Figure 6.4 in order to determine the presence of Au nanoparticles in PVP/Au nanofibers. The weight percentage of Au in PVP/Au nanofibers was 1.33 and showed the uniform distribution over the surface area of the nanofibers.

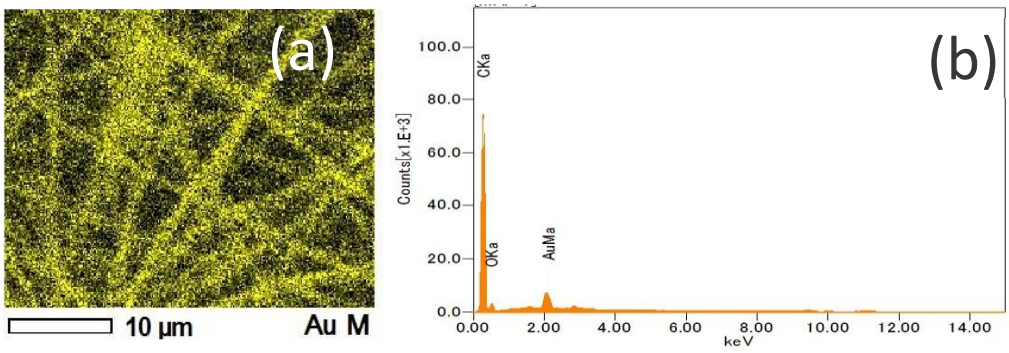

Figure 6.4. Selected area of nanofibers for mapping (a) and EDS spectrum of PVP/Au nanofibers (b).

6.3.3. FT-IR study

In order to investigate the chemical interaction between PVP and Au nanoparticles, Fourier Transform Infrared Spectroscope study was done as shown in Figure 6.5. Spectra showed that in neat PVP nanofibers there were O-H stretching at 3435 cm^{-1}, C-H asymmetric stretching at 2955 cm^{-1}, C=O stretching at 1661 cm^{-1}, CH_2 bending at 1424 cm^{-1} and C-N bending at 1291 & 1018 cm^{-1} and in PVP/Au nanofibers there were Au nanoparticles because in spectrum of PVP/Au there are additional stretching and bending at 2350 & 2095 cm^{-1} respectively, which are not present in neat PVP graph [31,32].

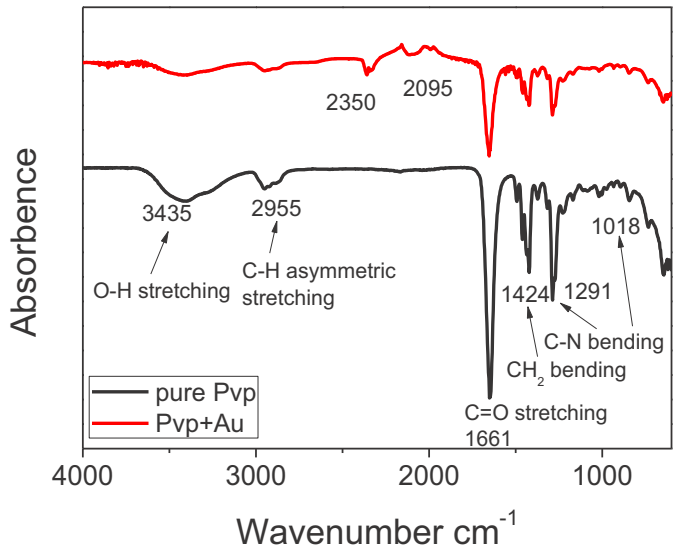

Figure 6.5. FT-IR spectra of PVP & PVP/Au nanofibers

6.3.4. Wide -angle X-ray diffraction (WAXD)

In order to investigate the crystal structure of PVP/Au nanofibers, WAXD patterns were studied. The neat PVP powder and nanofibers exhibit the peaks at 5 ^{o} and 12^{o} and therefore result might be attributed to crystallinity of the PVP crystalline domain, but the PVP/Au nanofibers exhibit the typical sharp peaks at 3^{o}, 5^{o}, 10^{o} and 12^{o} but low intensity as shown in Figure 6.6 [33]. It means blending of Au nanoparticles in PVP,

result might be attributed to enhance the crytallinity of the PVP crystalline domains, which was induced by enhancing the solution conductivity of the PVP/Au solution during electrospinning, because Au nanoparticles shows different crystallinity levels due to nanoaprticles sizes which have to blend. Valeri. et al in 2005 studied the diffraction patterns of Au nanoparticles in three different sizes; 3 nm, 15 nm and 30 nm. They showed that when size of nanoparticles was increased its crystalinity was increased [34]. So, resultant nanofibers based tubes has the appreciable crystalinity behavior for potential neuroscience applications.

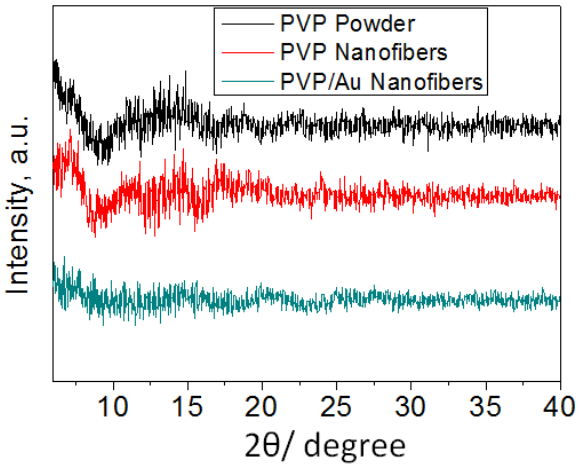

Figure 6.6. WAXD pattern of neat PVP and PVP/Au nanofibers based tubes

6.3.5. Stress-strain analysis

The tensile strength of PVP/Au tubes based on nanofibers, was investigated by the using the *Universal Tensile Testing Machine*. The PVP/Au tubes having diameter 0.2 mm has the highest tensile strength and stress than all other mentioned types of the tubes and when diameter of the tubes is increased, the tensile strength of the tubes is decreased as shown in the Figure 6.7a & 6.7b. In the S-S curve, when the diameter of tubes was increased, the tensile strength of tubes was reduced. It is due to two main reasons, one is high diameter tubes have course/thick nanofibers than smaller diameter tubes. The finer nanofibers have high elongation & strength than thicker nanofibers. Therefore, tube having 0.2 mm has the highest tensile strength than tube having 2.0 mm and second is scientific equation which showed that strength is reversible to diameter; when diameter of tubes is increased then tensile strength of tubes is decreased. Therefore, according to the equation (1), in the S-S curve, the tube having diameter of 0.2 mm has the highest tensile strength than other tubes.

$$\text{Stress (Strength)} = \frac{\text{load(N)}}{\text{Area } (\pi r^2)} \qquad (1)$$

The tensile strength of the PVP/Au tubes based on nanofibers, is 17 MPa, 4 MPa, 1.2 MPa, 0.8 MPa and 0.5 MPa of 0.2 mm, 0.5 mm, 1.0 mm, 1.5 mm and 2.0 mm diameter respectively. The Figure 7b is the magnified form for the graphs of tubes having diameter of 2 mm, 1.5 mm and 1.0 mm. But the main thing which is common in all PVP/Au nanofibers based tubes is bending behavior. These all types of tubes having diameter of 2.0 mm, 1.5 mm, 1.0 mm, 0.5 mm and 0.2 mm showed good bending behavior as shown in Figure 6.8a-e respectively.

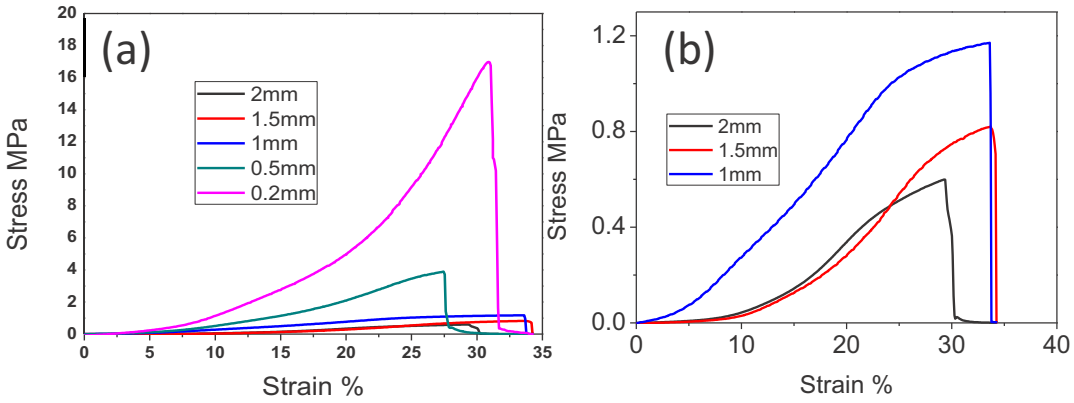

Figure 6.7. Stress-strain behavior of PVP/Au tubes of all diameters (a) and the magnified form of graph of PVP/Au tubes of 2, 1.5 & 1mm diameters (b)

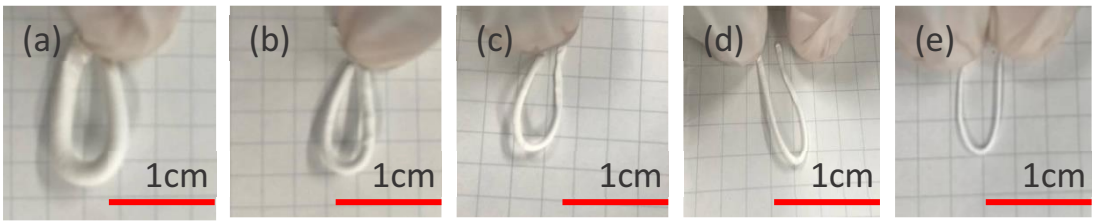

Figure 6.8. Bending behavior of PVP/Au tubes based on nanofibers

6.3.6. Efficiency of potential voltage

In order to investigate the capacity for potential of voltage in each nanofibers based tube, volt meter was used. It was analyzed that capacity of voltage carrying was increased as the diameter of the tubes was increased because when diameter is increased, the area of tube is also increased as shown in Figure 6.9. In the higher area there are more collisions of ions which create more voltage as compared to low area and the addition of Au nanoparticles in the PVP solution also increased the capacity for potential of voltage in the nanofibers based tubes, as mentioned in Figure 6.9.

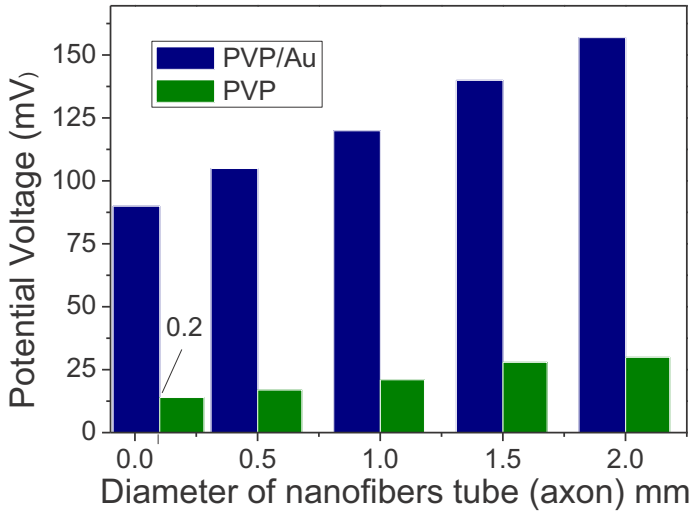

Figure 6.9. The capacity of potential voltage of axon having different diameters

The minimum potential voltage which is suitable for carrying neurosignal in axon must be in the range of -75 mV to +75 mV. The PVP nanofibers based tubes having very small potential voltage which is not suitable for axon. Therefore the nanofibers tubes were fabricated from PVP/Au to enhance the capacity of potential voltage. Obtained data showed that PVP/Au having good potential voltage which is required range for axon as shown in Figure 6.9, but the nanofibers tube having diameter of 0.2 mm made from PVP/Au is most suitable tube for the axon application which has the capacity of potential voltage upto 89 mV and good average diameter of 210 ± 25 nm for the nanofibers of the tube and suitable thickness of 0.039 mm for the tube wall.

6.4. Conclusion

Herein, nanofibers based tubes were successfully fabricated with PVP/Au via electrospinning. All tubes showed better morphology in terms of structural stability, formability and good dispersion of Au nanoparticles on the nanofibers. FT-IR spectra revealed that PVP/Au blend nanofibers exhibited the characteristics peaks of both PVP and Au. WAXD study demonstrated that crystallinity of PVP/Au nanofibers was increased by blending of Au nanoparticles. The study of stress & strain behavior showed that when the diameter of tubes was increased, the tensile strength of tubes was reduced. It is due to two main reasons, one is high diameter tubes have course/thick nanofibers than smaller diameter tubes. The finer nanofibers have high elongation & strength than thicker nanofibers. Therefore, tube having 0.2 mm has the highest tensile strength than tube having 2.0 mm and strength is reversible to diameter; when diameter of

tubes is increased then tensile strength of tubes is decreased. Therefore, according to the equation (1), in the S-S curve, the tube having diameter of 0.2 mm has the highest tensile strength than other tubes. The values of capacity for potential voltage of tubes showed that tubes which were made from neat PVP having very small potential voltage which is not suitable for the potential application of axon but the tubes made from PVP/Au having good potential voltage which was required range for axon. So, the nanofibers tube having diameter of 0.2 mm made from PVP/Au is most suitable tube for the axon application which has the capacity of potential voltage upto 89 mV and good average diameter of 210 ± 25 nm for the nanofibers of the tube and suitable thickness of 0.039 mm for the tube wall, good tensile strength upto 17 MPa and 33% elongation. On the bases of the characterization of PVP/Au, we conclude that this biomaterial may be a better substrate for further in vivo or in vitro investigation to make it useful for tissue engineering.

References

1. Ramakrishna, Seeram, et al. Electrospun nanofibers: solving global issues, *Materials today* 2006; 9.3: 40-50.
2. Davis, Michael E., et al. Local myocardial insulin-like growth factor 1 (IGF-1) delivery with biotinylated peptide nanofibers improves cell therapy for myocardial infarction, *Proceedings of the National Academy of Sciences* 2006; 103.21: 8155-8160.
3. Yoshimoto, H., et al. A biodegradable nanofiber scaffold by electrospinning and its potential for bone tissue engineering, *Biomaterials* 2003; 24.12: 2077-2082.
4. Li, Mengyan, et al. Electrospinning polyaniline-contained gelatin nanofibers for tissue engineering applications, *Biomaterials* 2006; 27.13: 2705-2715.
5. Silva, Gabriel A., et al. Selective differentiation of neural progenitor cells by high-epitope density nanofibers, *Science* 2004; 303.5662: 1352-1355.
6. Pham, Quynh P., Upma Sharma, and Antonios G. Mikos. Electrospinning of polymeric nanofibers for tissue engineering applications: a review, *Tissue engineering* 2006; 12.5: 1197-1211.
7. Sill, Travis J., and Horst A. von Recum. Electrospinning: applications in drug delivery and tissue engineering, *Biomaterials* 2008; 29.13: 1989-2006.
8. Vasita, Rajesh, and Dhirendra S. Katti. Nanofibers and their applications in tissue engineering, *International J. nanomedicine* 2006; 1.1: 15.

9. Chen, Rui, et al. Preparation and characterization of coaxial electrospun thermoplastic polyurethane/collagen compound nanofibers for tissue engineering applications, *Colloids and Surfaces B: Biointerfaces* 2010; 79.2: 315-325.
10. Ji, Yuan, et al. Dual‐Syringe Reactive Electrospinning of Cross‐Linked Hyaluronic Acid Hydrogel Nanofibers for Tissue Engineering Applications, *Macromolecular bioscience* 2006; 6.10: 811-817.
11. Ma, Zuwei, et al. Surface engineering of electrospun polyethylene terephthalate (PET) nanofibers towards development of a new material for blood vessel engineering, *Biomaterials* 2005; 26.15: 2527-2536.
12. Bakhshandeh, Haleh, et al. Poly (ε-caprolactone) nanofibrous ring surrounding a polyvinyl alcohol hydrogel for the development of a biocompatible two-part artificial cornea, *International J. nanomedicine* 2011; 6: 1509.
13. Warnke, Patrick H., et al. Primordium of an artificial Bruch's membrane made of nanofibers for engineering of retinal pigment epithelium cell monolayers, *Acta biomaterialia* 2013; 9.12: 9414-9422.
14. Li, Yumei, et al. Enhanced adhesion and proliferation of human umbilical vein endothelial cells on conductive PANI-PCL fiber scaffold by electrical stimulation, *Materials Science and Engineering: C* 2017; 72: 106-112.
15. Namekawa, Koki, et al. Fabrication of zeolite–polymer composite nanofibers for removal of uremic toxins from kidney failure patients, *Biomaterials Science* 2014; 2.5: 674-679.
16. Barnes, Catherine P., et al. Nanofiber technology: designing the next generation of tissue engineering scaffolds, *advanced drug delivery reviews* 2007; 59.14: 1413-1433.
17. Venugopal, J., and S. Ramakrishna. Applications of polymer nanofibers in biomedicine and biotechnology, *Applied biochemistry and biotechnology* 2005; 125.3: 147-157.
18. Ito, Yoshihiro, et al. A composite of hydroxyapatite with electrospun biodegradable nanofibers as a tissue engineering material, *J. Bioscience and Bioengineering* 2005; 100.1: 43-49.
19. Verreck, Geert, et al. Incorporation of drugs in an amorphous state into electrospun nanofibers composed of a water-insoluble, nonbiodegradable polymer, *J.Controlled Release* 2003; 92.3: 349-360.
20. Park, Honghyun, et al. Plasma-treated poly (lactic-co-glycolic acid) nanofibers for tissue engineering, *Macromolecular Research* 2007; 15.3: 238-243.

21. Albreiki, Raed M. Shubair, et al. Coding brain neurons via electrical network models for neuro-signal synthesis in computational neuroscience, *Electronic Devices, Systems and Applications (ICEDSA), 2016 5th International Conference on*. IEEE.
22. Liedler, A. and Gregor Remmert, Neurostimulation using AC and/or DC stimulation pulses, 2018; U.S. Patent Application No. 15/647,905.
23. Yogev, S. and Kang Shen, Establishing Neuronal Polarity with Environmental and Intrinsic Mechanisms, *Neuron* 2017; 96.3: 638-650.
24. Kaurav, H. and Deepak N. Kapoor, Implantable systems for drug delivery to the brain, *Therapeutic delivery 2017;* 8.12: 1097-1107.
25. Sahoo, Sambit, et al. Growth factor delivery through electrospun nanofibers in scaffolds for tissue engineering applications, *J. biomedical materials research Part A* 2010; 93.4: 1539-1550.
26. Pal, Pinki, Jay Prakash Pandey, and Gautam Sen. Synthesis of polyacrylamide grafted polyvinyl pyrollidone (PVP-g-PAM) and study of its application in algal biomass harvesting, *Ecological Engineering* 2017; 100: 19-27.
27. Cantu, Travis, et al. Conductive polymer-based nanoparticles for laser-mediated photothermal ablation of cancer: Synthesis, characterization, and in vitro evaluation, *International J. nanomedicine* 2017; 12: 615.
28. Schnell, Eva, et al. Guidance of glial cell migration and axonal growth on electrospun nanofibers of poly-ε-caprolactone and a collagen/poly-ε-caprolactone blend, *Biomaterials* 2007; 28.19: 3012-3025.
29. Tysseling-Mattiace, Vicki M., et al. Self-assembling nanofibers inhibits glial scar formation and promotes axon elongation after spinal cord injury, *J. Neuroscience* 2008; 28.14: 3814-3823.
30. Khatri, Zeeshan, et al. Preparation and characterization of electrospun poly (ε-caprolactone)-poly (l-lactic acid) nanofiber tubes, *J. Materials Science* 2013; 48.10: 3659-3664.
31. Abdelrazek, ElMetwally M., et al, Structural, optical, morphological and thermal properties of PEO/PVP blend containing different concentrations of biosynthesized Au nanoparticles, *Journal of Materials Research and Technology* 2017.
32. Cai, Wen, et al, Gold nanorods@ metal-organic framework core-shell nanostructure as contrast agent for photoacoustic imaging and its biocompatibility, *Journal of Alloys and Compounds* 2018.

33. Zhang, Xingwang, et al. Physical characterization of lansoprazole/PVP solid dispersion prepared by fluid-bed coating technique. *Powder technology* 2008; 182.3: 480-485.
34. Petkov, Valeri, et al. Structure of gold nanoparticles suspended in water studied by x-ray diffraction and computer simulations. *Physical review* 2005; *B* 72.19: 195402.

Chapter # 07

***In-vitro* assessment of dual-network electrospun tubes from poly (1, 4 cyclohexane dimethylene isosorbide terephthalate)/PVA hydrogel for blood vessel application**

7.1. Introduction

Tissue engineering is defined as the application of engineering fields to maintain and restore existing tissue structure or to enable tissue growth. The tissue is usually organized into three-dimensional structures as required for the body that believed to the development of specific biological function in the tissue. When used to develop the artificial tissue substitutes, the engineering approaches emphasize the importance of the structural design of the biomaterial employed as scaffolding structure [1-3].

The development of nanofibers has enhanced the scope for fabricating the scaffolds that can potentially mimic the architecture of human tissue at stated requirements. The high surface area to volume ratio of the nanofibers combined with their microporous structure favors the cell adhesion, proliferation, migration, and differentions are the highly desired properties for the tissue engineering applications. Therefore the current research in this area was driven towards the fabrication, characterization, and application of nanofibers as scaffolds for tissue engineering in many fields like ophthalmology, bone regeneration, drug delivery, wound dressings, neuroscience and vascular transplantation [4-8].

Large numbers of people suffer from cardiovascular disease and most of them need proper vascular grafts. Blood vessel tissue engineering has emerged as a promising approach for addressing the shortage of current therapies. A tissue engineering blood vessel should be biocompatible, having appropriate mechanical properties and its availability in a variety of size for grafting applications. It is now an actively investigated field for small diameter vascular graft [9-11]. Recently, the vascular transplantation has been commonly used for the treatment of cardiovascular or vascular diseases by knitted tubular fabrication system [12] and some scaffolds fabricated by the electrospinning of synthetic polymers such as polylactide, poly (lactide-co-glycolide), poly ($_{E}$- caprolactone), collagen and silk fibroin, but there was no good elongation, breaking strength and dimensional stability [13-19]. Very first time, we attempted to develop the blood vessel by dual network composite scaffolds. In which electrospun poly (1, 4 cyclohexane dimethylene isosorbide terephthalate) (PICT) nanofibers were coated with a hydrogel of polyvinyl alcohol (PVA). The hydrogel of PVA was coated on the PICT nanofibers tubes to form the stable, good elongation, suitable breaking strength,

and long-lasting blood vessels because the hydrogel can enhance the strength, mechanical properties and enhance the wetting ability of the composite [20-22]. The dual network composite enhances retention of cells viability and mechanical properties [23-26]. PVA is a biocompatible and biodegradable polymer [27-29] and PICT is new and aromatic semicrystalline co-polyester [30].

In this report, electrospun PICT nanofibers tubes had an inner diameter of 2.0 mm, were composed by coating with a hydrogel of PVA at three different concentrations. The morphology of scaffolds was characterized by SEM, chemical interactions by FT-IR, tensile strength by tensile strength tester, wetting behavior was analyzed by water contact angle meter by drop method and biocompatibility test was done by MTT test.

7.2. Experimental Section

7.2.1. Materials

Polyvinyl alcohol (PVA) (Mw: 85,000-124,000, 99% hydrolyzed was purchased from *Sigma-Aldrich*, USA. Poly (1, 4-cyclohexanedimethylene isosorbide terephthalate) (PICT) was kindly supplied by SK chemicals, Republic of Korea as pellet type. Trifluoroacetic acid (99.9%) and chloroform (99%) were purchased from *Wako Pure Chemical Industries, Ltd,* Japan, and deionized water was used.

7.2.2. Fabrication of nanofibers tubes as scaffolds for blood vessel

10% by weight PICT was dissolved in trifluoroacetic acid and chloroform in 1:3 ratios. The solution was loaded in a plastic syringe connected with capillary tips having an inner diameter of 0.60 mm, in which an electrode of Cu wire was adjusted. The distance from capillary tip to the collector was 15 cm and the supply of voltage was 10 kV. Nanofibers were formed at room temperature and at 45% humidity through electrospinning machine. A rotating & reciprocating element was used to form the nanofibers tubes as shown in Figure 7.1. The nanofibers tubes were fabricated in the same diameter of 2 mm. The resultant nanofibers tubes were immersed in the PVA hydrogel as scaffolds for a blood vessel. The solution of PVA hydrogel was prepared in three different concentrations of PVA (99% hydrolyzed); 5%, 7.5% and 10% by weight. These solutions were dissolved in deionized water and stirred at 70^{o}C for 6 hrs. Then PICT nanofibers tubes were immersed into the resultant PVA hydrogels at 80^{o}C for 12 hrs, frozen at -20^{o}C for 12 hrs and then dried for characterizations.

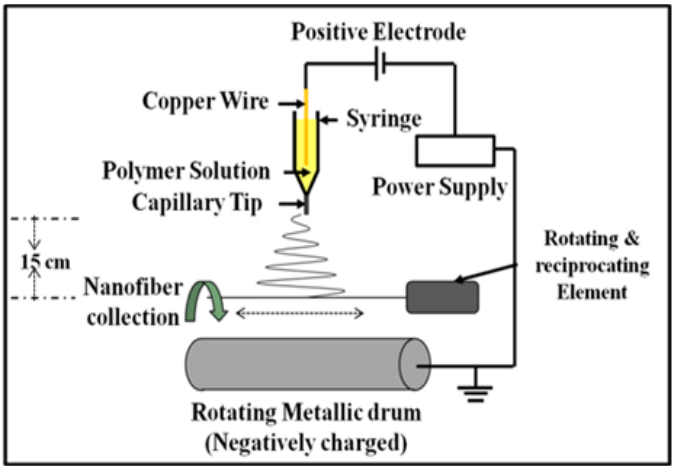

Figure 7.1. Preparation method of nanofibers tubes as scaffolds

7.2.3. Characterizations

The all characterizations of nanofibers based tubes were done according to the standard method of their testing, as described below**;**

Scan electron microscopy (SEM):

The surface morphology of the nanofibers tubes was evaluated by SEM (JSM-5300, JEOL Ltd., Japan) accelerated with the voltage of 12 kV. The average diameter of nanofibers was determined from 20 measurements of the random nanofibers tubes' using image analysis software (Image J, version 1.49) and thickness of tube wall was measured by digital micrometer MCD 130-25 with measuring the sensitivity of ± 1µm.

Fourier transform infrared (FT-IR):

The chemical interactions between PICT and PVA hydrogel were studied by Fourier transform infrared (FT-IR) spectra achieved by IR Prestige -21 (Shimadzu, Japan). The spectra were recorded from 400-4000 cm^{-1} with a resolution of 4 cm^{-1} and the addition of 128 scans.

Tensile Strength Test (ISO 13634*):*

The tensile strength test was performed to check the mechanical behavior of nanofibers by using the Universal Testing Machine (Tesilon RTC 250A, A&D Company Ltd., Japan). According to ISO 13634, the 5 specimens for each sample of different concentrations of PVA hydrogel were prepared under a cross-head

speed of 1 mm/min at room temperature and the values of stress and strain were calculated by the following formulas 1 & 2 respectively.

$$\text{Tensile Strength (MPa)} = \frac{\text{All values of load(N)}}{\text{Area } (\pi r^2)} \qquad (1)$$

$$\text{Elongation } (\%) = \frac{\text{change in length}(\Delta l)}{\text{initial length(l)}} \times 100 \qquad (2)$$

Water contact angle meter:

In order to investigate the wetting behavior of nanofibers tubes, static angle with a contact angle meter by drop method (Kyowa Interface Science, Japan), was used.

MTT study:

In order to investigate the cells attachment behavior of resultant scaffolds, MTT study was done for 72 hrs in line L929 with two-time repeat in triplicate for each sample and cell line. After sterilization, the samples were cultured for 72 hrs in DMEM/F12 with 10% FBS for L929. The cell viability was measured in the percentage of negative control. After 72 hrs, 15% of medium culture which containing *Thiazolyl Blue Tetrazolium Bromide* (MTT; 5mg/ml) was added to each wall and incubated in 37ºC with 5% CO_2 for 5 hrs. After this, the medium was removed and samples were washed with PBS. Formosan crystals were dissolved in 400 µl DMSO. The amount of 200 µl of each solution transferred into the new 96 wells and the absorbance was measured at 570 nm. To measure the dye absorption by the scaffolds, all samples without any cells were immersed in a medium culture with the addition of MTT, then washed with DMSO and absorbance was read at 570 nm. For the estimation of the number of cells adhering to the scaffolds, the absorbance of scaffolds was subtracted from the absorbance in the presence of cell line L929.

7.3. Results and discussion

7.3.1. Morphology Analysis

In order to investigate the surface morphology of the nanofibers tubes as scaffolds for a blood vessel, scan electron microscopy was studied as shown in Figure 7.2. It was analyzed that PICT nanofibers tubes and PICT/PVA nanofibers tubes have the good and dimensional stable morphology. PICT/PVA nanofibers tubes showed the relatively good cohesiveness in nanofibers that led the scaffolds compact with cross section close to a circular shape. The neat PICT nanofibers tubes were fixed and its nanofibers were entangled & overlapped to each other but PICT/PVA nanofibers tubes showed the elongated and flexible structure. This

study also showed that there was a great effect of coating the PVA hydrogel on the morphology and structure of PICT/PVA nanofibers tubes. Because when neat PICT nanofibers tubes were immersed in the PVA hydrogel at 80°C for 12 hrs, the PICT/PVA nanofibers tubes elongated and their thickness reduced. It is due to the extraction of nanofibers whcih converted into elongated structure and width of nanofibers tubes also decreased as shown in Figure 7.2 & Table 7.1.

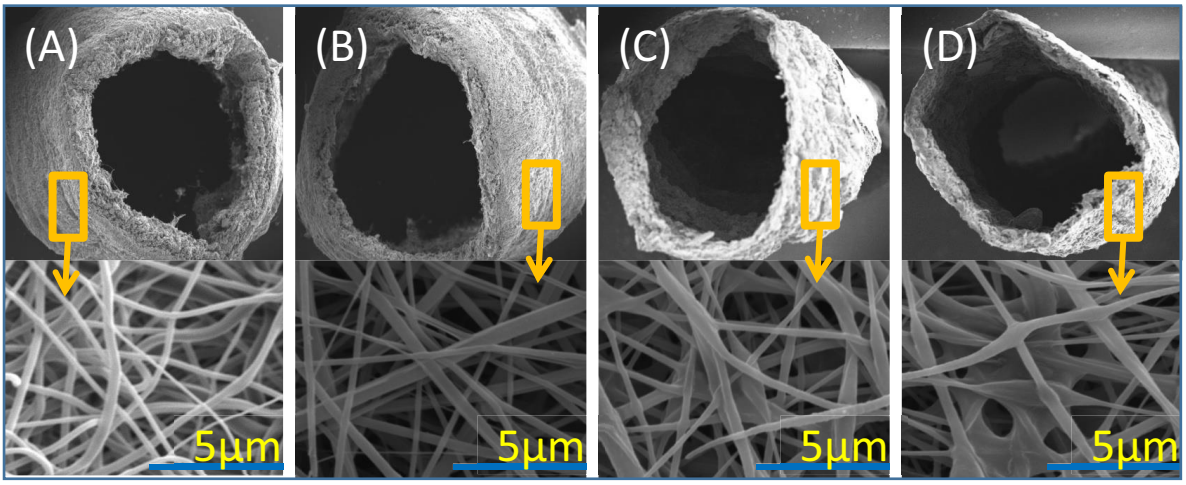

*Figure 7.2. SEM images of nanofibers tube having a diameter of 2.0 mm (a) neat PICT nanofibers tube, (b) 5% wt. PVA hydrogel in PICT/PVA nanofibers tube, (c) 7.5% wt. PVA hydrogel in PICT/PVA nanofibers tube, (d) 10% wt. PVA hydrogel in PICT/PVA nanofibers tube.**Figure 7.2. SEM images of nanofibers tube having a diameter of 2.0 mm (a) neat PICT nanofibers tube, (b) 5% wt. PVA hydrogel in PICT/PVA nanofibers tube, (c) 7.5% wt. PVA hydrogel in PICT/PVA nanofibers tube, (d) 10% wt. PVA hydrogel in PICT/PVA nanofibers tube.*

Table 7.1. Specifications of nanofibers tubes

Sr. #	The diameter of nanofiber tubes, (mm)	The thickness of tube wall (mm)	Materials
1	2.0	0.045 ± 0.010	Neat PICT
2	2.0	0.042 ± 0.013	5% PVA/PICT
3	2.0	0.040 ± 0.009	7.5% PVA/PICT
4	2.0	0.038 ± 0.011	10% PVA/PICT

7.3.2. Chemical Interactions Analysis

In order to investigate the chemical interactions analysis of neat PICT, PICT/PVA nanofibers tubes, FT-IR spectra were analyzed as shown in Figure 7.3. It was analyzed that there were successful chemical interactions between PICT and hydrogel of PVA as shown in Figure 7.3 & Table 7.2. FT-IR spectra showed that there was strong stretching of CH in CH and CH_2 groups in neat PVA, 5% PVA/PICT, 7.5% PVA/PICT and 10 % PVA/PICT nanofibers tubes at 2922 cm^{-1}, also there was CH bending in CH and CH_2 groups in neat PICT [31,32], 5% PVA/PICT, 7.5% PVA/PICT and 10 % PVA/PICT nanofibers tubes at 1455 cm^{-1}. The stretching of C-O group in neat PICT, 5% PVA/PICT, 7.5% PVA/PICT and 10 % PVA/PICT nanofibers tubes at 1050 cm^{-1} [33] also showed the successful chemical interaction between PICT and PVA hydrogel.

Table 7.2. FT-IR Spectra details

Functional Group	***Absorption(s)(cm^{-1})***	***Notes***
CH_2	2922	CH stretching in CH and CH2 groups (a)
C=O	1666	Stretching (a)
CH	1456	CH blending (a)
C=C	1580	Stretching (b)
Aromatic	1600	Strong stretching (b)
C=O	1641	Stretching (b)
CH	1455	CH blending (b)
C-O	1050	Stretching (b), (c), (d) and (e)
CH_2	2922	CH stretching in CH and CH2 groups (c), (d) and (e)
OH	3200	Stretching (a), (c), (d) and (e)

CH	1456	CH blending (c), (d) and (e)

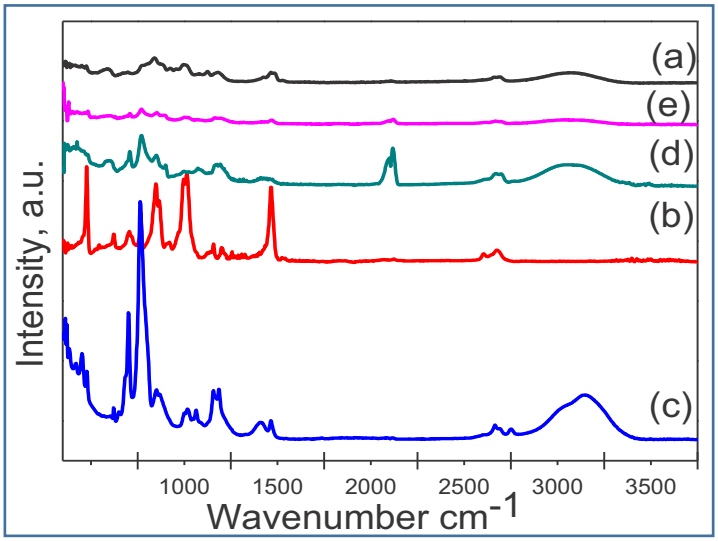

Figure 7.3. FT-IR spectra of nanofibers tube having a diameter of 2.0 mm (a) neat PVA, (b) neat PICT nanofibers tube (c) 5% wt. PVA hydrogel in PICT/PVA nanofibers tube, (d) 7.5% wt. PVA hydrogel in PICT/PVA nanofibers tube, (e) 10% wt. PVA hydrogel in PICT/PVA nanofibers tube.

7.3.3. Water contact angle analysis

In order to investigate the wetting behavior of PICT and PICT/PVA nanofibers tubes, static angle with a contact angle meter by drop method was used as shown in Figure 7.4. It was analyzed that neat PICT nanofibers are water resistant nanofibers and showed contact angle at 130 $\pm$5, but the PICT/PVA nanofibers tubes having 5% PVA hydrogel, 7.5% PVA hydrogel and 10% PVA hydrogel have contact angles at 108$\pm$2, 97$\pm$3 & 83$\pm$2, respectively as shown in Figure 7.4. It means water absorbency was increased as PVA hydrogel was coated/blended into PICT nanofibers because there were chemical interactions between PVA and PICT, OH group of PVA increased the hydrophilicity of PICT. Therefore when more PVA was coated, as more OH group was interacted into PICT/PVA nanofibers tubes, which made them hydrophilic [34]. It means this wetting behavior is appreciable for scaffolds as a blood vessel.

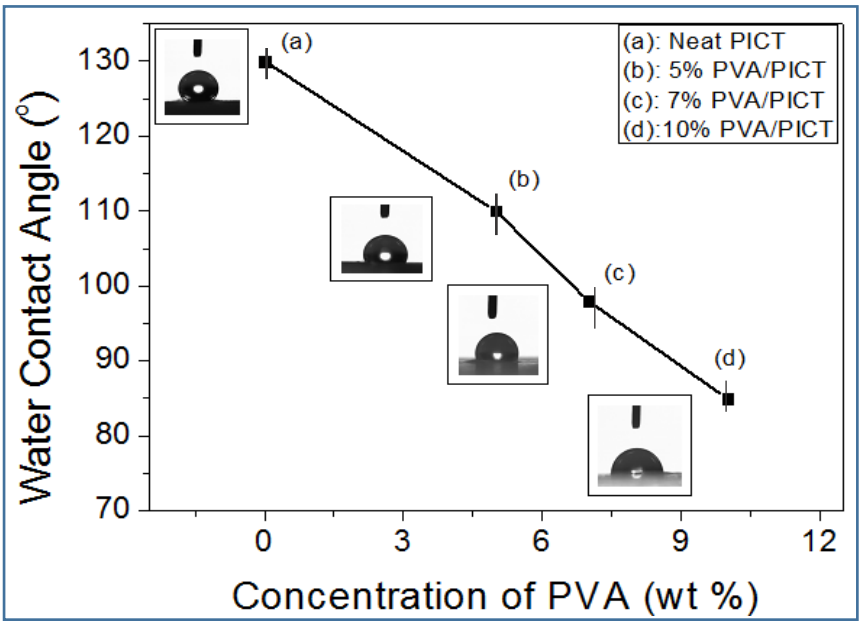

Figure 7.4. Wetting behavior of nanofibers tubes.

7.3.4. Tensile strength analysis (ISO 13634)

The stress-strain behavior of PICT and PICT/PVA nanofibers tubes was investigated by *Universal Testing Machine* and results were shown in **Figure 5**. It was observed that neat PICT nanofibers tubes have high capacity for bearing the stress up to 8 MPa and elongation up to 7%, but 5% PICT/PVA, 7.5% PICT/PVA and 10% PICT/PVA nanofibers tubes have the ability to bear the stress up to 3 MPa, 1.6 MPa & 0.75 MPa and elongation up to 13%, 38% & 47.5%, respectively. So, PICT/PVA nanofibers tubes have low stress but high elongation than neat PICT, but high stress and low elongation than neat PVA as shown in Figure 7.5. It also showed that when the concentration of PVA hydrogel was increased, the elongation of nanofibers tubes was increased but stress bearing ability was reduced. It is due to immersing of PICT into PVA hydrogel at 80°C, which elongated its dimensions. So, these properties about stress-strain behavior may good for scaffolds because for a blood vessel, elongation is necessary.

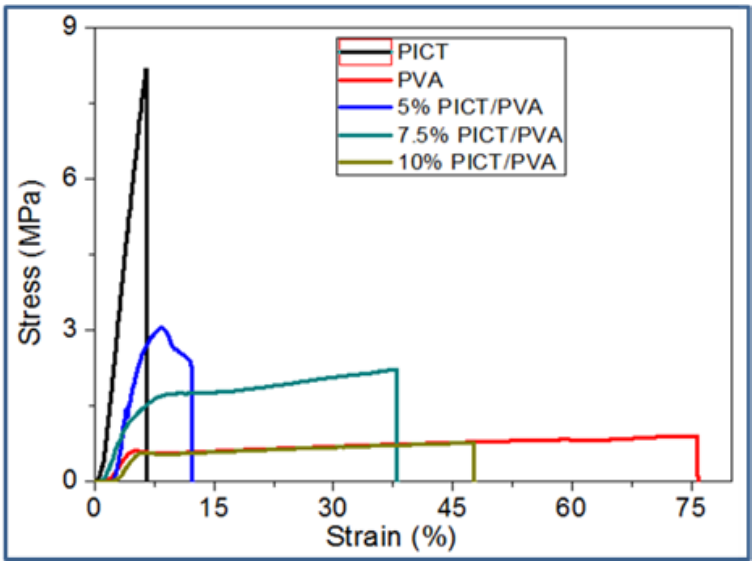

Figure 7.5. Stress-Strain Behavior of nanofibers tubes

7.3.5. *In-vitro* analysis

The *in-vitro* study was done to investigate the cytotoxicity with respect to the cell attachments of scaffolds by MTT assessment. The MTT assessment was done by using cell line L929 for 72 hrs. The resultant data was reported as a percentage of negative control as shown in Figure 6. It was analyzed that L929 cells attached to PICT/PVA scaffolds and cells attached in greatest numbers to scaffolds. Each sample showed well attachment of cells and no toxicity but 5% by weight PVA/PICT showed great potential for cells attachment than other samples as shown in Figure 7.6. The increasing concentration of PVA hydrogel in the scaffolds reduced the attachment of cells due to the blocking of pores in the scaffolds by overlapping the surface of the scaffolds, but the positive and negative controls showed the expected results against the cytotoxicity. The positive control showed that there was 99.9 % cell death (Figure 7.6e) but negative control showed no toxicity. It showed response with a few malformed cells due to physical damage raised from the overlying scaffolds as shown in Figure 7.6. It also showed that this composite is nontoxic due to the good performance of PVA in the PICT/PVA nanofibers composites. So, the resultant scaffolds are nontoxic to the human blood vessel.

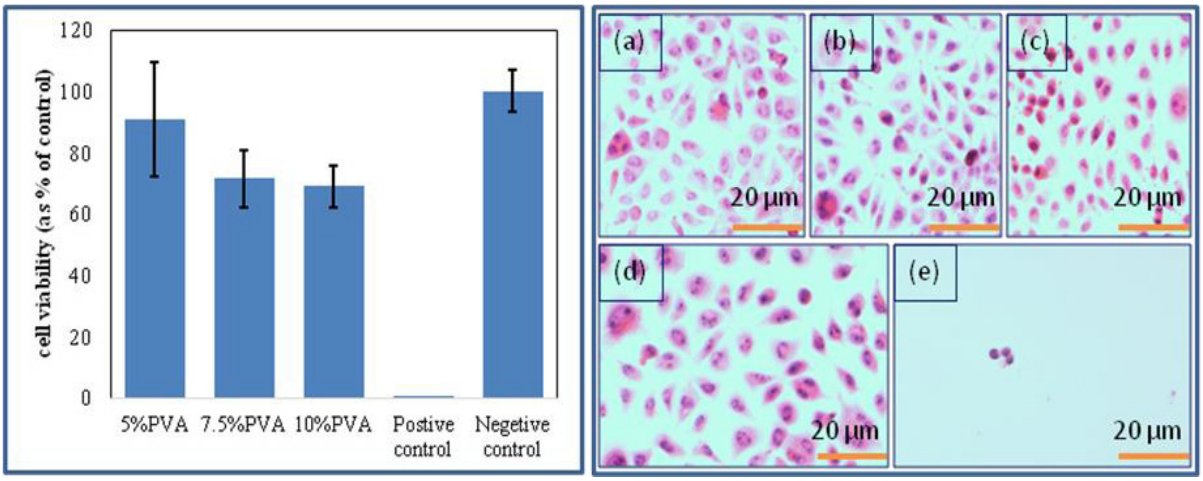

Figure 7.6. MTT analysis of PICT/PVA scaffolds. (a) 5% PICT/PVA nanofibers tubes, (b) 7.5% PICT/PVA nanofibers tubes, (c) 10% PICT/PVA nanofibers tubes, (d) Negative control and (e) Positive control

7.4. Conclusions

Herein, tubular scaffolds for blood vessel were fabricated successfully by coating poly (1, 4 cyclohexane dimethylene isosorbide terephthalate) electrospun nanofibers with PVA hydrogel. The scaffolds possessed dual network polymers may increase the main requirements to preparing artificial blood vessels as well as high tensile strength with excellent biocompatibility. All investigated characterization results showed that the resultant scaffolds are appropriate candidates for blood vessel tissue engineering due to its dual network performance, where PVA performed for biocompatibility and excelent elongation and PICT performed for approperiate tensile strength and dimensional stability for blood vessel. Therefore this research is fruitfull to fulfill the stated and implied needs of society.

References

[1]. L. Matthias W. and M. D. Menger, Trends in biotechnology. 2017, 35.2, 133-144.

[2]. M. Maya, P. Kedar, and Supriya Bansode, Tissue engineering. 2017, 2.4.

[3]. J. M. Steven and G. V. Novakovic, Tissue Engineering ja 2017.

[4]. M.Q. Khan, Lee, H., Khatri, Z., Kharaghani, D., Khatri, M., Ishikawa, T., Im, S.S. and Kim, I.S., Materials Science and Engineering: C. 2017, 81, pp.247-251.

[5]. M.Q. Khan, Lee, H., Koo, J.M., Khatri, Z., Sui, J., Im, S.S., Zhu, C. and Kim, I.S., Textile Research Journal. 2017, p.0040517517723026.

[6]. Hu, Jue, et al. Materials Science and Engineering: C. 2017, 70 1089-1094.

[7]. Qureshi, U.A., Khatri, Z., Ahmed, F., Khatri, M. and Kim, I.S., ACS Sustainable Chemistry & Engineering, 2017, 5(5), pp.4340-4351.

[8]. Lee, H., Xu, G., Kharaghani, D., Nishino, M., Song, K.H., Lee, J.S. and Kim, I.S., International journal of pharmaceutics. 2017, 531(1), pp.101-107.

[9]. Augustine, R., Dan, P., Sosnik, A., Kalarikkal, N., Tran, N., Vincent, B., Thomas, S., Menu, P. and Rouxel, D., Nano Research. 2017, 10(10), pp.3358-3376.

[10]. Wu, Y., Liu, G., Chen, W., Yang, M. and Zhu, C., Journal of Biomedical Materials Research Part B: Applied Biomaterials. 2017, 105(4), pp.744-752.

[11]. Ayala, P., Dai, E., Hawes, M., Liu, L., Chaudhuri, O., Haller, C.A., Mooney, D.J. and Chaikof, E.L., Journal of Biomedical Materials Research Part B: Applied Biomaterials, 2017.

[12]. Zhang, L., Ao, Q., Wang, A., Lu, G., Kong, L., Gong, Y., Zhao, N. and Zhang, X., Journal of biomedical materials research Part A. 2006, 77(2), pp.277-284.

[13]. Marcolin, C., Draghi, L., Tanzi, M., and Faré, S., J. Materials Science: Materials in Medicine, 2017, 28(5), 80.

[14]. Vaz, C.M., Van Tuijl, S., Bouten, C.V.C. and Baaijens, F.P.T., Acta biomaterialia. 2005, 1(5), pp.575-582.

[15]. He, W., Yong, T., Teo, W.E., Ma, Z. and Ramakrishna, S., Tissue engineering. 2005, 11(9-10), pp.1574-1588.

[16]. Badhe, R. V., Bijukumar, D., Chejara, D. R., Mabrouk, M., Choonara, Y. E., Kumar, P., and Pillay, V., Carbohydrate polymers, 2017, *157*, 1215-1225.

[17]. Khatri, Z., Nakashima, R., Mayakrishnan, G., Lee, K.H., Park, Y.H., Wei, K. and Kim, I.S., Journal of Materials Science. 2013, 48(10), pp.3659-3664.

[18]. Hasan, A., Memic, A., Annabi, N., Hossain, M., Paul, A., Dokmeci, M.R., Dehghani, F. and Khademhosseini, A., Acta biomaterialia. 2014, 10(1), pp.11-25.

[19]. Augustine, R., Dan, P., Sosnik, A., Kalarikkal, N., Tran, N., Vincent, B. and Rouxel, D., Nano Research, 2017 *10*(10), 3358-3376.

[20]. Koike, N., Fukumura, D., Gralla, O., Au, P., Schechner, J.S. and Jain, R.K., Nature. 2004, 428(6979), p.138.

[21]. Bhowmick, S., Mohanty, S. and Koul, V., Journal of Materials Science: Materials in Medicine. 2016, 27(11), p.160.

[22]. Nonoyama, T., Wada, S., Kiyama, R., Kitamura, N., Mredha, M., Islam, T., Zhang, X., Kurokawa, T., Nakajima, T., Takagi, Y. and Yasuda, K., Advanced Materials. 2016, 28(31), pp.6740-6745.

[23]. Rodell, C.B., Dusaj, N.N., Highley, C.B. and Burdick, J.A., Advanced materials. 2016, 28(38), pp.8419-8424.

[24]. Nonoyama, T., Wada, S., Kiyama, R., Kitamura, N., Mredha, M., Islam, T., Zhang, X., Kurokawa, T., Nakajima, T., Takagi, Y. and Yasuda, K., Advanced Materials. 2016, 28(31), pp.6740-6745.

[25]. Choi, S., Choi, Y.J., Jang, M.S., Lee, J.H., Jeong, J.H. and Kim, J., Adv. Funct. Mater. 2017, 27(42).

[26]. Gong, J.P., Katsuyama, Y., Kurokawa, T. and Osada, Y., Advanced Materials. 2003, 15(14), pp.1155-1158.

[27]. Yuan, F., Ma, M., Lu, L., Pan, Z., Zhou, W., Cai, J., Luo, S., Zeng, W. and Yin, F., Cellular and molecular biology (Noisy-le-Grand, France). 2017, 63(5), pp.32-35.

[28]. Kumar, A. and Han, S.S., International Journal of Polymeric Materials and Polymeric Biomaterials. 2017, 66(4), pp.159-182.

[29]. Asghari, F., Samiei, M., Adibkia, K., Akbarzadeh, A. and Davaran, S., Artificial cells, nanomedicine, and biotechnology. 2017, 45(2), pp.185-192.

[30]. Nam, D., Hoik L., and Kim, I.S., Nanomaterials. 2017, 8(2), p.56.

[31]. Khan, M. Q., Lee, H., Khatri, Z., Kharaghani, D., Khatri, M., Ishikawa, T., and Kim, I. S., Materials Science and Engineering: C. 2017*81*, 247-251.

[32]. Phan, D. N., Lee, H., Choi, D., Kang, C. Y., Im, S. S., and Kim, I. S., Nanomaterials. 2018, *8*(2), 56.

[33]. Kharaghani, D., Lee, H., Ishikawa, T., Nagaishi, T., Kim, S. H., and Kim, I. S., Textile Research Journal. 2018, 0040517517753635.

[34]. Zheng, Q., Cai, Z., & Gong, S., Journal of Materials Chemistry A. 2014*2*(9), 3110-3118.

Chapter # 08

The fabrications and characterizations of antibacterial PVA/Cu nanofibers composite membranes by synthesis of Cu nanoparticles from solution reduction, nanofibers reduction and immersion methods.

8.1. Introduction

Over the past decade, nano-sized metal materials have attracted much technological and scientific attention as a result of their interesting size dependent chemical and physical properties and wide applications in biotechnology, electronics, magnetism, and optics. Among all metals, copper (Cu) is the most commonly used metal because of its antibacterial and high electrical conductivity. A number of methods have been developed to fabricate the uniform and controllable dimensions of Cu nanoparticles, such as reduction of Cu compounds, vacuum vapor deposition, vapor-solid reaction growth and electrochemical deposition [1-5]. However, the main concern with utilizing Cu NPs is their tendency to aggregate when they blended with a polymer matrix, which results in low efficiency and resulting composites that have non uniform characteristics but eco-friendly issues associated with the tendency of Cu nano composites to release Cu. This is concern that the presences of CuNPs in aquatic environment could potentially cause adverse impacts on ecosystem and human health. So, preventing the release of CuNPs from composite materials is essential if it has to be used as commercial products [6]. The composites materials which made from electrospun nanofibers have several advantages due to the high surface area, high area to volume ratio and high porosity which make it promising materials for use as separation filters, protective clothing, sensors, wound dressings and tissue scaffolds [7-11].

The biomedical field is one of the important application areas of the electrospun nanofibers. electrospinning has attracted great interest among researchers because it is very simple, low cost and with effective technology to produce polymer nanofibers [12,13]. By utilizing electrospinning technique, the biomedical field can be enriched widely due to synthesis methods used to produce metal composite nanofibers [14]. Typically, Cu NPs are embedded with a polymer matrix to prepare the electrospinning solution because it is the simplest way to fabricate the Cu loaded nanofibers. Another method is the immersion/dipping method in which nanofibers are immersed/dipped in the solution that contains Cu particles or Cu^{+} ions, resulting in the Cu species absorbed by the electrospun nanofibers. In addition, the reduction of Cu^{+} ion is an important step in the preparation of Cu loaded PVA nanofibers[15-20]. However, in these methods, there was no investigation regarding to determine the best method of synthesis of Cu nanoparticles for the promising

nanofibers composites which have the strong attractions between Cu and desired or stated polymers for providing disparity to produce huge amount of Cu nanoparticles on the surface of nanofibers and also no antibacterial study was done. Therefore we attempted to synthesize the Cu nanoparticles for loading on the cross linked PVA nanofibers in three different ways to make the antibacterial nanofibers membranes. The objective was to investigate and optimize methods for preventing the release of Cu nanoparticles from the PVA nanofibers in order to provide the high amount of Cu nanoparticles on the nanofibers for antibacterial properties.

In this report, we developed the antibacterial PVA/Cu nanofibers membranes through different fabrication methods of effective loading of Cu nanoparticles on the PVA nanofibers. We fabricated the Cu nanoparticles in three different methods; a) Nanofibers Reduction method, b) Solution Reduction method & c) Immersion method. The resultant membranes were characterized by SEM & TEM for morphology of nanofibers, FTIR for chemical interactions between PVA and Cu, XPS for presence of Cu element, Tensile test for the stress-strain behavior, ICP for release behavior, water contact angle for suitable absorbency and antibacterial activity was done to analyze the efficiency of the membranes for bacteria resistance.

8.2. Experimental

8.2.1. Materials

All of the chemical materials were analytical grade which was used in the experiment. Copper sulfate ($CuSO_4$, purity of 99.8%), sodium hydroxide (NaOH, purity of 97.0%) and hydrochloric acid (HCl, 35.0-37.0%) were purchased from Wako Pure Chemical Industries, Ltd. Poly vinyle alcohol (PVA, MW: 85,000-124,000, 87-89% hydrolyzed) was purchased from Sigma Aldrich Chemicals, and glutaraldehyde (GA, 50% in aqueous solution) was purchased from MP Biomedical. The deionized water was used in the experiment.

8.2.2. Preparations of PVA/Cu nanofibers membranes

The aqueous solution of PVA (10 wt%) was prepared by stirring the solution vigorously at 70 ºC for 5 hrs and 0.024 wt% of Ga was blended with PVA solution at room temperature. The copper wire connected as a +ve electrode. The distance from plastic tip to the collector was 13 cm and 12 kV voltages were supplied for electrospinning. In all methods, the prepared solutions were loaded in the plastic syringe with capillary tips having an inner diameter of 0.60 mm. Every method is described below.

Nanofiber reduction method: $CuSO_4$ (0.1 wt% to PVA/Ga solution) was added in the prepared PVA/Ga solution and followed by stirring 1 hr. The Cu^+/PVA/Ga solution was prepared and loaded in the plastic syringe for electrospinning to fabricate the Cu^+-loaded PVA nanofibers. After drying the resultant nanofibers were exposed to HCl vapor in desiccators at 40 ^oC for 60 seconds, and then the nanofibers mat was immersed in a 0.1 wt% NaOH solution for 24 hrs to reduce the Cu^+ ions to Cu nanoparticles on the nanofibers.

Solution reduction method: $CuSO_4$ (0.1 wt% to PVA/Ga solution) was added in the prepared PVA/Ga solution and followed by stirring 1 hr. Then NaOH (1:1 ratio with Cu^+) was added to the solution to reduce the Cu^+ ions to Cu nanoparticles. During stirring, the color of the solution changed to dark brown due to the reduction of Cu^+ to Cu nanoparticles. The solution of Cu nanoparticles and PVA was loaded for electrospinning to fabricate the PVA/Cu nanofibers. The resultant nanofibers mat was dried at ambient conditions to remove the residual solvent and nanofibers mat was exposed to HCl vapor in desiccators at 40 ^oC for 60 seconds. HCl & Ga reacted to generate the 3D network structure in the PVA nanofibers which enhanced the water resistance of the nanofibers.

Immersion method: The prepared PVA/Ga solution was loaded for electrospinning to fabricate the nanofibers. The resultant nanofibers were placed in HCl atmosphere to generate the cross-linked nanofibers for the resistance of water. The crosslinked PVA nanofibers mat was immersed for 24 hrs in 0.1 wt% $CuSO_4$ solution and then these resultant nanofibers mat was again immersed in 0.1 wt% NaOH solution for 24 hrs to reduce the Cu^+ to Cu nanoparticles.

All of the resultant nanofibers membranes were washed with deionoized water for the removal of any excessive HCl or NaOH from the nanofibers. The nanofibers mat was immersed in deionized water for 30 minutes and water was changed in every 10 minutes. The PVA/Cu nanofibers were dried at ambient conditions for 24 hrs to remove any residual solvent.

8.2.3. Characterizations

The morphology of PVA nanofibers and PVA/Cu nanofibers was investigated by scanning electron microscopy (SEM)(S-3000N, Hitachi Co., Japan) at 12 kV accelerating voltage. For the analysis of Cu nanoparticles dispersion on the PVA nanofibers, transmission electron microscopy (2010 Fas TEM, JEOL Japan) was used at 200 kV accelerating voltage. The average diameter of the PVA & PVA/Cu nanofibers

was determined by analyzing the SEM images using the image J software. Fourier transform infrared (FT-IR) spectra were recorded between the wavelengths of 400-4000 cm^{-1} using an IR Prestige-21 (Shimadzu Co., Ltd) and studied for the chemical interactions between PVA & Cu nanoparticles. For the confirmation of the presence of Cu nanoparticles in the PVA/Cu nanofibers, X-ray photoelectron spectroscopy (XPS) was used. XPS was conducted on a Shimadzu-Kratos AXIS-ULTRA HAS SV (Shimadzu Co., Ltd) using an Al X-ray source, set at 10 kV and 15 mA. The release behavior of the Cu from the PVA/Cu nanofibers was examined by an inductively coupled plasma (ICP) atomic emission spectrometer (SHIMADZU/ICPS, 10000IV, Japan) over a period of 72 hrs by immersing the nanofibers in deionized water and stirring very slowly at room temperature.

8.3. Results and discussions

8.3.1. Morphology analysis

In order to investigate the surface morphology of the PVA & PVA/Cu nanofibers, scanning electron microscope was used. It was analyzed that surface morphology was changed as Cu nanoparticles were embedded in or synthesized on the PVA nanofibers as shown in Figure 8.1. The surface morphology was clearly changed in nanofibers reduction method as shown in Figure 8.1b and nanofiber's diameter size was also changed due to the blending of Cu nanoparticles into the PVA nanofibers as shown in Figure 8.1. The diameter size of neat PVA nanofibers is smaller than others method. The highest diameter size is in PVA/Cu nanofibers which were obtained from the immersion method as shown in Figure 8.1c.

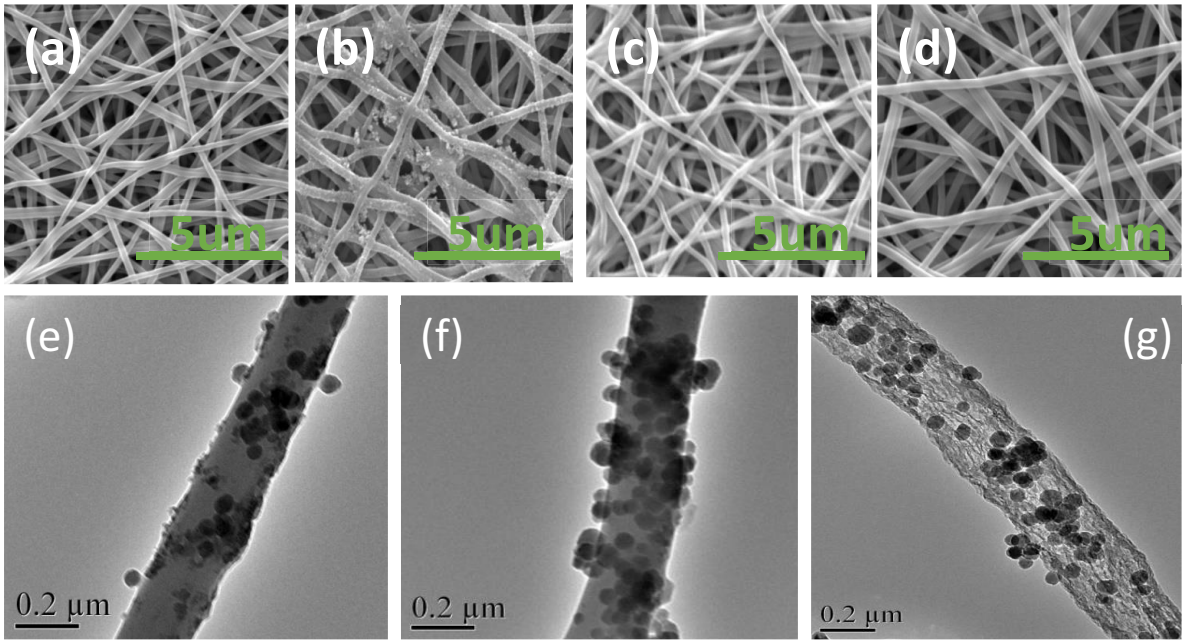

Figure *8.1. SEM results of (a) neat PVA nanofibers, (b) PVA/Cu nanofibers by nanofibers reduction, (c) PVA/Cu nanofibers by solution reduction, (d) PVA/Cu nanofibers by immersion method. TEM results of (e) nanofibers reduction, (f) solution reduction, (g) immersion method.*

In order to further investigation of the morphology of PVA/Cu nanofibers and dispersion of Cu nanoparticles on the surface of PVA/Cu nanofibers, transmission electron microscopy was studied. It was observed that in all methods of synthesis of Cu nanoparticles in the PVA nanofibers, the dispersion of Cu nanoparticles was uniform and appreciable dispersion which is good for wound dressings effect as shown in Figure 8.1e, 8.1f & 8.1g and the amount Cu nanoparticles was differently loaded on PVA/Cu nanofibers in all methods, but the amount of Cu nanoparticles loaded by immersion method was highest than all other methods as shown in Figure 8.1g due to good dispersion and absorption on the high surface of nanofibers because in immersion method Cu^{+} ions on the surface of nanofibers were reduced by immersing the nanofibers in NaOH solution. Therefore Figure 8.1g showed a relatively large amount of Cu nanoparticles in PVA nanofibers as compared to other methods. The amount of Cu nanoparticles was highest in the immersion method which was 28 NPs/µm^2. In other two methods, there were 22 NPs/µm^2 and 20 NPs/µm^2 in nanofibers reduction method and solution reduction method respectively.

8.3.2. FR-IR study

In order to investigate the chemical interactions between PVA & Cu nanoparticles, FT-IR spectra were studied as shown in Figure 8.2a. It was observed that the extensive band at 3350 cm^{-1} for PVA nanofibers was related to the stretching vibrations of OH functional group and the band at 2920 cm^{-1} was assigned to

the stretching vibrations of CH_2. The PVA/Cu nanofibers prepared by nanofibers reduction & immersion method showed different spectra than the spectra of neat PVA and PVA/Cu nanofibers by solution reduction method. The difference between the synthesis methods was at the point where reduction happened. In both nanofibers reduction method and immersion method Ag^+ ions to nucleate the Ag nanoparticles after generating a chemical interaction between Ag^+ ions and OH group in PVA nanofibers but in the solution reduction method Ag^+ ions reduced in the PVA solution. In solution reduction method the peak intensity at 1730 cm^{-1} showed the carbonyl group of Ga and its intensity was decreased in other methods as shown in Figure 8.2a due to interaction of carbonyl group of Ga with Ag^+ ions and Ag nanoparticles, similarly the peak intensity of C-O stretching of PVA at 1247 cm^{-1} was also decreased in nanofibers reduction and immersion methods than neat PVA and PVA/Cu nanofibers by solution reduction method. So it is concluded that there were successful chemical interactions between PVA and Cu nanoparticles through all methods.

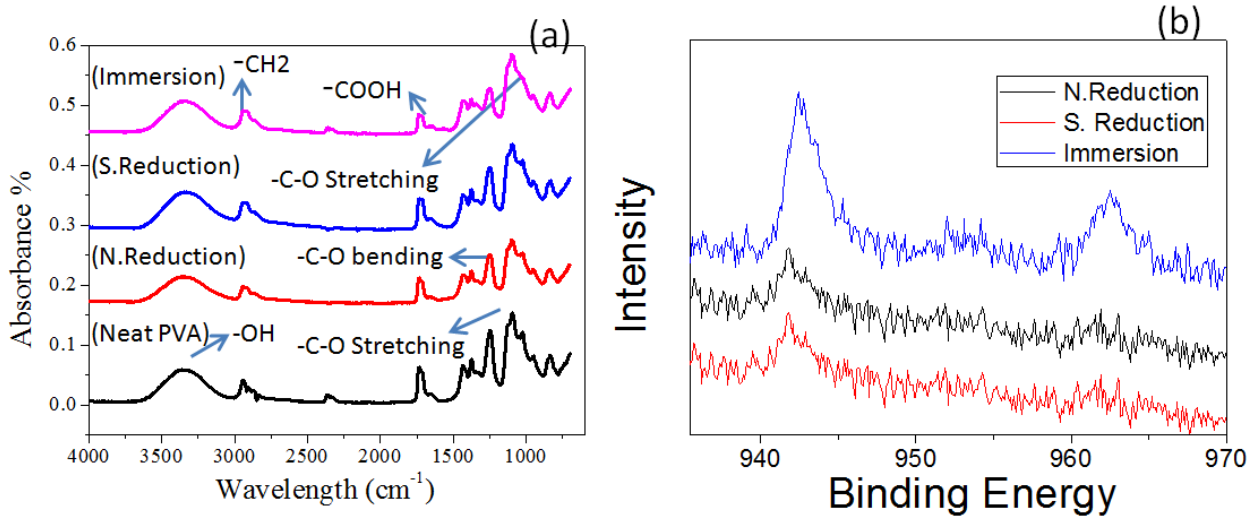

Figure 8.2. Chemical interactions of (a) FT-IR Spectra of neat PVA nanofibers, PVA/Cu nanofibers by nanofibers reduction, PVA/Cu nanofibers by solution reduction, and PVA/Cu nanofibers by immersion method. (b) XPS study of PVA/Cu nanofibers by nanofibers reduction, solution reduction, and immersion method.

8.3.3. XPS study

In order to investigate the presence of the Cu in the PVA/Cu nanofibers, XPS spectra were studied as shown in Figure 8.2b. It was analyzed that Cu was successfully synthesized through all methods. Cu 2p peaks of all PVA/Cu nanofibers were presented in two peaks, one at 942 .5 eV and other at 952 eV. The binding energy peaks of 942 .5 eV and 952 eV were assigned to $2p3_{/2}$ and $2p_{1/2}$, respectively. Typically, the area of the peak represents the amount of Cu nanoparticles and these spectra also strongly implied that immersion method has

the largest amount of Cu nanoparticles in the PVA/Cu nanofibers as shown in the Figure 8.2b. The ratios of the peak areas for three different methods were 8:3:2.8. It showed that Cu naoparticles were successfully synthesized by all methods for wound dressings.

8.3.4. EDS spectra

In order to investigate the element contribution in PVA & PVA/Cu nanofibers, EDS spectra were studied as shown in Figure 8.3. It was observed that in neat PVA there are no Cu nanoparticles as shown in Figure 8.3a but Figure 8.3b, Figure 8.3c, and Figure 8.3d showed that Cu nanoparticles were well embedded in PVA/Cu nanofibers by nanofibers reduction, solution reduction and immersion methods. There were well weight percentages of Cu nanoparticles in PVA/Cu nanofibers through each method. There was 1.03, 0.91 and 0.45 weight percentage of Cu nanoparticles in the PVA/Cu nanofibers by immersion method, solution reduction and nanofibers reduction methods, respectively as shown in Figure 8.3.

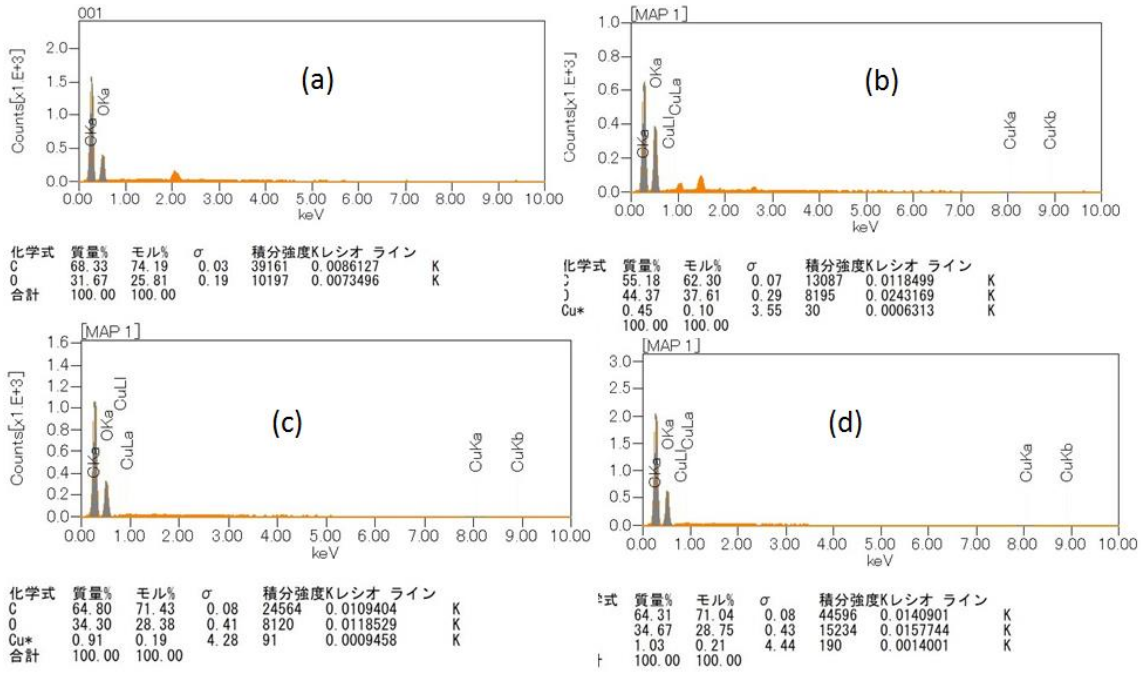

Figure 8.3. EDS spectra of (a) neat PVA nanofibers, (b) PVA/Cu nanofibers by nanofibers reduction, (c) PVA/Cu nanofibers by solution reduction, (d) PVA/Cu nanofibers by immersion method.

8.3.5. Water contact angle

In order to investigate the wetting behavior of PVA & PVA/Cu nanofibers, static angle with a contact angle meter by drop method was used as shown in Figure 8.4. It was analyzed that neat PVA nanofibers are water absorbent nanofibers at contact angle 78 $\pm$5. But the PVA/Cu nanofibers having absorbency at contact angle

55±5, 48±5 & 57±5 for nanofibers reduction method, solution reduction method and immersion method respectively as shown in Figure 8.4. It means water absorbency was increased as Cu nanoparticles were blended into PVA nanofibers.

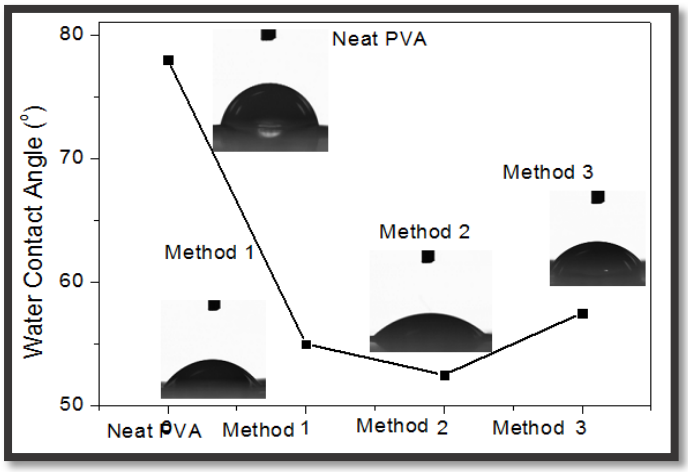

Figure 8.4. Water contact angle results of (a) neat PVA nanofibers, (b) PVA/Cu nanofibers by nanofibers reduction, (c) PVA/Cu nanofibers by solution reduction, and (d) PVA/Cu nanofibers by immersion method.

8.3.6. Stress-strain behavior

The stress-strain behavior of PVA & PVA/Cu nanofibers was investigated by *Universal Testing Machine* and results were shown in Figure 8.5a. It was observed that neat PVA nanofibers have low strength and elongation as compared to PVA/Cu nanofibers. The PVA nanofibers have 0.037 MPa stress and 15% elongation but PVA/Cu nanofibers where Cu nanoparticles were synthesized by nanofibers reduction method has stress 0.078 MPa and elongation 70%, PVA/Cu nanofibers where Cu nanoparticles were synthesized by solution reduction method has stress 0.108 MPa and elongation 68% and PVA/Cu nanofibers where Cu nanoparticles were synthesized by immersion method has stress 0.110 MPa and elongation 78%. It means immersion method to load the Cu nanoparticles on PVA nanofibers is the good method because it has good strength and also elongation efficiency than other methods as shown in Figure 8.5a.

8.3.7. ICP study

In order to investigate the release behavior of Cu nanoparticles from the PVA/Cu nanofibers, inductively coupled plasma (ICP) study was done as shown in Figure 8.5b. In this study, 0.02 grams amount of PVA/Cu nanofibers was solved in 5ml of H_2SO_4 to calculate the amount of Cu nanoparticles and for the analysis of the Cu release the 1 g of PVA/Cu nanofibers were dissolved in deionized water and measured during 72 hrs. It was observed that samples leached Cu into the deionized water 4, 9 & 16 ppm for nanofibers reduction

method, solution reduction method and immersion method, respectively. The resultant graphs showed that in the immersion method the highest amount of Cu nanoparticles were released as shown in the Figure 8.5b. The ICP study confirmed that PVA/Cu nanofibers membranes are the significant and appreciable efficiency of antibacterial properties.

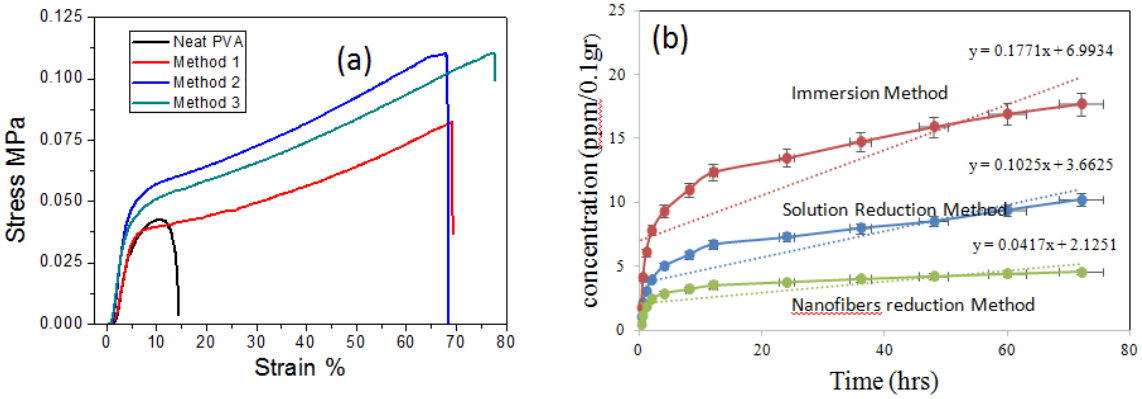

Figure 8.5. (a) Stress-strain behavior of neat PVA nanofibers, PVA/Cu nanofibers by nanofibers reduction, PVA/Cu nanofibers by solution reduction, PVA/Cu nanofibers by immersion method and (b) Release behavior of PVA/Cu nanofibers by nanofibers reduction, PVA/Cu nanofibers by solution reduction, PVA/Cu nanofibers by immersion method.

8.3.8. Antibacterial activity

In order to investigate the antibacterial properties of PVA & PVA/Cu nanofibers membranes, disc diffusion method was used. In this method, the selected bacteria stain such as; *Gram-negative Escherichia coli and Gram-positive Staphylococcus aurous* were used to observe the antibacterial potential of PVA & PVA/Cu nanofibers. For the disc diffusion assay nutrient, agar was prepared. Agar media was transferred in 6 inches. The wick paper sheet was used to prepare discs for standards. PVA & PVA/Cu nanofibers membranes were made 6 mm in size. The discs 6 mm size were impregnated with 100 µL standard samples. The Rifampicin was used as standard for the bacteria at the concentration of 1000 µg/mL. The respective solvent of extracts and fractions were used as negative control. The discs were placed in the incubated plates. After the incubation period, Petri dishes were incubated for 24 hrs at 37^{o}C bacteria strains respectively. The zone of discs was measured in mm by Image J software.

The resultant antibacterial properties are shown in Figure 8.6 and Table 8.1. It was observed that neat PVA nanofibers membranes have no antibacterial properties but PVA/Cu nanofibers membranes have good potential for antibacterial properties. The PVA/Cu nanofibers membranes prepared by immersion method of

synthesis of Cu nanoparticles have the highest potential of antibacterial properties against *Escherichia coli* and *Staphylococcus aurous* bacteria than solution reduction method and nanofibers reduction method as shown in Figure 8.6 and Table 8.1.

Table 8.1. Antibacterial activity by zone of inhibition in millimeter (mm)

Sr. No	Sample specifications	E.Coli bacterium	S. Aureus bacterium
1	Neat PVA membranes	Not active	5
2	PVA/Cu (Nanofiber reduction)	12	10
3	PVA/Cu (Solution reduction)	10	12
4	PVA/Cu (Immersion method)	17	15
Rifampicin (+ve standard)		26	24

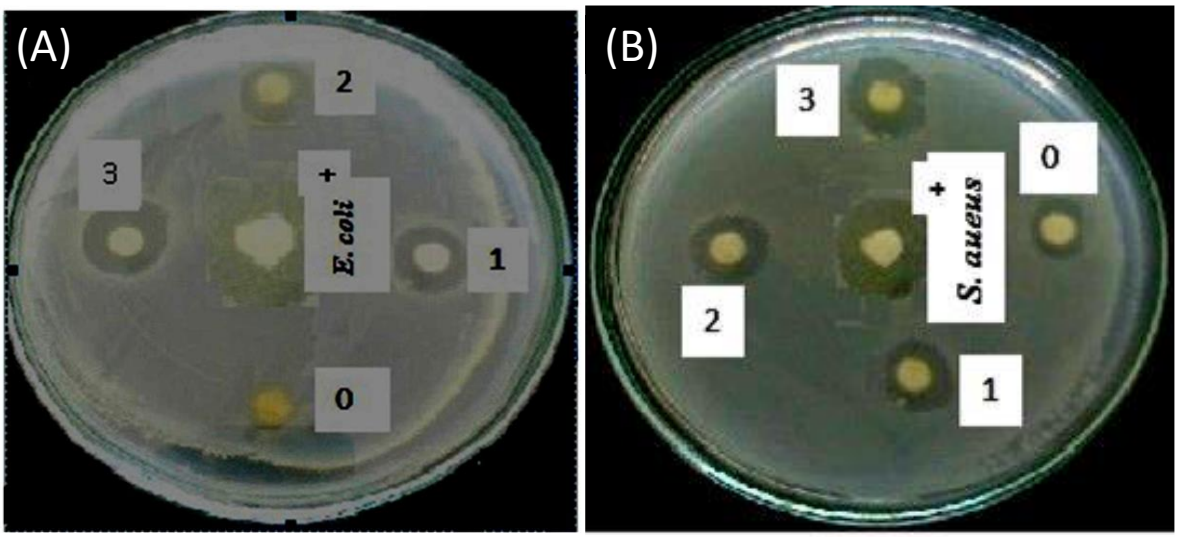

Figure 8.6: Results of antibacterial properties against (a) Escherichia coli bacterium and (b) Staphylooccus aureus bacterium.

8.4. Conclusion

Herein, we successfully fabricated the antibacterial PVA/Cu nanofibers membranes by synthesized and loaded the Cu nanoparticles in different methods. The resultant antibacterial membranes showed appreciable results in all characterizations. It was concluded that PVA/Cu nanofibers membranes having great potential for antibacterial properties but the membranes in which Cu nanoparticles were loaded by immersion method have the highest potential than other nanofiber reduction and solution reduction methods because these PVA/Cu nanofibers membranes have 17 & 15 inhibition zone against *Gram-negative Escherichia coli and Gram–positive Staphylococcus aurous* bacteria which is near to Rifampicin (+ve standard) 26 & 24 respectively. So the PVA/Cu antibacterial membranes prepared by immersion method can fulfill the stated and implied needs of customers.

References

1. Zhang, D. W., Zhang, J., et al. Novel electrochemical milling method to fabricate copper nanoparticles and nanofibers. Chemistry of materials 2005; 17(21), 5242-5245.
2. Chernousova, S., Epple, M. Silver as antibacterial agent: ion, nanoparticle, and metal. Angewandte Chemie International Edition 2013; 52(6), 1636-1653.
3. Hazer, B., Kalaycı, Ö. A. High fluorescence emission silver nano particles coated with poly (styrene-g-soybean oil) graft copolymers: Antibacterial activity and polymerization kinetics. Materials Science and Engineering: C 2017; 74, 259-269.
4. Song, R., Chai, Y., et al. An ultra-long and low junction-resistance Ag transparent electrode by electrospun nanofibers. RSC advances 2016; 6(94), 91641-91648.
5. Dong, C., Xiao, X., et al. Synthesis of stearic acid-stabilized silver nanoparticles in aqueous solution. Advanced Powder Technology 2016; 27(6), 2416-2423.
6. Gebeyehu, M. B., Murakami, R. I., et al. Fabrication and characterization of continuous silver nanofiber/polyvinylpyrrolidone (AgNF/PVP) core–shell nanofibers using the coaxial electrospinning process. RSC Advances 2016; 6(59), 54162-54168.
7. Dubey, P., Gopinath, P. PEGylated graphene oxide-based nanocomposite-grafted chitosan/polyvinyl alcohol nanofiber as an advanced antibacterial wound dressing. RSC Advances 2016; 6(73), 69103-69116.

8. Khan, M. Q., Kim, I. S., et al. Fabrication and characterization of nanofibers of honey/poly (1, 4-cyclohexane dimethylene isosorbide trephthalate) by electrospinning. Materials Science and Engineering: C 2017; 81, 247-251.
9. Coimbra, P., Ferreira, P., et al. (). Coaxial electrospun PCL/Gelatin-MA fibers as scaffolds for vascular tissue engineering. Colloids and Surfaces B: Biointerfaces 2017; 159, 7-15.
10. Vashisth, P., Pruthi, V., et al. Ofloxacin loaded gellan/PVA nanofibers-Synthesis, characterization and evaluation of their gastroretentive/mucoadhesive drug delivery potential. Materials Science and Engineering: C 2017; 71, 611-619.
11. Drozdova, M. G., Markvicheva, E. A., et al. Macroporous modified poly (vinyl alcohol) hydrogels with charged groups for tissue engineering: Preparation and in vitro evaluation. Materials Science and Engineering: C 2017; 75, 1075-1082.
12. Chen, S., Xie, J., et al. Recent advances in electrospun nanofibers for wound healing. Nanomedicine 2017; (0).
13. Xue, J., Xia, Y., et al. Electrospun Nanofibers: New Concepts, Materials, and Applications. Accounts of chemical research 2017; 50(8), 1976-1987.
14. Senthamizhan, A., Balusamy, B., Uyar, T. Electrospinning: A versatile processing technology for producing nanofibrous materials for biomedical and tissue-engineering applications. In Electrospun Materials for Tissue Engineering and Biomedical Applications 2017; (pp. 3-41).
15. Liang, Y., Wang, X., et al. Decorating of Ag and CuO on Cu Nanoparticles for Enhanced High Catalytic Activity to the Degradation of Organic Pollutants. Langmuir 2017; 33(31), 7606-7614.
16. Li, H., Li, C., et al. A facile method to fabricate Cu 0 supported on nanofibers as efficient catalyst using N-arylation reactions. Molecular Catalysis 2017; 431, 49-56.
17. Shabnam, L., & Gomes, V. G., et al. Doped graphene/Cu nanocomposite: A high sensitivity non-enzymatic glucose sensor for food. Food chemistry 2017; 221, 751-759.
18. Parveen, F., Pathan, H. M., et al. Copper nanoparticles: Synthesis methods and its light harvesting performance. Solar Energy Materials and Solar Cells 2016; 144, 371-382.
19. Gawande, M. B., Varma, R. S., et al. Cu and Cu-based nanoparticles: synthesis and applications in catalysis. Chemical reviews 2016; 116(6), 3722-3811.

20. Wang, J., Du, M., et al. Small and well-dispersed Cu nanoparticles on carbon nanofibers: self-supported electrode materials for efficient hydrogen evolution reaction. International Journal of Hydrogen Energy 2016; 41(40), 18044-18049.

Chapter # 09

Fabrication of novel antibacterial electrospun cellulose acetate/ silver-sulfadiazine nanofibers composites for wound dressings applications

9.1. Introduction

Silver sulfadiazine (SSD) is the most effective and ambient applicator for antibacterial factor to save the skin of human beings from bacterial infections and exterior contaminations. SSD is a leading agent for controlling the microbial infections in the second class burn wounds. SSD is the silver (Ag) salt of sulfadiazine (SD) and a molecule of polymeric type, in which Ag ions are tertracoordinated and surrounded with three different deprotonated molecules of SD, where each SD molecule bounded with three Ag ions (Agnes et al. 2014). The Ag ion is the active part of SSD and SD is the supportive factor for achieving more antibacterial properties than sodium alginate, bacterial cellulose and metallic nanoparticles (Wei et al 2015). Recently, the considerable research has been attracted to fabricate the high performance scaffolds due to recent emphasis on environmentally sustainable materials and technology. Therefore, there has been a lot of interest in the fabrication of bio-composites based on cellulose polymers (Ali. Et al., 2015). Cellulose is a regenerated fibers which also known as a natural polysaccharide (A. Ashori et al., 2015). It is one of the highest naturally abundant and extensively used renewable materials due to its multi characteristic like excellent thermal stability, chemical resistance, biodegradability and biocompatibility (Lee et al., 2018). In the same way, regenerated cellulose fibers of one nano/micro scale dimensions are attractive for various applications such as scaffolds, biosensor, packaging films, filter and chemo sensor (Cho, et al. 2007). Nano-scale cellulose fibers which are fabricated by electrospinning have significant scientific and technological attractions due to its proportionally larger surface area and consequently more surface atoms than its micro scale (Jordon et al. 2005).

In the current research authors attempted to develop the antibacterial wound dressings by using the blended cellulose acetate/ silver-sulfadiazine nanofibers via electrospinning. The doping of silver-sulfadiazine (SSD) into spinning solution for electrospinning, is first time attempted for wound dressing of burn infections. Many researchers attempted to fabricate the antibacterial assessment with CA nanofibers by using metals such as silver nanoparticles with low antibacterial efficiency and also side effects (Chen et al., 2016), A. Ashori et al., analyzed the efficiency of antibacterial on the cellulose/polylactic acid composites coated with ethanolic

materials in 2017, R. Liu et al., also examine the antibacterial activity of cellulose nanofibers with hydrogels in 2018, but none of them examine the antibacterial efficiency of SSD on the CA nanofibers with SSD.

9.2. Materials and methods

9.2.1. Materials

Cellulose acetate (CA) (MW = 30000 gmol-1) and silver (1) sulfadiazine (SSD) (98%, powder form, MW = 357.14 g/mol) were provided by Sigma-Aldrich Co., Ltd. (Louis, Missouri, USA). Acetone (99.5%), Sodium hydroxide (NaOH, Purity of 97.0%) and dimethylformamide 98% (DMF) were provided by Wako Pure Chemical Industries, Ltd. (Osaka, Japan)

9.2.2. Method

CA with 24 wt% was dissolved in DMF/acetone (6:4). The solution was prepared with constant stirring for 6 hrs at room temperature, then SSD was dissolved in that CA solution with constant stirring for 4 hrs in four different concentrations such as 0.125 wt%, 0.25 wt%, and 0.37 wt 5 and 0.5 wt %. The resultant solution of CA/SSD of each concentration was loaded in the plastic syringe of 5ml with a capillary tip of 0.6 mm internal diameter. This capillary tip was used to inject the solution on the collector by the supplied voltage. The distance between capillary tip to collector was 15 cm and supplied voltage was 12 kV. The electrospinning used for this purpose has the capacity of voltage up to 80 kV and provide by Har-100* 12, Matsusada Co.,Tokyo Japan. The resultant CA & CA/SSD nanofibers were de-acetalized by NaOH for 3 hrs. The illustration scheme of fabrication of CA/SSD nanofibers was shown in the Figure 1.

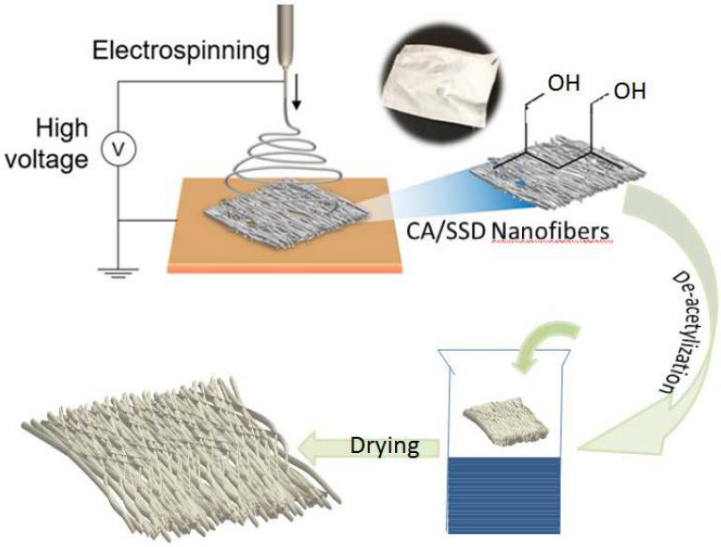

Figure 9.1: Illustration scheme of fabrication of CA/SSD nanofibers.

9.2.3. Characterizations

The morphology of CA nanofibers and CA/SSD nanofibers were investigated by scanning electron microscopy (SEM)(S-3000N, Hitachi Co., Japan) at 12 kV accelerating voltage. For the analysis of SSD particles dispersion on the CA nanofibers, transmission electron microscopy (2010 Fas TEM, JEOL Japan) was used at 200 kV accelerating voltage. The average diameter of the CA & CA/SSD nanofibers was determined by analyzing the SEM images using the image J software. Fourier transform infrared (FT-IR) spectra were recorded between the wavelengths of 400-4000 cm-1 using an IR Prestige-21 (Shimadzu Co., Ltd) and studied for the chemical interactions between CA & SSD. In order to investigate the wetting behavior of CA & CA/SSD nanofibers, static angle with a contact angle meter by drop method was used. X-ray diffraction (XRD) was performed at room temperature using a rotaflex RTP300 (Rigaku Co., Japan and operating at 50 kV and 200mA. The antibacterial analysis of the CA nanofibers & CA/SSD nanofibers against Escherichia coli and B. Subtilis bacteria was determined by using agar diffusion test. The nanofibers of 12 mm diameter were placed for examination on agar plates seeded in log phase with bacterial cells and incubated at 37 °C overnight. This test was repeated three times on different samples. The diameter of inhibition zone was examined in triplicate using ImageJ. Thermal degradation of CA & CA/SSD nanofibers and confirmation of SSD in the CA/SSD nanofibers were performed by thermo-gravimetric analysis (TGA). It was performed on the thermo- plus TG-8120 (Rigaku Corporation, Osaka, Japan). It was operated in a static mode under air temperature at heating rate of 10oC/min with temperature range of 0-600oC.

9.3. Results and discussion

9.3.1. Morphology of nanofibers

In order to investigate the surface morphology of cellulose acetate and cellulose acetate/SSD nanofibers, SEM images were studied as shown in Figure 9.2. It was observed that addition of SSD in the cellulose acetate nanofibers, the morphology and diameter of nanofibers wad not affected. The diameter of neat cellulose acetate was 290 ± 50 but the diameter of 0.125 wt% CA/SSD, 0.25 wt% CA/SSD, 0.37 wt% CA/SSD and 0.5 wt% CA/SSD was 292 ± 20, 287 ± 44, 293 ± 30 and 286 ± 60, respectively as shown in Figure 9.2f.

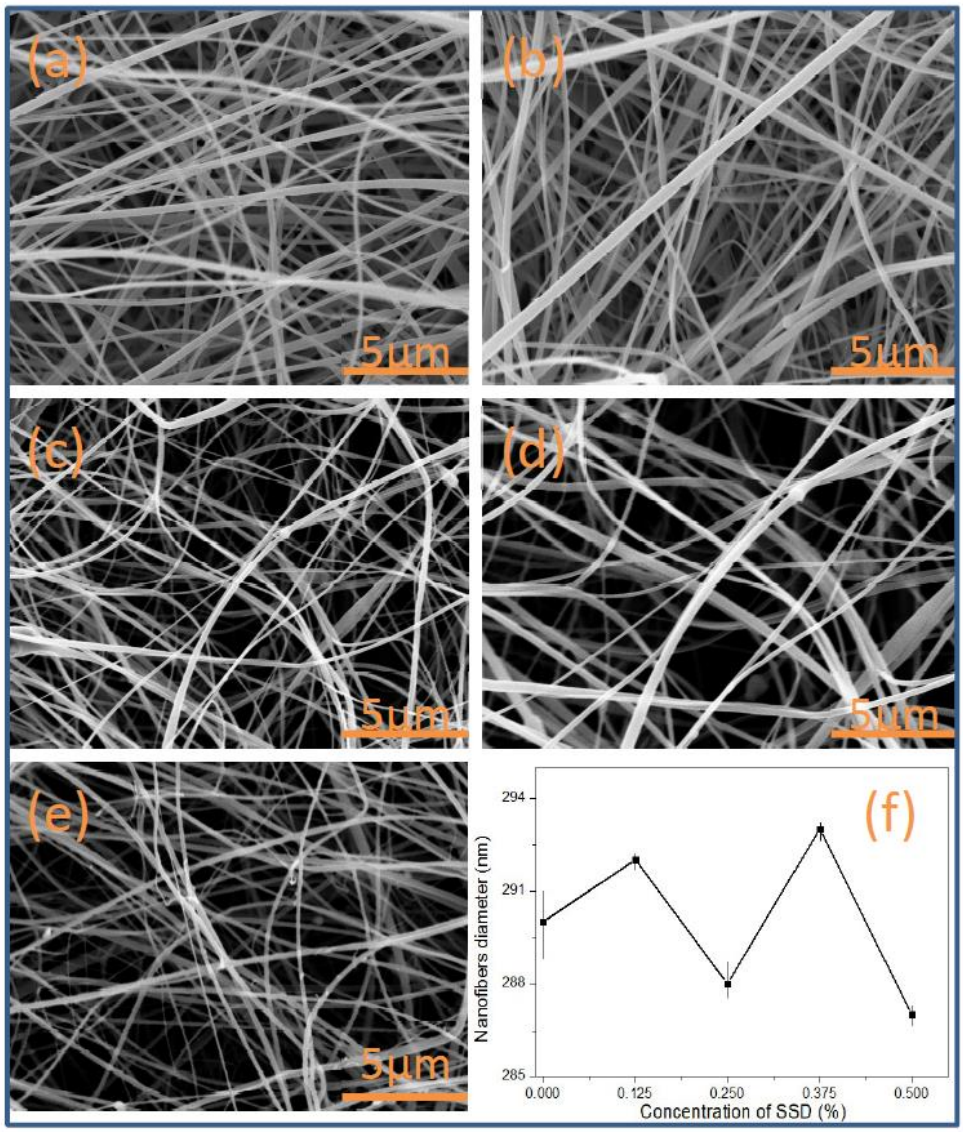

Figure 9.2: SEM images of (a) neat cellulose acetate, (b) 0.125 wt% CA/SSD nanofibers, (c) 0.25 wt% CA/SSD nanofibers, (d) 0.37 wt% CA/SSD nanofibers and (e) 0.5 wt% CA/SSD nanofibers and (f) Nanofibers diameter distributions graph.

In order to further investigation of morphology with respect to the particles distribution on the surface of nanofibers, TEM images were studied as shown in Figure 9.3. It was observed that particles of SSD were uniformly distributed throughout the nanofibers. When the concentration of SSD was increased the visibility of particles was increased as shown in Figure 9.3d. TEM images also confirmed that addition of SSD in the cellulose acetate solution did not affect the surface and diameter of nanofibers also didn't affected.

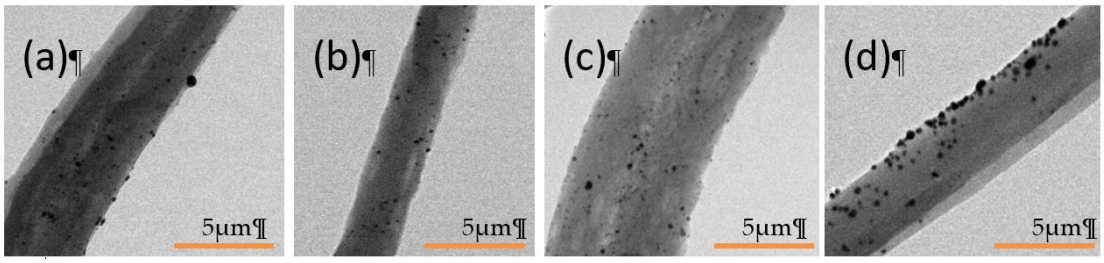

Figure 9.3. TEM images of (a) 0.125 wt% CA/SSD nanofibers, (b) 0.25 wt% CA/SSD nanofibers, (c) 0.37 wt% CA/SSD nanofibers and (d) 0.5 wt% CA/SSD nanofibers.

9.3.2. Chemical interactions analysis

In order to investigate the chemical interactions between cellulose acetate and SSD, FT-IR spectra were studied as shown in Figure 9.4.It was observed that there was successful chemical interactions between SSD and CA. in the CA/SSD nanofibers there were intense and well defined characteristic peaks asymetric of SO2 at 1250 cm-1 and there were also characteristics peaks of NH bending of SSD at 1594 cm-1 (Boating et al. 2015, Augozi et al. 2014) and NH stretching at 3300 cm-1 (Wei et al. 2014). The characteristics peaks of C=O, C-CH3 and C-O-C of cellulose acetate at 1775, 1370 and 1100 cm-1,(Khatri et al. 2012) respectively were shifted in CA/SSD nanofibers at 3100, 2300 and 1775 cm-1, respectively as shown in Figure 9.4.

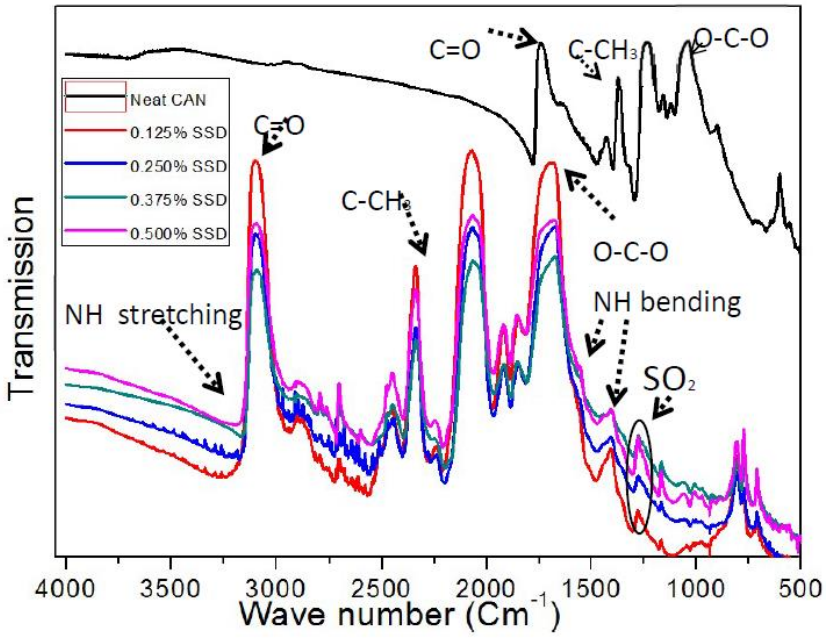

Figure 9.4: FTIR spectra of CA nanofibers and CA/SSD nanofibers.

9.3.3. XRD analysis

In order to investigate the crystalline structure of CA nanofibers and CA/SSD nanofibers, XRD spectra were studied as shown in Figure 9.5. It was observed that crystalline structure of CA/SSD was increased by addition of SSD in the CA nanofibers. It was due to polymeric nature of SSD which has hydrophilic behavior. The characteristics peaks of SSD/CA were at 8o, 8.5o and 18o in all types of CA/SSD nanofibers as shown in the Figure 9.5, but the intensity of these peaks was increased as the content of SSD was increased in the CA nanofibers. Aguzzi et al. in 2013 studied XRD spectra of SSD/chitosan composite and confirmed that SSD showed characteristic peaks at 8o and 10o. Wen et al. in 2015 studied that SSD had great effect on the crystallinity of the partner materials as like CA nanofibers and showed the characteristics peaks at 8o and 18o.So, our proposed XRD results confirmed that SSD has blended in the CA nanofibers which affected the crystalline structure of CA/SSD nanofibers as shown in Figure 9.5.

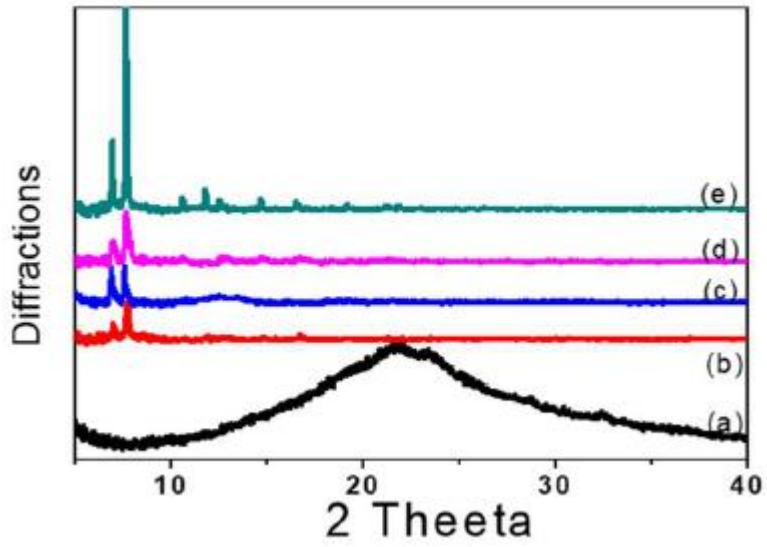

Figure9.5: XRD spectra of CA nanofibers and CA/SSD nanofibers.

9.3.4. Water contact angle analysis

In order to investigate the wetting behavior of CA & CA/SSD,Water contact angle analysis was done as shown in Figure 9.6. It was observed that both CA nanofibers and CA/SSD nanofibers showed the hydrophilic behavior which is appreciable for wound dressing to recover the wound, but the water absorbing property of CA/SSD was reduced as the concentration of SSD was increased as shown in the Figure 9.6. 0.5 wt % CA/SSD nanofibers showed the lowest water absorbency than CA nanofibers and CA/SSD nanofibers. Neat CA nanofibers showed the water content at 28^{o} but 0.125 wt% CA/SSD, 0.25 wt% CA/SSD, 0.37% CA/SSD and 0.5 wt % CA/SSD nanofibers showed 30^{o}, 37^{o}, 40^{o} and 50^{o}, respectively. It is due to the addition of SSD with CA nanofibers which increases the crystalline structure of the CA/SSD nanofibers as shown in the XRD spectra. So, when crystalline structure was increased water absorbency was decreased.

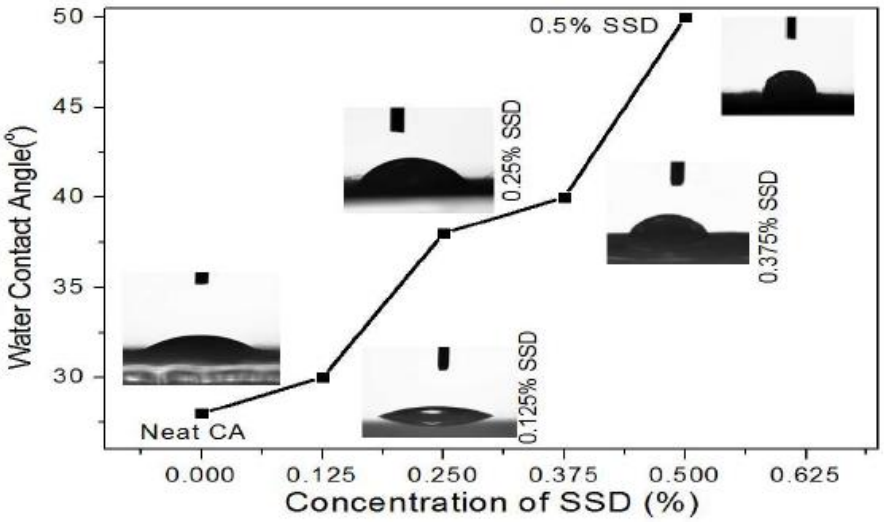

Figure 9.6: water contact angle measurements of CA and CA/SSD nanofibers.

9.3.5. Thermo-gravimetric analysis (TGA)

Thermal degradation of CA & CA/SSD nanofibers and confirmation of SSD in the CA/SSD nanofibers were performed by thermo-gravimetric analysis (TGA). It was performed on the thermo- plus TG-8120 (Rigaku Corporation, Osaka, Japan). It was operated in a static mode under air temperature at heating rate of 10^{o}C/min with temperature range of 0-600^{o}C. It was observed that the thermal degradation of CA/SSD nanofibers was increased by addition of SSD in the CA/SSD nanofibers as shown in Figure 9.7A. TGA spectra also confirmed the presence of SSD in the CA/SSD nanofibers as shown in the Figure 9.7. TGA spectra showed that 0.5 wt % CA/SSD nanofibers have more than 16% SSD in the 6 mg of CA/SSD nanofibers which is higher concentration of SSD than others samples as confirmed by Figure 9.7B. The TGA spectra also showed that when concentration of SSD was increased the thermal stability of CA/SSD nanofibers was increased and content of SSD also increased.

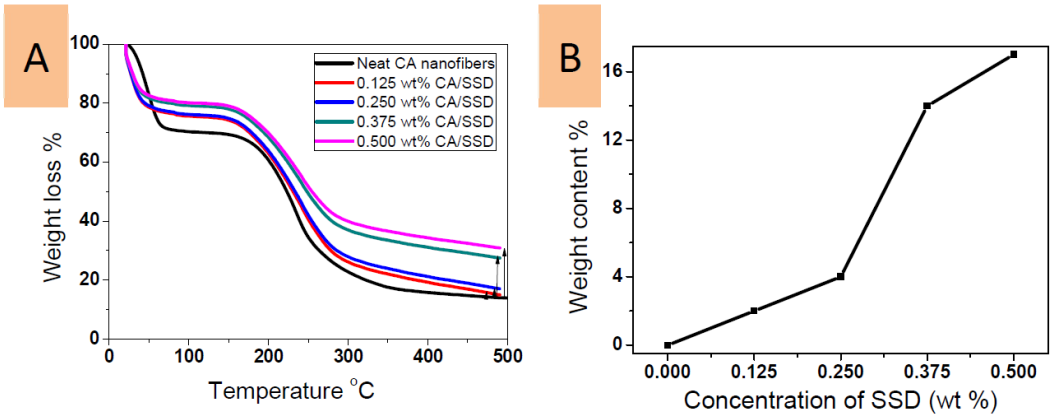

Figure 9.7: TGA spectra of (A) CA & CA/SSD nanofibers (B) weight content of SSD in CA/SSD nanofibers.

9.3.6. Antibacterial analysis

In order to investigate the antibacterial activity, agar disk diffusion method was employed as shown in the Figure 9.8. In this activity, Gram negative E.Coli and Gram positive B. Subtilis were studied. Bare CA nanofibers were used as a negative control during the antibacterial activity. The CA/SSD nanofibers showed the appreciable activity against both types of bacteria strains and exhibit the inhibition zone. It was observed that with low amount of SSD in cellulose acetate nanofibers, CA/SSD nanofibers have very appreciable potential of antibacterial activity. In contrast, there no activity by CA nanofibers was noticed but 0.125 wt% CA/SSD nanofibers were started initiation to antibacterial zone and it was measured around 2 mm for Gram negative E. coli bacteria and 1 mm for Gram positive B. Subtilis bacteria. The CA/SSD nanofibers have great potential of antibacterial activity against Gram negative E. coli bacteria than Gram positive B. Subtilis bacteria as shown in Figure 8a, b & c, which might be attributed to the difference in the cell wall structures of Gram positive and Gram negative bacteria. It has been accepted that Gram negative bacteria are more difficult to kill than Gram positive bacteria since the cell walls of Gram negative bacteria contain a complex and highly asymmetric biological barrier composed of phospholipids and lip polysaccharides as an outer membrane, in addition to a thin peptidoglycan layer adjacent to the cytoplasm membrane, making them much less permeable to most antibacterial agents than Gram positive bacteria (Zhang et al. 2011), but SSD has great potential to bind more Ag and S with Gram negative bacteria than Gram positive (Beveridge et al. 1985), therefore, CA/SSD showed great effect against Gram negative bacteria than Gram positive bacteria

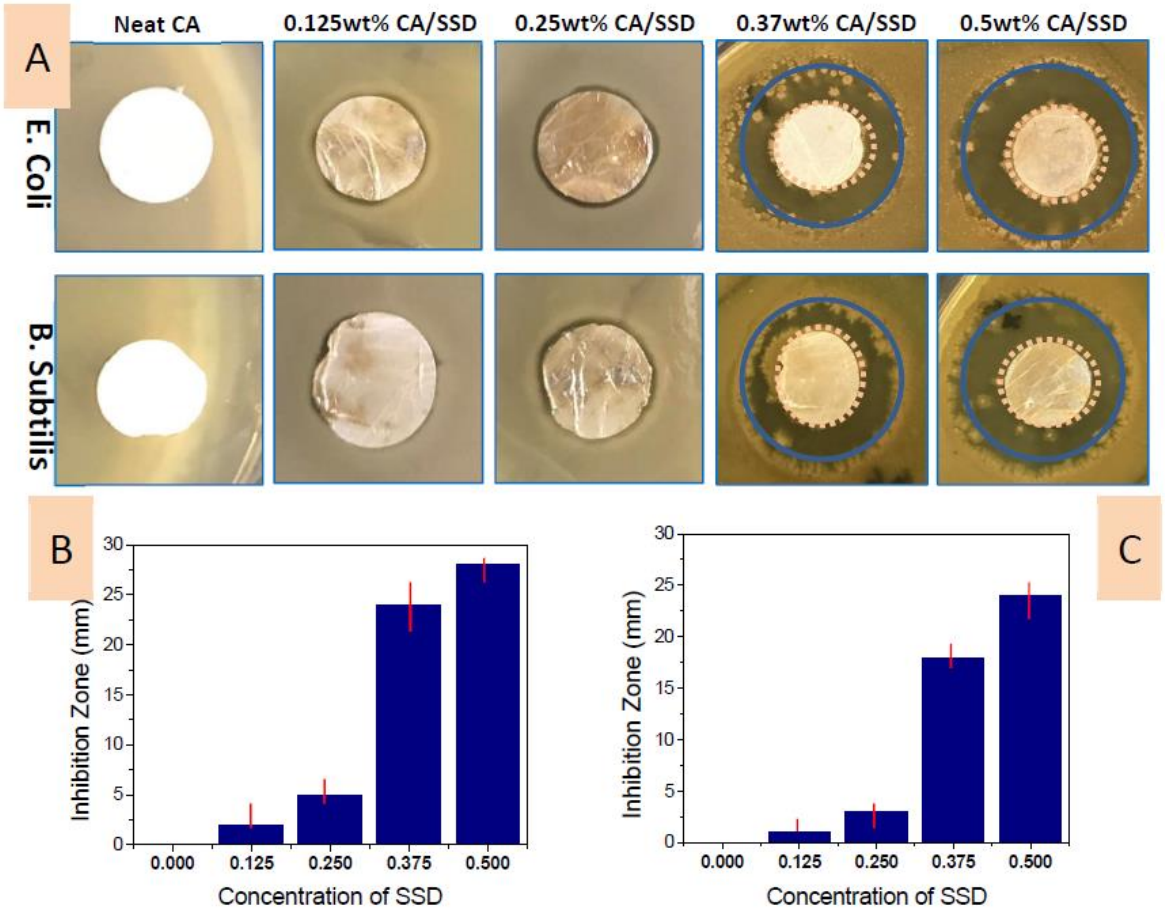

Figure 9.8: Antibacterial activity (A) of CA CA/SSD nanofibers (B) inhibition zone against E. Coli (C) inhibition zone against B. Subtilis.

9.4. Conclusion

Herein, we successfully fabricated the electrospun CA/SSD nanofibers for wound dressings of burn infections. SEM & TEM images revealed that CA/SSD nanofibers have suitable morphology with uniform distributions of SSD particles in the CA/SSD nanofibers. FT-IR spectra and TGA analysis revealed that CA/SSD nanofibers having strong chemical interactions between SSD and CA. The XRD spectra and water contact angle test also showed that CA/SSD nanofibers revealed the suitable water absorbency as required for scaffoldings. The resultant CA/SSD nanofibers exhibited the appreciable antimicrobial activity against Gram-negative Escherichia Coli and Gram-positive Bacillus Subtilis bacteria with considerable sustainability for repetitive use. In addition, CA/SSD nanofibers revealed the appreciable biocompatibility. So, CA/SSD nanofibers can be used as a promising & distinguish product for wound dressings applications and it can be fulfill the stated and implied needs of customers.

References

1. Chen, Honglei, Guangqian Lan, Luoxiao Ran, Yang Xiao, Kun Yu, Bitao Lu, Fangying Dai, Dayang Wu, and Fei Lu. "A novel wound dressing based on a Konjac glucomannan/silver nanoparticle composite sponge effectively kills bacteria and accelerates wound healing." Carbohydrate polymers 183 (2018): 70-80.
2. Siafaka, Panoraia I., Asimina P. Zisi, Maria K. Exindari, Ioannis D. Karantas, and Dimitrios N. Bikiaris. "Porous dressings of modified chitosan with poly (2-hydroxyethyl acrylate) for topical wound delivery of levofloxacin." *Carbohydrate polymers* 143 (2016): 90-99.
3. Dhand, Chetna, Mayandi Venkatesh, Veluchami Amutha Barathi, Sriram Harini, Samiran Bairagi, Eunice Goh Tze Leng, Nandhakumar Muruganandham et al. "Bio-inspired crosslinking and matrix-drug interactions for advanced wound dressings with long-term antimicrobial activity." *Biomaterials*138 (2017): 153-168.
4. Caló, Enrica, Lucy Ballamy, and Vitaliy V. Khutoryanskiy. "Hydrogels in Wound Management." *Hydrogels: Design, Synthesis and Application in Drug Delivery and Regenerative Medicine* (2018): 128.
5. Mele, Elisa. "Electrospinning of natural polymers for advanced wound care: towards responsive and adaptive dressings." *Journal of Materials Chemistry B* 4, no. 28 (2016): 4801-4812.
6. Abrigo, Martina, Sally L. McArthur, and Peter Kingshott. "Electrospun nanofibers as dressings for chronic wound care: advances, challenges, and future prospects." *Macromolecular Bioscience* 14, no. 6 (2014): 772-792.
7. Nherera, Leo M., Paul Trueman, Christopher D. Roberts, and Leena Berg. "A systematic review and meta-analysis of clinical outcomes associated with nanocrystalline silver use compared to alternative silver delivery systems in the management of superficial and deep partial thickness burns." *Burns* 43, no. 5 (2017): 939-948.
8. Maharjan, Bikendra, Mahesh Kumar Joshi, Arjun Prasad Tiwari, Chan Hee Park, and Cheol Sang Kim. "In-situ synthesis of AgNPs in the natural/synthetic hybrid nanofibrous scaffolds: Fabrication, characterization and antimicrobial activities." *Journal of the mechanical behavior of biomedical materials* 65 (2017): 66-76.

9. Szegedi, Ágnes, Margarita Popova, Krassimira Yoncheva, Judit Makk, Judith Mihály, and Pavletta Shestakova. "Silver-and sulfadiazine-loaded nanostructured silica materials as potential replacement of silver sulfadiazine." *Journal of Materials Chemistry B* 2, no. 37 (2014): 6283-6292.
10. Shao, Wei, Hui Liu, Xiufeng Liu, Shuxia Wang, Jimin Wu, Rui Zhang, Huihua Min, and Min Huang. "Development of silver sulfadiazine loaded bacterial cellulose/sodium alginate composite films with enhanced antibacterial property." *Carbohydrate polymers* 132 (2015): 351-358.
11. Abdulkhani, Ali, Jaber Hosseinzadeh, Alireza Ashori, and Hossein Esmaeeli. "Evaluation of the antibacterial activity of cellulose nanofibers/polylactic acid composites coated with ethanolic extract of propolis." *Polymer Composites* 38, no. 1 (2017): 13-19.
12. Lee, Hoik, Masayoshi Nishino, Daewon Sohn, Jung Soon Lee, and Ick Soo Kim. "Control of the morphology of cellulose acetate nanofibers via electrospinning." *Cellulose* (2018): 1-9.
13. Cao, Xiaodong, Hua Dong, and Chang Ming Li. "New nanocomposite materials reinforced with flax cellulose nanocrystals in waterborne polyurethane." *Biomacromolecules*8, no. 3 (2007): 899-904.
14. Jordan, Jeffrey, Karl I. Jacob, Rina Tannenbaum, Mohammed A. Sharaf, and Iwona Jasiuk. "Experimental trends in polymer nanocomposites—a review." *Materials science and engineering: A* 393, no. 1-2 (2005): 1-11.
15. Chen, Hao, Lei Guo, Joshua Wicks, Christopher Ling, Xin Zhao, Yufei Yan, Jin Qi, Wenguo Cui, and Lianfu Deng. "Quickly promoting angiogenesis by using a DFO-loaded photo-crosslinked gelatin hydrogel for diabetic skin regeneration." *Journal of Materials Chemistry B* 4, no. 21 (2016): 3770-3781.
16. Liu, Rui, Lin Dai, Chuanling Si, and Zhaogang Zeng. "Antibacterial and hemostatic hydrogel via nanocomposite from cellulose nanofibers." *Carbohydrate polymers* 195 (2018): 63-70.
17. Boateng, Joshua, Rocio Burgos-Amador, Obinna Okeke, and Harshavardhan Pawar. "Composite alginate and gelatin based bio-polymeric wafers containing silver sulfadiazine for wound healing." *International journal of biological macromolecules* 79 (2015): 63-71.
18. Aguzzi, Carola, Giuseppina Sandri, Cristina Bonferoni, Pilar Cerezo, Silvia Rossi, Franca Ferrari, Carla Caramella, and César Viseras. "Solid state characterisation of silver sulfadiazine loaded on montmorillonite/chitosan nanocomposite for wound healing." *Colloids and Surfaces B: Biointerfaces* 113 (2014): 152-157.

19. Shao, Wei, Hui Liu, Xiufeng Liu, Shuxia Wang, Jimin Wu, Rui Zhang, Huihua Min, and Min Huang. "Development of silver sulfadiazine loaded bacterial cellulose/sodium alginate composite films with enhanced antibacterial property." *Carbohydrate polymers* 132 (2015): 351-358.
20. Wen, Xiaoxiao, Yudong Zheng, Jian Wu, Lina Yue, Cai Wang, Jiabin Luan, Zhigu Wu, and Kaisheng Wang. "In vitro and in vivo investigation of bacterial cellulose dressing containing uniform silver sulfadiazine nanoparticles for burn wound healing." *Progress in Natural Science: Materials International*25, no. 3 (2015): 197-203.
21. Zhang, Lifeng, Jie Luo, Todd J. Menkhaus, Hemanthram Varadaraju, Yuyu Sun, and Hao Fong. "Antimicrobial nano-fibrous membranes developed from electrospun polyacrylonitrile nanofibers." *Journal of membrane science*369, no. 1-2 (2011): 499-505.
22. Beveridge, T. J., and W. S. Fyfe. "Metal fixation by bacterial cell walls." *Canadian Journal of Earth Sciences* 22, no. 12 (1985): 1893-1898.

Chapter # 10

Conclusion

Herein, we have shown that electrospun anofibers have appericiable properties to fabricate biomedical products and functional textiles. PICT/honey nanofibers were successfully fabricated by electrospinning for potential of antibacterial applications. Polymer solution containing 20% of the honey was maximum percentage of honey concentration to obtain bead free PICT/honey nanofibers. The release of honey was complete in 15 minutes and the maximum release of honey was 72 mg/L in 10 minutes. Therefore, PICT/honey nanofibers containing 15% of honey are more suitable for good elastic behavior and tensile strength as compared to other concentrations of honey used in the polymer solution. We successfully developed the multifunctional nanocomposite for the surgical gown by blending of PVA/ZnO through electrospinning. The blending of ZnO nanoparticles with PVA was in three different concentrations; 5wt%, 7wt% & 9wt% and uniformly dispersion on nanofibers was achieved. The resultant nanofibers have good chemical interactions between PVA & ZnO nanoparticles, crystallinity and strength of the blended nanofibers were increased as concentration of ZnO nanoparticles was increased. The photo-catalysis efficiency of the PVA/ZnO nanofibers was increased as the concentration of the ZnO nanoparticles was increased. The UV transmission of the PVA/ZnO nanofibers was decreased as the concentration of ZnO nanoparticles was increased. The antibacterial efficiency of PVA/ZnO nanofibers was increased as the concentration of the ZnO nanoparticles was increased. So this nanocomposite is very beneficial for the medical surgeon to fulfill the stated and implied needs of the customer.

Furthermore, we successfully fabricated the antibacterial PVA/Cu nanofibers membranes by synthesized and loaded the Cu nanoparticles in different methods. The resultant antibacterial membranes showed appreciable results in all characterizations. It was concluded that PVA/Cu nanofibers membranes having great potential for antibacterial properties but the membranes in which Cu nanoparticles were loaded by immersion method have the highest potential than other nanofiber reduction and solution reduction methods because these PVA/Cu nanofibers membranes have 17 & 15 inhibition zone against *Gram-negative Escherichia coli and Gram–positive Staphylococcus aurous* bacteria which is near to Rifampicin (+ve standard) 26 & 24 respectively. So the PVA/Cu antibacterial membranes prepared by immersion method can fulfill the stated and implied needs of customers.

We also have successfully fabricated the electrospun CA/SSD nanofibers for wound dressings of burn infections. SEM & TEM images revealed that CA/SSD nanofibers have suitable morphology with uniform distributions of SSD particles in the CA/SSD nanofibers. FT-IR spectra and TGA analysis revealed that CA/SSD nanofibers having strong chemical interactions between SSD and CA. The XRD spectra and water contact angle test also showed that CA/SSD nanofibers revealed the suitable water absorbency as required for scaffoldings. The resultant CA/SSD nanofibers exhibited the appreciable antimicrobial activity against Gram-negative Escherichia Coli and Gram-positive Bacillus Subtilis bacteria with considerable sustainability for repetitive use. In addition, CA/SSD nanofibers revealed the appreciable biocompatibility. So, CA/SSD nanofibers can be used as a promising & distinguish product for wound dressings applications and it can be fulfill the stated and implied needs of customers.

Herein, we successfully developed self-cleaning PVA/ZnO & PVA/TiO_2 nanofibers by electrospinning in three different concentrations of ZnO and TiO_2 NPs. On the basis of the characterization results, it was concluded that these PVA/ZnO & PVA/TiO_2 nanofibers have self-cleaning properties, but PVA/ZnO nanofibers have higher self-cleaning properties than PVA/TiO_2 nanofibers because 9% by weight PVA/ZnO nanofibers has 95% self-cleaning properties, which is higher than 9% by weight PVA/TiO_2 nanofibers. This innovative research is essential to form intelligent textiles for stain eliminating from non-washable & non-woven products, such as surgical gown, wound dressings, and home textiles. This research will be fruitful to fulfill the stated and implied needs of customers.

Nanofibers based tubes were successfully fabricated with PVP/Au via electrospinning. All tubes showed better morphology in terms of structural stability, formability and good dispersion of Au nanoparticles on the nanofibers. Therefore, tube having 0.2 mm has the highest tensile strength than tube having 2.0 mm and strength is reversible to diameter; when diameter of tubes is increased then tensile strength of tubes is decreased. Therefore, according to the equation (1), in the S-S curve, the tube having diameter of 0.2 mm has the highest tensile strength than other tubes. The values of capacity for potential voltage of tubes showed that tubes which were made from neat PVP having very small potential voltage which is not suitable for the potential application of axon but the tubes made from PVP/Au having good potential voltage which was required range for axon. So, the nanofibers tube having diameter of 0.2 mm made from PVP/Au is most suitable tube for the axon application which has the capacity of potential voltage upto 89 mV and good

average diameter of 210 ± 25 nm for the nanofibers of the tube and suitable thickness of 0.039 mm for the tube wall, good tensile strength upto 17 MPa and 33% elongation. On the bases of the characterization of PVP/Au, we conclude that this biomaterial may be a better substrate for further in vivo or in vitro investigation to make it useful for tissue engineering.

Furthermore, tubular scaffolds for blood vessel were fabricated successfully by coating poly (1, 4 cyclohexane dimethylene isosorbide terephthalate) electrospun nanofibers with PVA hydrogel. The scaffolds possessed dual network polymers may increase the main requirements to preparing artificial blood vessels as well as high tensile strength with excellent biocompatibility. All investigated characterization results showed that the resultant scaffolds were appropriate candidates for blood vessel tissue engineering due to its dual network performance, where PVA performed for biocompatibility and excelent elongation and PICT performed for approperiate tensile strength and dimensional stability for blood vessel. Therefore this research is fruitfull to fulfill the stated and implied needs of society.

We successfully fabricated ZnO/PICT nanofibers by the electrospinning technique. The electrospun nanofibers demonstrated efficient self-cleaning activity. The TEM results clearly showed that the uniformity in the dispersion of the ZnO nanoparticles on the PICT nanofibers was increased as the concentration increased. The photo-catalytic activity of 9 wt% ZnO/PICT nanofibers had about 50% efficiency within 1 hr, and it increased gradually to around 99% within 3 hrs, while, at 3 wt%, the ZnO/PICT had 40% self-cleaning efficiency in the same time. Based on these results, it was apparent that the higher concentration of ZnO provided a more effective self-cleaning performance, and the contamination was fully degraded and removed within3 hrs. The results of this innovative research should be very useful in developing intelligent textile products that self-eliminate stains. These results should be helpful in academic and industrial applications in that they can help textile researchers and manufacturers to meet the stated and implied needs of customers.

Accomplishments

List of journal publications

1. Muhammad Qamar Khan, Hoik Lee, Zeeshan Khatri, Davood Kharaghani, Muzamil Khatri, Takahiro Ishikawa, Seung-Soon Im, Ick Soo Kim. Fabrication and characterization of nanofibers of Honey/Poly (1, 4 cyclohexane dimethylene isosorbide trephthalate) by Electrospinning. Materials Science and Engineering: C. 2017. 81, 247-251. (https://doi.org/10.1016/j.msec.2017.08.011)

2. Muhammad Qamar Khan, Hoik Lee, Jun Mo Koo, Zeeshan Khatri, Jianhua Sui, Seung Soon Im, Chunhong Zhu, Ick Soo Kim. Self-cleaning effect of electrospun poly (1, 4-cyclohexanedimethylene isosorbide terephthalate) nanofibers embedded with zinc oxide nanoparticles, "Textile Research Journal. 2017. 88, 21, 2493-2498. (https://doi.org/10.1177%2F0040517517723026)

3. Muhammad Khan, Davood Kharaghani, Sana Ullah, Muhammad Waqas, Abdul Abbasi, Yusuke Saito, Chunhong Zhu, Ick Soo Kim. Self-Cleaning Properties of Electrospun PVA/TiO2 and PVA/ZnO Nanofibers Composites. Nanomaterials. 2018. 8, no. 9: 644. (https://doi.org/10.3390/nano8090644)

4. Muhammad Qamar Khan, Davood Kharaghani, Nazish Nishat, Takahiro Ishikawa, Sana Ullah, Hoik Lee, Zeeshan Khatri, Ick Soo Kim. The development of nanofiber tubes based on Nanocomposites of Polyvinylpyrolidone incorporated gold nanoparticle (PVP/Au) as scaffold for neuroscience application in Axon. Textile Research Journal. 2018. (0040517518801185). (https://doi.org/10.1177%2F0040517518801185)

5. Muhammad Qamar Khan, Davood Kharaghani, Nazish Nishat, Sanaullah, Amir Shahzad, Yuma Inoue, Ick Soo Kim. In-Vitro Assessment of Dual-Network Electrospun Tubes from Poly (1, 4 Cyclohexane Dimethylene Isosorbide Terephthalate)/PVA Hydrogel for Blood Vessel Application. Journal of Applied Polymer Science. 2018.135. 47222. (https://doi.org/10.1002/app.47222)

6. Muhammad Qamar Khan, Davood Kharaghani, Nazish Nishat, Tanveer Hussain, Sanaullah, Muhammad Waqas, Ick Soo Kim. Preparation and Characterizations of Multifunctional PVA/ZnO Nanofibers Composite membranes for Surgical Gown Application. Journal of Materials Research and Technology. 2018. (10.1016/j.jmrt.2018.08.013). (https://doi.org/10.1016/j.jmrt.2018.08.013)

7. Muhammad Qamar Khan, Davood Kharaghani, Sanaullah, Amir Shahzad, Y. Saito, Yamamoto T, Ogasawara H, Ick Soo Kim. Fabrication of antibacterial electrospun cellulose acetate/silver-sulfadiazine nanofibers composites for wound dressings applications. Polymer Testing. 2019;74:39-44. (https://www.sciencedirect.com/science/article/pii/S0142941818316945)

8. Davood Kharaghani, Muhammad Qamar Khan, Amir Shahzad, Yuma Inoue, Takayuki Yamamoto, Selene Rozet, Yasushi Tamada, and Ick Kim. Preparation and In-Vitro Assessment of Hierarchal

Organized Antibacterial Breath Mask Based on Polyacrylonitrile/Silver (PAN/AgNPs) Nanofiber. Nanomaterials. 2018. 8, no. 7: 461.
(https://doi.org/10.3390/nano8070461)

9. Amir Shahzad, Naseer Ahmad, Zulfiqar Ali, Ali Afzal, Muhammad Bilal Qadir, Zubair Khaliq, Muhammad Qamar Khan. Statistical analysis of yarn to metal frictional coefficient of cotton spun yarn using Taguchi design of experiment. The Journal of Strain Analysis for Engineering Design. 53, no. 7 (2018): 485-493.
(https://doi.org/10.1177%2F0309324718786373)

10. Davood Kharaghani, Yun Kee Jo, Muhammad Qamar Khan, Yeonsu Jeong, Hyung Joon Cha, Ick Soo Kim. Electrospun antibacterial polyacrylonitrile nanofiber membranes functionalized with silver nanoparticles by a facile wetting method. European Polymer Journal. 2018. 108: 69-75.
(https://doi.org/10.1016/j.eurpolymj.2018.08.021)

11. Amir Shahzad, Zulfiqar Ali, Usman Ali, Zubair Khaliq, Muhammad Zubair, Ick Soo Kim, Tanveer Hussain, Muhammad Qamar Khan, Abher Rasheed, Muhammad Bilal Qadir. Development and characterization of conductive ring spun hybrid yarns. The Journal of Textile Institute. (2018): 1-10.
(https://doi.org/10.1080/00405000.2018.1507695)

12. Muzamil Khatri, Farooq Ahmed, Irfan Shaikh, Duy-Nam Phan, Muhammad Qamar Khan, Zeeshan Khatri, Hoik Lee, Ick Soo Kim. Dyeing and characterization of regenerated cellulose nanofibers with vat dyes. Carbohydrate polymers. 2017. 174: 443-449.
(https://doi.org/10.1016/j.carbpol.2017.06.125)

13. Davood Kharaghani, Muhammad Qamar Khan, Amir Shahzad, Yuma Inoue, Takayuki Yamamoto, Selene Rozet, Yasushi Tamada, Ick Soo Kim. Fabrication of electrospun antibacterial PVA/Cs nanofibers loaded with CuNPs and AgNPs by an in-situ method. Polymer Testing. 72 (2018): 315-321.
(https://doi.org/10.1016/j.polymertesting.2018.10.029)

14. Hassan, M. Aamir, Usman Ali, Amir Shahzad, Muhammad Bilal Qadir, Zubair Khaliq, Ahsan Nazir, Sharjeel Abid, Muhammad Qamar Khan, and Tanveer Hussain. "Bullet-Spinneret based needleless electrospinning; a versatile way to fabricate continuous nanowebs at low voltage." Materials Research Express 6, no. 2 (2018): 025053.
(https://doi.org/10.1088/2053-1591/aaf137)

15. Sanaullah, Mutahira Hashmi, Muhammad Qamar Khan, Davood kharaghani, Ick Soo Kim, Silver sulfadiazine loaded zein nanofiber mats as a novel wound dressing, RCS Advances, 9(1):268-277

Book chapter

16. Muhammad Qamar Khan, Davood Kharaghani, Ick Soo Kim. Nanofibers for medical textiles. Hand book of nanofibers. Springer International Publishing AG (2018). 1-17.

(https://link.springer.com/referenceworkentry/10.1007%2F978-3-319-42789-8_57-1)

17. Davood Kharaghani, Muhammad Qamar Khan, Ick Soo Kim. Application of nanofibers in ophthalmic tissue engineering. Hand book of nanofibers. Springer International Publishing AG 2018. 978-3-319-42789-8.

(HTTPS://LINK.SPRINGER.COM/REFERENCEWORKENTRY/10.1007%2F978-3-319-42789-8_56-1)

List of conference publications

1. Muhammad Qamar Khan, Davood Kharaghani, Ick Soo Kim. Nanofibers based tubes for medical applications. Eurpeon Microbiology Research Conference Valencia, Spain 2018. (https://europeanmicrobiology.madridge.com/)

2. Davood Kharaghani, Muhammad Qamar Khan, Ick Soo Kim. Antimicrobial PAN/Ag nanofibers based washable mask. Eurpeon Microbiology Research Conference Valencia, Spain 2018. (https://europeanmicrobiology.madridge.com/)

3. Muhammad Qamar Khan, Davood Kharaghani, Ick Soo Kim. The development of nanofibers based tubes for neuroscience application. Fifth International Nanofiber Symposium –NANOFIBERS2018, ANEX 2018. Japan. (https://anex2018.com/symposium)
4. Davood Kharaghani, Muhammad Qamar Khan, Ick Soo Kim. The fabrication of nanofibers web/Nonwoven antibacterial mask. Fifth International Nanofiber Symposium –NANOFIBERS2018, ANEX 2018. Japan. (https://anex2018.com/symposium)
5. Muhammad Qamar Khan, Hoik Lee, Davood Kharaghani, Ick Soo Kim. Hydrogel nanofiber with cross-linked poly(vinyl alcohol). Gelsympo2017. Nihon University Narashino Chiba 275-8575, Japan. (https://www.gelsympo2017.com/tentative-program)

6. Davood Kharaghani, Muhammad Qamar Khan, Hoik Lee, Ick Soo Kim. Comparison of fabrication methods for the effective loading of Ag onto PVA nanofibers. Gelsympo 2017. Nihon University Narashino Chiba 275-8575, Japan. (https://www.gelsympo2017.com/tentative-program)

7. Muhammad Qamar Khan, Ick Soo Kim. The Development of Self-cleaning Nanocomposite via Electrospinning. The 70th annual conference of the Japan Textile Machinery Society 2017, Osaka, Japan. (http://tmsj.or.jp/annual/70/postersession.html)

8. Muhammad Qamar Khan, Ick Soo Kim. The Development of Photo-catalytic Nanocomposites via Electrospinning. International Congress on Polymers for Emerging Technologies 2017, Jeju, Korea. (https://iupac.org/event/iupac-faps-2017-polymer-congress/)